Yokohama National University
Graduate School of Urban Innovation

Durability Assessment of High RAP Mixture with Rejuvenator using SATS Conditioning

再生添加剤を併用し再生骨材配合率を高めた再生アスファルト混合物の
SATS コンディショニングを用いた耐久性評価

by

Masahiko Iwama

Thesis submitted to Yokohama National University
for the degree of Doctor of Engineering

February 2023

Abstract

In many countries, and especially in developed countries, assessing the durability of aging infrastructures has become an urgent issue, as the number aging infrastructures failing during their service has been increasing. Meanwhile, increases in torrential rainfalls and heat waves have become apparent worldwide, and might be related to global warming. Therefore, many aging infrastructures will be exposed to more severe environments; accordingly, the possibility of further failures during their service is expected to increase. In particular, the durability of road pavements is a concern because they are directly subjected to heavy rainfall and heat waves while withstanding traffic loading.

In the field of road pavements, the use of reclaimed asphalt pavement (RAP) has increased for asphalt pavements owing to the aim of preserving natural resources, resulting in increased demand for RAP mixture production. Recently, approaches to reusing RAP have been repeatedly implemented. Therefore, providing durability assessments of RAPs is especially important. For this reason, several studies have investigated the effects of moisture on the mechanical and physical properties of RAP mixtures, as moisture plays an important role in the durability of asphalt mixtures. It is known that moisture induces a loss of cohesion in asphalt mixtures, resulting in the loss of stiffness of the mixture. Moisture also leads to stripping in asphalt mixtures during service, owing to the loss of adhesion at the interface between the aggregate and binder. Thus far, the previous results obtained using RAP mixtures have suggested that RAP mixtures have better resistance to moisture than virgin hot mix asphalt (HMA) mixtures.

In terms of environmental concern, warm-mix asphalt (WMA) mixture have been widely used in practice, which has contributed to reduction in carbon dioxide (CO_2) and preservation of natural resource. WMA technology can save energy and prevent bitumen from aging at asphalt mixture production. One of effective measures in the WMA technology is binder modification via wax. Binder viscosity significantly decreases, resulting in the reduction in the temperatures of asphalt mixtures at the production and the layering. Therefore, the application to WMA technology is also examined for RAP mixture.

However, aging caused by thermal degradation and oxidation also appears during the service, i.e., while the moisture attacks the RAP. Despite this fact, few efforts have been made to investigate the combined effects of moisture, heat, and oxidation, referred to as "combined aging," on the durability of RAP mixtures. In recent years, RAP mixtures with high RAP contents blended with rejuvenator agents have appeared in practice for the repeated use of RAPs. Owing to this situation, there is a need to understand how the performances of RAP mixtures with high RAP contents and rejuvenator agents change when the mixtures are subjected to combined aging. However, there have been no detailed studies on how the durability of such RAP mixtures changes when subjected to combined aging, or how it differs from that of ordinary HMA and WMA mixtures, not only in terms of the mixture, but also in terms of the binder properties.

Therefore, in this study, the mechanical and physical properties of RAP mixtures with 30% and 60% RAP contents blended with two types of rejuvenator agents were experimentally investigated, with and without combined aging. Saturation aging tensile stiffness (SATS) conditioning was used to simulate the combined aging that would occur in the field. The properties of the binders extracted from the mixtures with and without combined aging were also examined. The test results were compared with those of HMA and WMA mixtures. The binder properties as obtained through a two-stage extraction process were also examined. Details of the experimental program and test results are described in this thesis. Based on the obtained test results, certain aspects of the damage mechanisms for RAP mixtures subjected to combined aging are discussed.

Acknowledgements

This research project would not have been completed without the support of many people. In particular, I would like to thank the following people and organisations:

First and foremost, I gratefully acknowledge the supervision provided by Professor Kimitoshi Hayano. Hayano-sensei has always encouraged and supported my research work, even on his weekend. In addition, he has constantly been on hand to provide guidance and advice through e-mails and video meeting, and helped me prepare for journal preparation. He has spent time and energy to guide me through research and journal paper. I am very fortunate to have met such a good supervisor.

Secondly, I am grateful to the members of NIPPO Corporation for giving me the opportunity to study and conduct research during my doctoral research. Without their assistance, I could not have continued this study.

Last, but not least, I would like to say a big “thank you” to my family, Natsumi, Mei, Katsuhiko and Shouko, for their love and encouragement. Without their support, I could not have continued this research during the research period.

Declaration

The work described in this thesis was conducted at Yokohama National University, Graduate School of Urban Innovation between October 2018 and February 2023. I declare that the work is my own and has not been submitted for a degree of another university.

Masahiko Iwama
February 2023

Table of Contents

Page

List of Figures

List of Tables

CHAPTER 1

Introduction

1.1 BACKGROUND

1.1.1 Global warming and pavement

Asphalt pavement has played an important role as a major infrastructure over the years. It has supported our economic activities, as well as social activities, as part of our transport infrastructure. In recent years, however, demand for asphalt pavement has changed due to growing awareness of environmental issues, such as global warming and climate change. This kind of problem has become more pronounced worldwide, where the air temperature during recent summers has tended to set new records, the surface of asphalt pavements may reach 60°C or more, the number of heavy rain has been rising (see Figure 1.1). In general, high surface temperatures and moisture in pavement adversely affect the longevity of pavement materials, by accelerating the pace of rutting, aging and fatigue. For the reasons, the increase in temperatures and torrential rain have become a serious problem for asphalt pavement (see Figure 1.2). In addition, bearing in mind recent demand for recycling technology to preserve natural resource, it is desirable to re-use existing paving materials for road maintenance. Therefore, the countermeasure for climate change and resource preservation has become an increasingly important issue, in terms of sustainability as well as the environment. In order to tackle this problem from a paving perspective, the use of Reclaimed Asphalt Pavement (RAP) mixture and Warm-Mix Asphalt (WMA) technologies has been accelerated on site.

Figure 1.1 Influence of global warming on at an airport infrastructure

https://mainichi.jp/articles/20180910/k00/00e/040/143000c

Figure 1.2 Cross section of an asphalt pavement after long-term service

(Hirato 2017）

1.1.2 Global warming for RAP mixture

In recent years, there is growing awareness that increases in heat wave and torrential rain are caused by serious environmental issue such as climate change. According to the report from International Panel for Climate Change (IPCC), these issues might be related significantly to global warming (Intergovernmental Panel on Climate Change 2021). On the other hand, for the field of civil engineering, aging infrastructure such as the collapse of bridges and tunnels are becoming urgent issue during service life (Levy, S. M. 2008). In particular, asphalt pavements are exposed to harsh conditions among road structures since it was directly subjected repeated heavy traffic loading, as well as summer heat and heavy rain.

Past studies suggested the existence of moisture leads to stripping in asphalt mixture during service (see Figure 1.3). This leads to the loss of adhesion related to aggregate – binder interface, resulting the premature failure of asphalt mixtures. In general, moisture damage causes the loss of adhesion and cohesion among aggregate and binder in asphalt mixtures. This means that adhesion between aggregate and binder leads to stripping whilst cohesion results in the loss of stiffness in the mixture. In case of hot mix asphalt (HMA), the loss of adhesion should carefully be considered because virgin aggregates and binders are attached during service life. In order to overcome such difficulties, a various types of laboratory test methods focused on moister sensitivity were developed and studies through past research. Although those asphalt mixtures are assessed enough in the experiments, stripping is still caused due to insufficient test condition, compared with field. Past study suggested that the reason for this poor correlation is caused by the lack of theoretical recognition for moister damage and modification of test method for moister susceptibility. Therefore, a number of studies have been carried out, especially looking at the three topics: air continuous void, moisture transportation and physical properties for adhesion between aggregates and binder.

In terms of preservation of natural resource, the use of Reclaimed Asphalt Pavement (RAP) has been widely used in practice as the amount of RAP mixture production has been risen in past ten years (National Asphalt Pavement Association 2017). In addition, the repeated recycling with high RAP contents are also conducted in practice. In such social environment, many studies conducted the durability assessment of RAP mixtures under moister condition or oxidation aging

(Karlsson & Isacsson 2006, Mogawer *et al*. 2012, Tarbox *et al*. 2012, Tran *et al*. 2012, Yin *et al*. 2017). Past study suggested that RAP mixture is advantageous for moister sensitivity because of strong bonding between aged binder and aggregates, compared with that of virgin HMA (Shu *et al*. 2012, Zhao *et al*. 2012). This results in entire strength for moister susceptibility. However, few research efforts have been conducted for high RAP mixture with combined aging (i.e. moister, oxidation and heat). In particular, the use of rejuvenator agent related to aging is not understood for RAP mixtures, although many research efforts have been made for rejuvenated RAP binder. In other words, moisture and aging damage mechanism of RAP mixture with rejuvenator are not studied correlated to combined aging conditions. Therefore, the combined aging properties of RAP mixtures should be studied related to the use of rejuvenator, if the durability of RAP mixture is carefully assessed, in terms of field application.

Figure 1.3 Stripping of pavement surface an airport runway
http://www.jice.or.jp/award/detail/47

1.1.3 Global warming for WMA mixture

In terms of reduction in carbon dioxide (CO_2) and preservation of natural resource, the use of warm-mix asphalt (WMA) mixture and Reclaimed Asphalt Pavement (RAP) has been widely used in practice as the amount of RAP mixture production has been risen (see Figure 1.4). Inevitably, these two technologies are combined and applied on site. However, few research efforts have been conducted for WMA and high RAP mixture with combined aging (i.e. moister, oxidation and heat). Past studies demonstrated that WMA mixture with wax additive was better than HMA mixture, in terms of fatigue performance (Hearon *et al*. 2008, Haggag *et al*. 2011, Silva *et al*. 2010, Yang *et al*. 2009). Meanwhile, drawback of WMA additive technology is reduction in stripping resistance under wet condition although the additive technology shows improvement in wettability, resulting in better adhesion between binder and aggregates (Arabani *et al*. 2011). In terms of RAP mixture with WMA, there are some concerns about blending between RA and virgin binders because lower production temperature (i.e 130°C) was expected rather than conventional temperature (i.e. 160°C or more) (Hamzah *et al*. 2010, Jamshidi *et al*. 2012).

However, recent increase in RAP ratio faces the utilization of rejuvenator. Despite the fact that many research studies were conducted for WMA and RAP mixtures, its combination with rejuvenator was not examined in detail. In addition, the influence of combined aging on RAP-WMA mixture with rejuvenator and those damage mechanism were not studied past. Therefore, these assessments with due consideration for recent issue such as moisture are required especially focusing on stiffness, fatigue and combined aging.

(a)  (b) 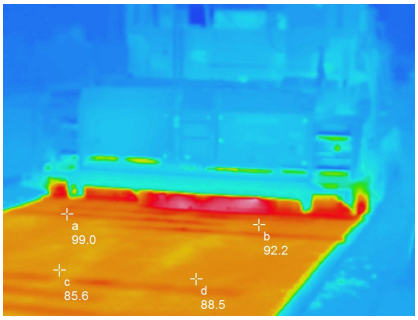

Figure 1.4 Asphalt laying work with WMA mixture
(a) Photographic image, (b) Thermographic image

1.2 SCOPE OF THE RESEARCH

This thesis consists of seven parts. In Chapter 2, a literature review related to the durability of Reclaimed Asphalt Pavement (RAP), Warm-Mix Asphalt (WMA) and RAP-WMA mixtures will be presented. Firstly, the durability of RAP mixtures with rejuvenator will be examined and explained. Secondly, the durability of WMA mixture will be described through past studies. Thirdly, RAP-WMA mixture with rejuvenator will be demonstrated based on previous research related to durability assessments.

The research methodology for this project will be presented in Chapter 3. In this chapter, the preparation works for the experiment part, such as gradation curve, mixture and binder testing methods used in this study are highlighted. The Nottingham Asphalt Tester (NAT) is used to perform the Indirect Tensile Stiffness Modulus (ITSM) and Indirect Tensile Fatigue Test (ITFT) to compare Hot-Mix Asphalt (HMA), RAP mixture, WMA mixture and RAP-WMA mixtures in terms of aging and moisture as a function of RAP ratio. The influence of rejuvenator related to mechanical properties is also analysed using laboratory specimens (i.e. 100 mm diameter specimens). Furthermore, test method for dynamic shear rheometer (DSR) will be described to conduct dynamic mechanical analysis for binders used in this study. In addition, testing methods of aging and moisture using saturation aging tensile stiffness (SATS) test will be highlighted in this chapter. Finally, the research methodology for this project will be presented.

Results of mechanical testing for HMA mixture and RAP mixture with rejuvenator will be discussed in Chapter 4. The Nottingham Asphalt Tester (NAT) is used to perform the Indirect Tensile Stiffness Modulus (ITSM) tests and Indirect Tensile Fatigue Test (ITFT) with and without SATS conditioning. In this chapter, relationship between retained tensile stiffness ratio and retained saturation will be indicated using HMA and RAP mixtures. In addition, these results are discussed with stripping results of the mixtures. Furthermore, extracted binder from specimens will also be analysed using DSR tests.

In terms of warm-mix asphalt (WMA) mixture, the durability of RAP mixture with

rejuvenator will be examined in Chapter 5. The same assessment as HMA mixture and RAP mixture with rejuvenator will be conducted in this chapter. In terms of binder, the influence of wax additive will be examined related to DSR tests.

Chapter 6 will concentrate on the durability assessment based on rheological property of extracted binders. In this chapter, the two types of rejuvenators will be compared to assess the combined aging effects of HMA mixture, RAP mixture, WMA mixture and RAP-WMA mixtures. In addition, the rheological characteristics of extracted binders with and without the conditioning will also be evaluated through Dynamic Shear Rheometer (DSR). Furthermore, inner and outer layers of bitumen coats are extracted from compacted specimens through staged-extraction process. These results will be analyzed in relation to the deterioration mechanism of the four mixture in this study.

Finally, Chapter 7 will provide a summary of the main findings and conclusions from the study and recommendations for further research.

CHAPTER 2

Literature Review

2.1 INTRODUCTION

Many studies related to the durability assessments for high RAP mixture have been carried out over the years. This literature review provides information on durability assessment on RAP mixture with rejuvenator, warm-mix asphalt and RAP-WMA mixture with rejuvenator through various types of mechanical testing. The chapter is divided into the following sections:

- Durability of RAP mixture with Rejuvenator
- Durability of Warm-Mix Asphalt
- Durability of RAP-WMA mixture

2.2 DURABILITY OF RAP MIXTURE WITH REJUVENATOR

A number of studies for RAP mixture with rejuvenator were conducted, related to durability, especially in aging and moisture. Zhang *et al*. (2021) examines three types of asphalt mixtures (i.e. new asphalt mixture, 40% RAP mixture and 60% RAP mixture with rejuvenator). They described from the Hamburg Wheel Tracking (HWT) test results that their RAP mixture with rejuvenator demonstrated better performance than that of new asphalt if the amount of rejuvenator were increased (see Figure 2.1). These trends were found in rutting, stiffness and fatigue test results in their experiments.

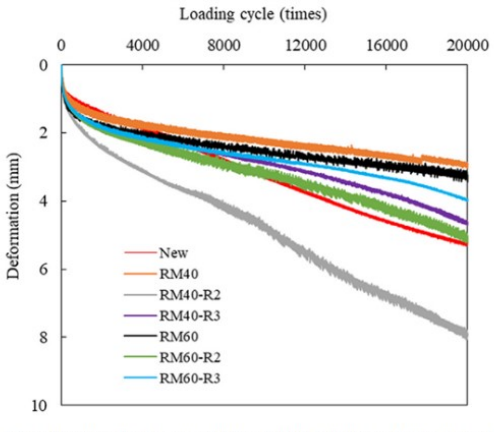

(a)

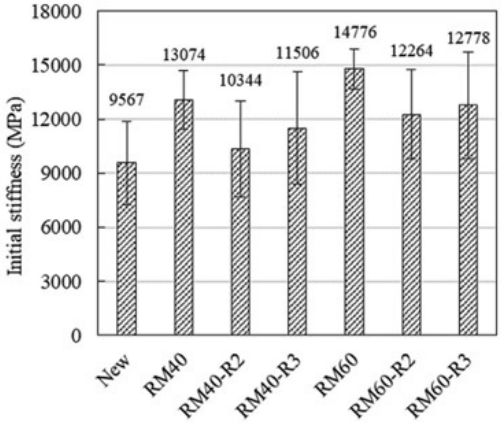

(b)

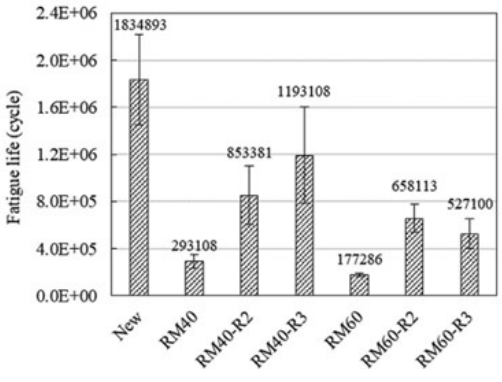

(c)

Figure 2.1 Hamburg Wheel Tracking (HWT) test results of RAP mixture with rejuvenator (Zhan *et al*. 2021) (a) Permanent deformation, (b) Stiffness results, (c) Fatigue results

Meanwhile, the HWT test in Mogawer *et al*. (2013) showed that the rejuvenators rose the rutting and moisture susceptibility of 40% RAP mixture. However, they also demonstrated that there were no significant differences with and without rejuvenator, in terms of fatigue properties. Similarly, Mirhosseini *et al*. (2019) demonstrated that the Tensile Strength Ratio (TSR) values for recycled asphalt mixtures with 20 to 40% RAP with and without rejuvenators decreased with the increase in the RAP content (see Figure 2.2). They suggest that other methods should be found if RAP contents will be increased more than 40%. They also demonstrated fatigue test results with rejuvenators. They concluded that fatigue life was improved when rejuvenator was added to RAP mixtures. Furthermore, Pradhan & Sahoo (2022) demonstrated that for 30 and 40% RAP mixtures, the TSR values were slightly increased (see Figure 2.3). However the TSR should be reduced if the RAP contents will be increased from 40%. Considering the past studies, there seems no universal findings about RAP mixture with rejuvenator. Thus, the effect of RAP contents and other factors on the moisture durability of RAP mixture with rejuvenators is still unclear.

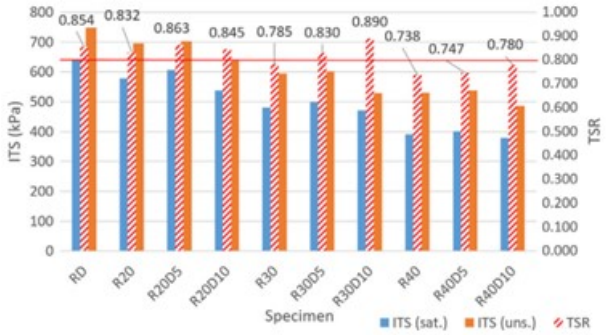

(a)

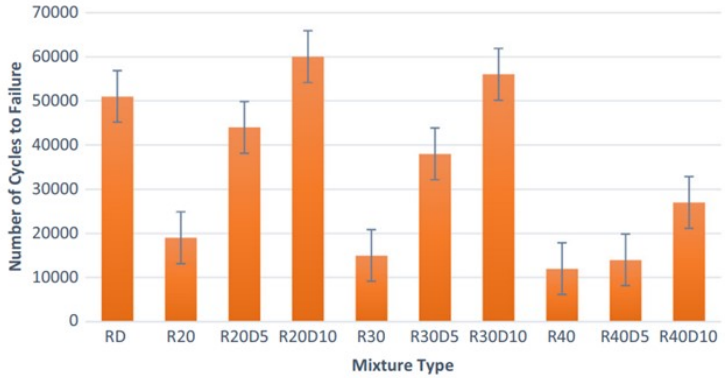

(b)

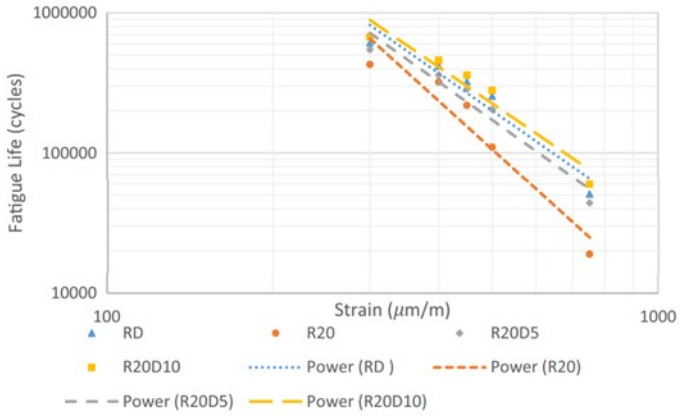

(c)

Figure 2.2 Performance evaluation of RAP mixture with rejuvenator (Mirhosseini *et al*. 2019) (a) Moisture susceptibility, (b) Beam bending tests, (c) Fatigue results

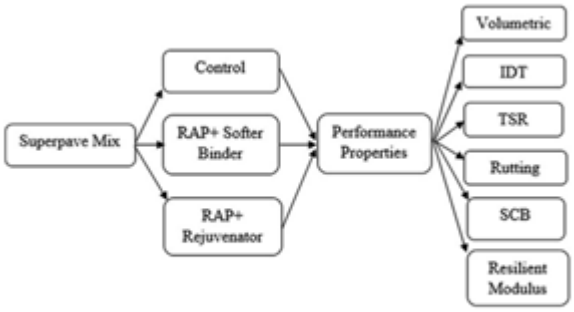

(a)

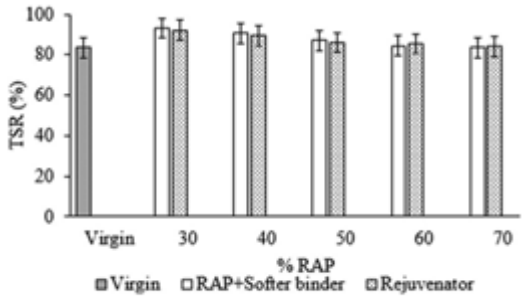

(b)

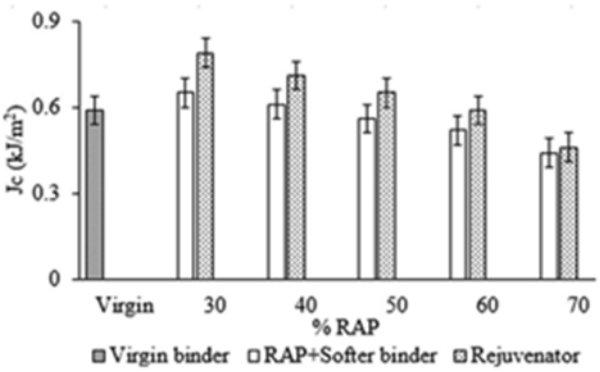

(c)

Figure 2.3 Performance evaluation of RAP mixture with rejuvenator (Pradhan & Sahoo 2022) (a) Experimental plan, (b) Tensile strength ratio results, (c) Semi-circular bending test results

Regarding the effect of aging on durability, Ziari *et al*. (2019) investigated the effect of rejuvenators on the aging resistance of recycled asphalt mixtures (see Figures 2.4 and 2.5). They concluded that RAP mixture with rejuvenator will be affected by moisture sensitivity. This effect was more sever if aging condition was subjected to the RAP mixture. In addition, the effect of aging was more pronounced for the fatigue behavior of RAP mixture with rejuvenator. The fatigue performance of the RAP mixture with rejuvenator was decreased, compared with conventional mixture. Meanwhile, Mogawer *et al*. (2015) indicated that no significant effects were found for RAP mixture with and without rejuvenator after long-term aging, in terms of fatigue properties. Thereby, there seems no universal agreement about the effect of aging on the fatigue behaviour of RAP mixture with rejuvenator.

(a)

Rejuvenator property	Cyclogen	Rapiol	WCO
Base	Oil	Oil	Organic
Physical state at room temperature	Liquid	Liquid	Liquid
Color	Black	Yellow	Yellow
Odor	No	No	No
Water solubility	No	No	No
Viscosity at 135 °C (s)	10	13	30
Flash point (°C)	218	255	320
Specific gravity (g/cm^3)	0.973	1.091	0.981

(b)

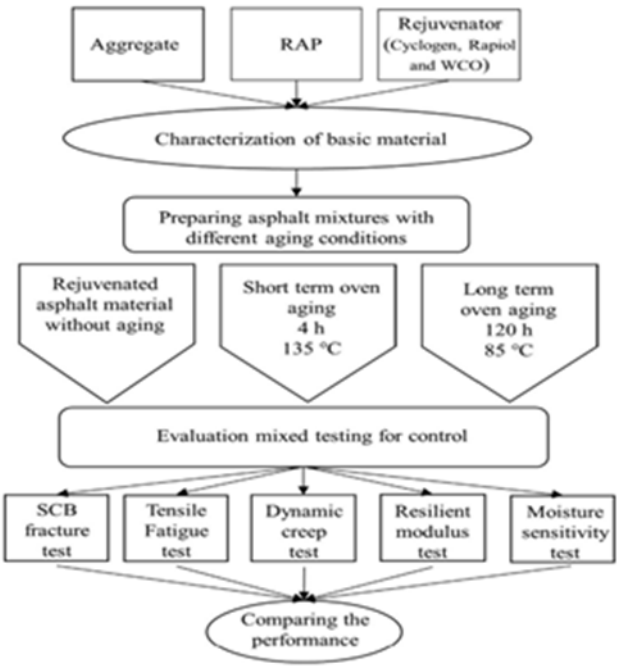

Figure 2.4 Effect of RAP mixture with rejuvenator (Ziari *et al*. 2019) (a) Rejuvenator types, (b) Experimental plan

(a)

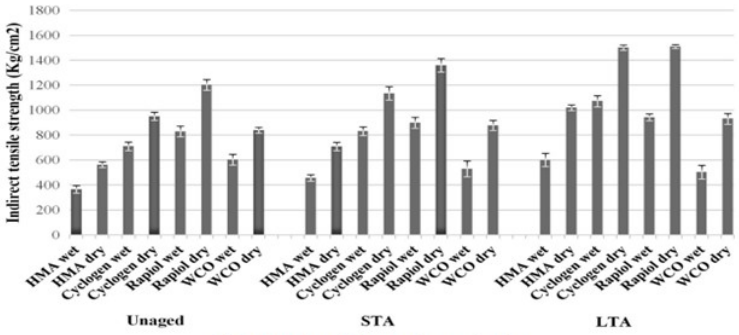

Fig. 5. Dry and wet indirect tensile strength values.

(b)

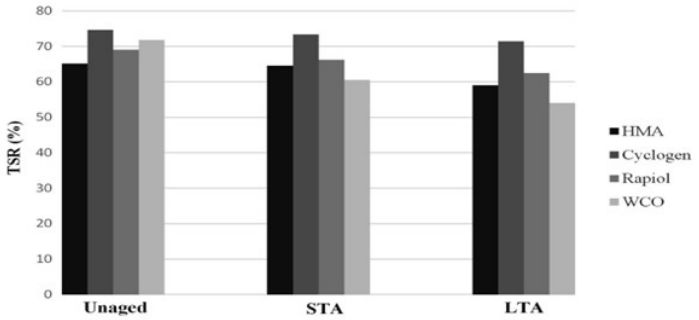

Fig. 6. The TSR values.

(c)

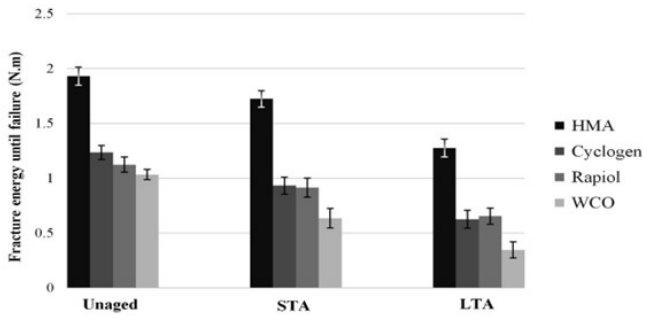

Fig. 8. The fracture energy until the peak load of the specimens with crack length of 25 mm.

(d)

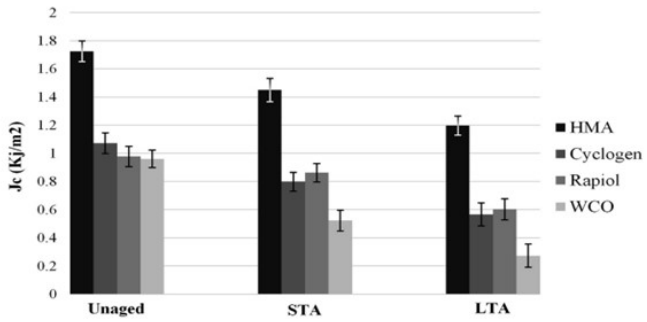

Fig. 9. The critical values of J integral.

Figure 2.5 Evaluation of RAP mixture with rejuvenator after laboratory tests (Ziari *et al*. 2019) (a) Indirect tensile strength test results, (b) Tensile strength ratio results, (c) Fracture energy in semi-circular bending test, (d) Critical value in semi-circular bending test

2.3 DURABILITY OF WMA MIXTURE

Warm-mix asphalt (WMA) mixture with reclaimed asphalt pavement (RAP) have been widely applied in practice, which has contributed to reduction in carbon dioxide (CO_2) and preservation of natural resource both in production and paving work. WMA technology can save energy and prevent bitumen from aging at asphalt mixture production. One of effective measures in the WMA technology is binder modification using wax. Binder viscosity will be significantly decreased by the effect of the modification, resulting in the reduction in the temperatures of asphalt mixtures at the production and the layering. In particular, Fisher-Tropsch (FT) wax, which is a production during oil refinery can reduce binder viscosity at temperatures for the production and the paving, while it increases the viscosity at in-service temperatures due to wax crystallization (see Figure 2.6, Simonofske *et al*. 2016).

Hureley and Prowell (2005) evaluated utilization of WMA mixture using FT wax (i.e. Sasobit®) (see Figure 2.7). It was found from their results that the wax did not influence on resilient modulus and rutting resistance of asphalt mixture. However, they implied that the reduction in the production temperatures might be related to moisture damage of WMA mixture. Kantipong *et al*. (2012) investigated moisture sensitivity of wax-based WMA, changing types of gradation and aggregate. They concluded that wax-based WMA has higher permanent deformation resistance than HMA mixture although WMA showed high in moister sensitivity compared with HMA. Sobhi *et al*. (2020) stated that wax additive improved workability and stiffness of WMA mixture although its moisture sensitivity was deteriorated. Similar findings were also suggested from past studies (Wassluddin *et al*. 2008, Kantipong *et al*. 2012, Ghabchi *et al*. 2013). Wassluddin *et al*. (2008) examined moisture sensitivity of wax-based WMA looking at aggregates used in WMA mixtures. They showed that adhesion between aggregates and binder were decreased due to the wax additive, resulting the reduction in lower moisture resistance although its wettability to aggregates were improved. Jamshidi *et al*. (2013) suggested from their literature review that wax additive might also cause reduction in cohesion amongst binder-filler mastics, as well as adhesion between aggregates and binder.

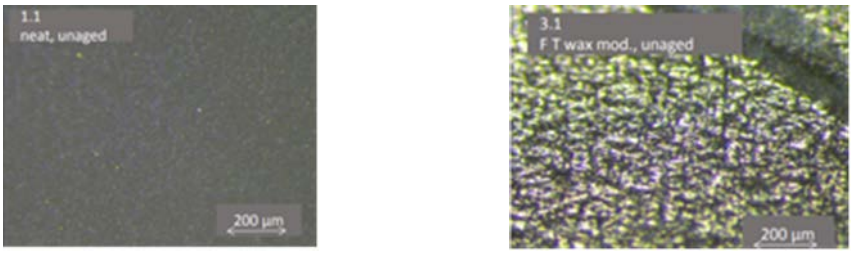

(a) (b)

Figure 2.6 Stereo scope results (Simnofske *et al*. 2016) (a) conventional asphalt binder, (b) Wax-modified asphalt binder

(a) (b)

Figure 2.7 An example of F-T wax (i.e. Sasobit®) (Hureley and Prowell, 2005) (a) Flakes, (b) Particles

2.4 DURABILITY OF RAP-WMA MIXTURE

So far, many research efforts have been made for RAP-WMA mixtures using wax additives. Yousef *et al*. (2021) demonstrated the effect of WMA additive including wax, related to RAP aggregates (see Figure 2.8). They indicated that wax modified RAP -WMA mixture showed similar results to that of HMA in terms of moisture sensitivity. Ameri *et al*. (2020) also studied the performance of RAP-WMA mixture using WMA additive (see Figure 2.9). They suggested that WMA additives improved moisture sensitivity of RAP-WMA mixtures. In particular, wax additive enhanced rutting and fatigue performance, as well as moisture sensitivity. In addition, Goli and Latifi (2020) also studied moisture sensitivity of RAP-WMA mixture using wax additive, and they concluded that RAP-WMA mixture modified by a wax additive improved moisture sensitivity, stiffness and fatigue resistance, compared to WMA mixture.

In terms of moisture sensitivity of RAP-WMA mixtures with rejuvenators, many efforts were made through past studies. For example, Hamburg wheel tracking (HWT) test results in a previous study showed that RAP-WMA with rejuvenators might contribute to permanent deformation and moisture sensitivity (Solaimanian *et al*. 2003). In addition, the tensile strength ratio (TSR) conducted to evaluate moisture susceptibility supported that the use of RAP and rejuvenator might increase the moisture damage of the mixtures with an increase in the RAP contents (Shu *et al*. 2012, Song *et al*. 2018, Rahman *et al*. 2021). These test results were performed in limited moister conditioning such as heat and water. However, on-site pavement surface would experience complex aging conditions such as heat, oxidation and moisture. Therefore, the combination amongst these conditions needs to be considered through laboratory experiments.

Regarding the influence of high temperature on RAP-WMA mixture with rejuvenator, Nahar *et al*. (2014) showed that the use of rejuvenator restores chemical composition of aged binder, and this results in improvement of mixture performance during high temperature. Meanwhile, Farooq *et al*. (2018) indicated that the increase use of rejuvenator leads to poor performance of RAP-WMA mixture such as Marshall stability and rutting. Lu *et al*. (2019) also supports this

result. Furthermore, micro-scale analysis related to these results were not discussed in detail through the previous studies. Thereby, the influence of high temperature on RAP-WMA mixture with rejuvenator is still unclear.

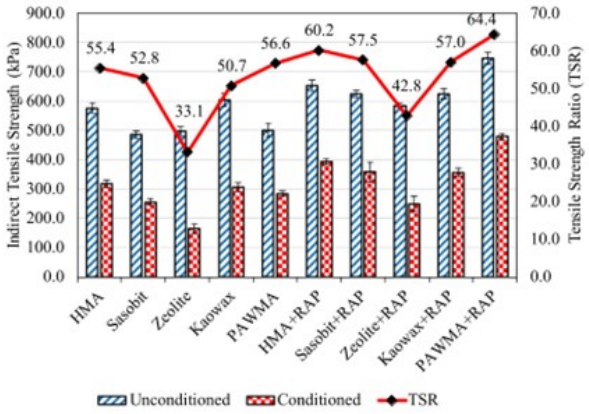

Figure 2.8 Indirect tensile strength and tensile strength ratio results (Yousef *et al*. 2021)

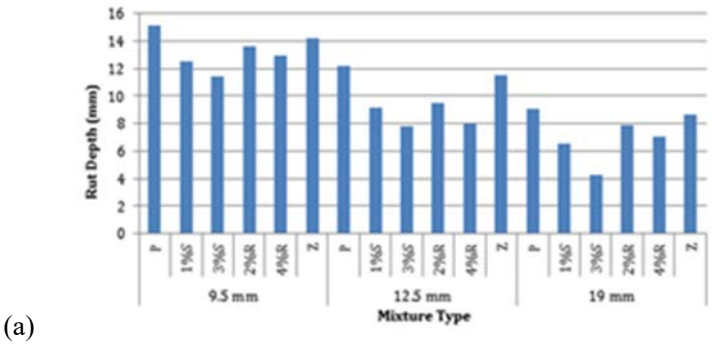

(a)

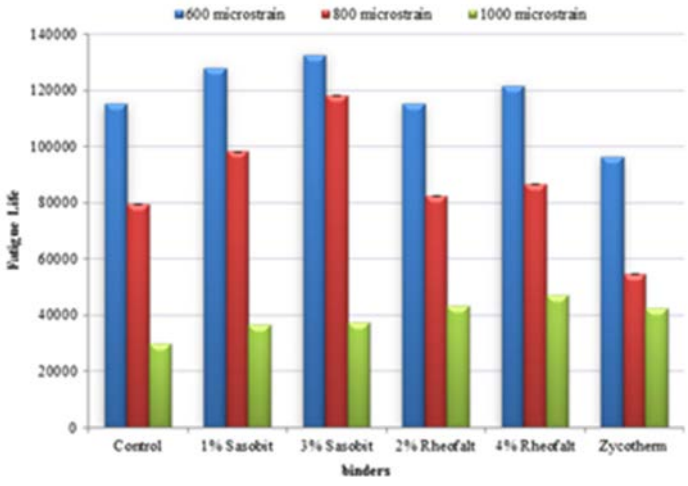

(b)

Figure 2.9 Laboratory evaluation of RAP-warm-mix asphalt (WMA) mixtures (Ameri *et al*. 2020) (a) Rutting test results, (b) Fatigue test results

2.5 DURABILITY ASSESSMENT OF ASPHALT MIXTURE

Past studies suggested the existence of moisture leads to stripping in asphalt mixture during service. This leads to the loss of adhesion related to aggregate – binder interface, resulting the premature failure of asphalt mixtures (Terrel, R.L. and Shute, J. W. 1989, Kandhal, P.S. 1994, Kennedy, T. W, 1985, Terrel, R. L. and Al-Swailmi, S. 1994). In general, moisture damage causes the loss of adhesion and cohesion among aggregate and binder in asphalt mixtures. This means that adhesion between aggregate and binder leads to stripping whilst cohesion results in the loss of stiffness in the mixture (Airey and Choi 2002). In case of hot mix asphalt (HMA), the loss of adhesion should carefully be considered because virgin aggregates and binders are attached during service life. In order to overcome such difficulties, a various types of laboratory test methods focused on moister sensitivity were developed and studies through past research (Lottman 1982, Terrel and Al-Swailmi 1993, Aschenbrener *et al*. 1995, Airey and Choi 2002, Solaimanian *et al*. 2003). Although those asphalt mixtures are assessed enough in the experiments, stripping is still caused due to insufficient test condition, compared with field. Past study suggested that the reason for this poor correlation is caused by the lack of theoretical recognition for moister damage and modification of test method for moister susceptibility (Caro et al, 2008). Therefore, a number of studies have been carried out, especially looking at the three topics: air continuous void, moisture transportation and physical properties for adhesion between aggregates and binder (Masad *et al*. 2006c, 2007, Krishnan and Rao 2001, Chen *et al*. 2004, Kassen *et al*. 2006, Masad *et al*. 2006a, Little and Jones 2003, Hefer *et al*. 2005, Song *et al*. 2005, Bhasin *et al*. 2006a, 2006b, Copeland *et al*. 2006, Masad *et al*. 2006b). However, previous studies looking at RAP and RAP-WMA mixtures with rejuvenator were not examined, especially in rheological assessments related to mixture properties. Therefore, the durability assessment of high RAP mixtures with rejuvenator should be examined with HMA and WMA mixtures.

2.6 RESEARCH PURPOSE

Although many studies were implemented for HMA, RAP, WMA and RAP-WMA mixtures, few research efforts have been conducted with combined aging (i.e. moister, oxidation and heat). In addition, although the mechanical properties of RAAP and RAP-WMA mixtures were examined in the past studies, rheological properties related to WMA additive and rejuvenator were not conducted. Furthermore, the durability assessment of RAP and RAP-WMA mixtures related to the mechanism for moisture sensitivity were inconclusive. Thereby, there seems no universal agreement about the effect of aging and moisture on the mechanical properties of high RAP contents (i.e. RAP ratio more than 30%) with rejuvenator, in terms of HMA and WMA mixtures. Therefore, these assessments with due consideration for recent issue such as aging and moisture are required, especially focusing on stiffness, fatigue and combined aging.

In terms of practical consideration, the adjustment of penetration grade to the target grade is major method when rejuvenator is used to recover binder property to the original level, especially for high RAP mixture. Although penetration grade is major factor for the mixture design of RAP and RAP-WMA mixtures, there should be the effects of RAP ratio, rejuvenator types, wax etc. on the durability of the mixtures.

In order to examine these influences, the aim of this research is to examine the durability of high RAP mixture with rejuvenator using Saturation Aging Tensile Stiffness (SATS) conditioning. In particular, the focus of this study are:

- To investigate the effect of RAP ratio (RAP ratio: 30% and 60%) with and without SATS conditioning,
- To examine the differences of rejuvenators (Rejuvenator 1 and 2) on the mechanical properties of RAP mixtures and binders, and
- To study the influence of WMA additive (i.e. wax) to RAP mixtures and

binders.

Finally, this study clarify the mechanism of the difference in the durability induced by above mentioned factors, based on the findings through experiments.

CHAPTER 3

Research Methodology

3.1 INTRODUCTION

In order to assess the durability of high RAP mixtures, a series of laboratory experiments need to conduct in this research. In addition, since RAP aggregates (i.e. aged aggregate) are obtained and recovered through asphalt plants and rejuvenators respectively, the mechanical properties of RAP mixtures might be complex, in terms of both mixture and binder aspects. Therefore, both mixture and binder tests need to analyse through laboratory experiments. Furthermore, research methodology should be established, based on material test methods. Therefore, the properties of material and mechanical test method should be reviewed before undertaking experiments. The aim of this chapter is to describe the four factors: Reclaimed Asphalt Pavement (RAP) and rejuvenator, Warm-Mix Asphalt (WMA), mechanical tests, and research methodology.

- Reclaimed Asphalt Pavement (RAP) and rejuvenators,
- Warm-Mix Asphalt (WMA)
- Mechanical tests
- Research methodology

3.2 RECLAIMED ASPHALT PAVEMENT (RAP)

Dense Asphalt Mixture was used in this study. The nominal aggregate size was 13

mm and three levels of RAP content were examined to evaluate the mixture: RAP 0% (i.e. virgin mixture), RAP 30% and RAP 60%. In terms of reclaimed asphalt pavement, RAP aggregates were obtained from an asphalt plant (see Figure 3.1 (a)). As shown in Figure 3.1 (b), the composition of bitumen is divided into to four components (i.e. Saturates, Aromatics, Resins, Asphaltenes, SARA). However, these compositions are changed as bitumen is aged during service in pavement. Therefore, the application of rejuvenator has to be considered looking SARA components.

For the virgin mixture, the Marshall method was applied for the mixture design. For the RAP mixture, the Japan Road Association specifications were followed (see Figure 3.2). Under this method, aged asphalt was extracted from RAP aggregate. The amount of rejuvenator was determined based on penetration and indirect tensile tests. After that, the virgin binder needed for the RAP mixture was determined. These production procedure is depicted in Figure 3.2.

(a)

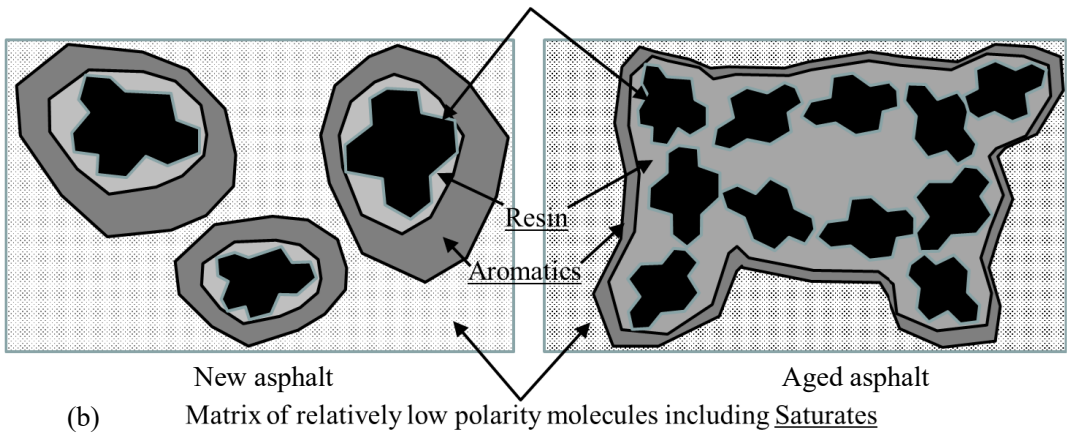

(b)

Figure 3.1 RAP aggregates and aged binder (a)Aged aggregates stored in a plant, (b) chemical composition of new asphalt and aged asphalt (after, Little, Allen, Bhasin, 2018)

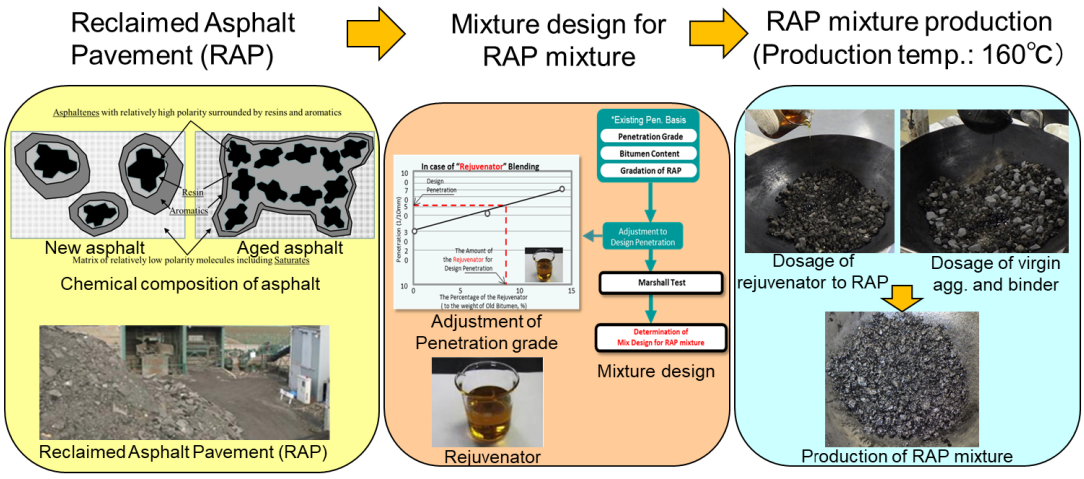

(a)

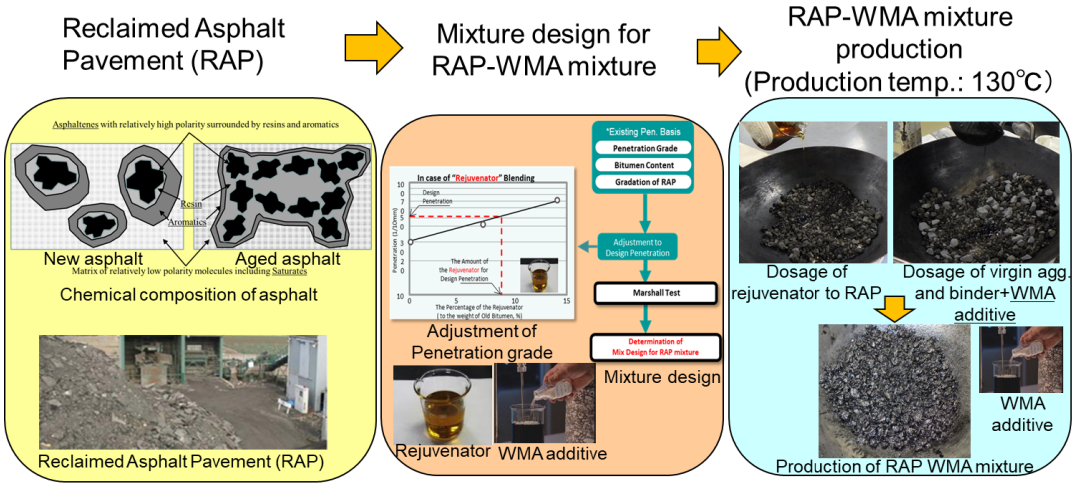

WMA additive: Venkatachalam *et al*. 2015

(b)

Figure 3.2 Production flow (a) Reclaimed Asphalt Pavement (RAP) mixture, (b) RAP-Warm-Mix Asphalt (WMA) mixture

3.2.1 Binder characteristics

In this research, four types of asphalt mixtures were studied experimentally: hot-mixed asphalt (HMA) mixture, reclaimed asphalt pavement (RAP) mixture, warm-mix asphalt (WMA) mixture and RAP-WMA mixture. For the conventional mixture, straight run asphalt 60/80 pen bitumen was used as binder. In the case of the reclaimed asphalt mixture, 30% and 60% RA mixtures were selected in this study. Here, the penetration grade of RA binders was restored using rejuvenators, and blended with fresh binder (see Table 3.1). The penetration grade was designed to be 70 pen grade. The blending protocol was as per the criteria of the Japan Road Association (2010).

Table 3.1 Binder characteristics

	Penetration at 25C (1/10 mm)	Softening Point (C)	Viscosity at 120C (mPa·s)
Virgin 60/80	63	48.5	835.6
Extracted RAP binder	12	80.5	21300

3.3 REJUVENATOR (Oil Based)

As described in the previous section, four types of asphalt mixtures were studied experimentally: HMA mixture, RAP mixture, WMA mixture and RAP-WMA mixture. For the HMA mixture, straight run asphalt 60/80 pen bitumen was used as binder. In the case of the reclaimed asphalt mixture, 30% and 60% RA mixtures were selected in this study.

In terms of RAP mixture, firstly old asphalts were extracted from RAP aggregated, then the extracted binder was recovered through rejuvenator. In this process, the penetration grade of the extracted binder was adjusted to the target penetration grade, 70 pen in this research. By changing the rejuvenator amount, optimum rejuvenator amount was decided. In this research, oil-based rejuvenator was used and added to recover the aged binder (see Figure 3.3).

After deciding the amount of rejuvenator, the Marshall design method were carried out to decide optimum asphalt amount for HMA and RAP mixtures. This design procedure was followed through Japan Road Association methods in this research.

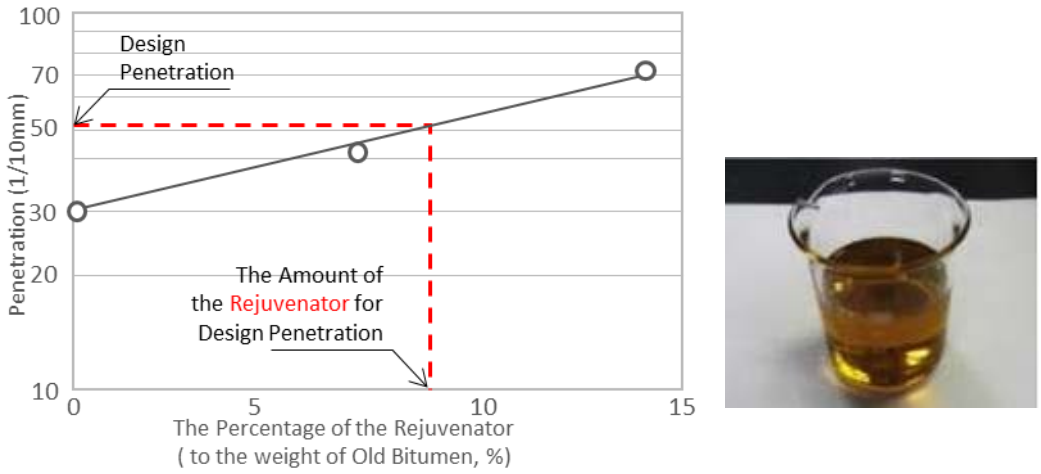

Figure 3.3 Process of optimum rejuvenator amount

3.4 WARM-MIX ADDITIVE

Recently, there has been growing awareness that the use of warm-mix asphalt technology is a highly effective way of reducing the production temperature in asphalt pavements (Huschek 1994, Gabrera & Zoorab 1994, 1996). This technology has been applied to several types of pavements such as dense-graded asphalt and reclaimed asphalt pavements. However, despite the fact that the production volume of recycled asphalt mixtures has been rapidly increasing in order to preserve natural resources, there has been insufficient research into the application of WMA technology to RAP mixtures. Therefore, more research into WMA with RAP is needed. Accordingly, a series of experiments examining the mixture performance were conducted, based on a wax based WMA technology. This research describes Warm-mix Asphalt technology using a wax additive, and the research examines the combination of a RAP mixture with rejuvenator.

In terms of warm-mix asphalt, a wax additive called "Sasobit®" was used as the additive agent (see Figure 3.4). Sasobit® is a synthetic material using Fisher-Tropsch wax. It increases the durability of the asphalt mixture as well as reducing its production temperature. Since it is widely used in practice, the additive was blended with fresh binders (i.e. virgin binder) when the specimens were manufactured. The dosage amount of wax additive was 3% of total binder (i.e both virgin and aged binders) in this research.

Figure 3.4 Sasobit® wax

3.5 MIXTURE GRADATION

In this study, the aggregate gradation used was continuous grading and dense asphalt mixtures (AC13) produced in the laboratory. For the RAP mixture, RA content of 30% and 60% were selected to assess the characteristics of the RAP mixture, and those RAP aggregates were blended with fresh aggregate, adjusted as much as possible to AC 13 mixture limits (see Figure 3.5). The design penetration was set at 70 pen grade using both fresh binder and rejuvenator. As for the warm-mix asphalt, 3% of the additive (i.e. Sasobit®) was added to the binder, then it was mixed with conventional and reclaimed asphalt mixture at 130°C, respectively.

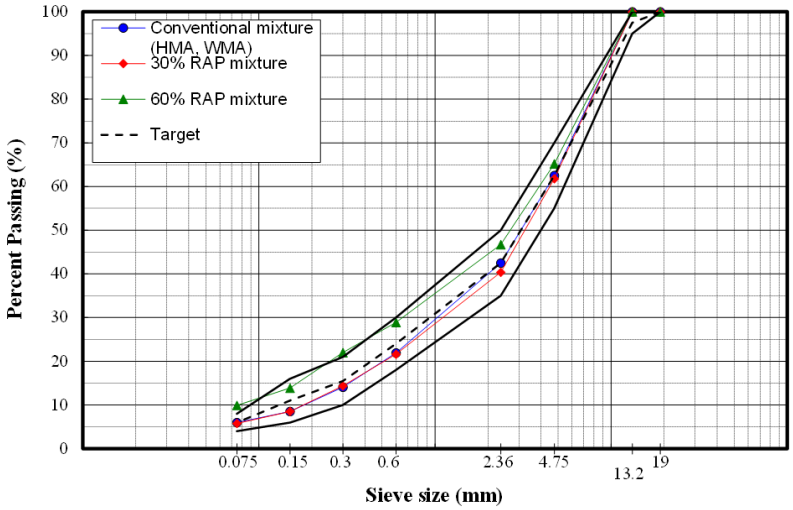

Figure 3.5 Gradation curve for AC 13 and RAP mixtures

3.6 MECHANICAL TESTING OF ASPHALT MIXTURES

3.6.1 Indirect Tensile Stiffness Modulus

The Indirect Tensile Stiffness Modulus (ITSM) test is used to determine the stiffness modulus of asphalt mixture specimens (Figure 3.6). The ITSM test is usually performed in accordance with British Standard BS 213 (1993). During the test a load pulse is applied along the vertical diameter of a cylindrical specimen and the resultant peak transient deformation measured along the horizontal diameter. The stiffness modulus is then calculated as a function of load, deformation, specimen dimensions and an assumed Poisson's ratio of 0.35.

During the ITSM test, five conditioning pulses are followed by five test pulses, which are averaged to obtain the stiffness modulus for that test. The test is then repeated after rotating the specimen through 90° and the mean stiffness from the two tests is recorded as the stiffness modulus of the asphalt mixture specimen.

- Horizontal deformation: 5 μm
- Rise time: 124 ms
- Specimen diameter: 100 mm
- Specimen height: 50 mm
- Test temperature: 20°C

By using these assumptions, the elastic stiffness of the asphalt mixture specimens was calculated. In order to determine elastic stiffness, the stress applied to the specimen was calculated using the following equation:

$$\sigma_{x\max} = \frac{2P}{\pi dt} \tag{3.1}$$

$$\sigma_{y\max} = -\frac{6P}{\pi dt} \tag{3.2}$$

where P = applied vertical force (N), d = diameter of the specimen (m), t = thickness of the specimen (m),

Also, the strain is derived from Hooke's law,

$$\varepsilon_{x\max} = \frac{\sigma_{\text{xmax}}}{S_{\text{m}}} - \frac{\upsilon\sigma_{y\max}}{S_{\text{m}}} \tag{3.3}$$

where $\upsilon =$ Poisson's ratio, S_{m} = stiffness modulus of the specimen (Pa), $\sigma_{x\max}$ = maximum horizontal tensile stress at the centre of the specimen (N/m^2), $\sigma_{y\max}$ = maximum vertical compressive stress at the centre of the specimen (N/m^2) and $\varepsilon_{x\max}$ = maximum initial horizontal tensile strain at the centre of specimen.

Alternatively, equation 3.3 can be derived using equations 3.1 and 3.2.

$$\varepsilon_{x\max} = \frac{2P}{\pi dtS_{\text{m}}} + \frac{\upsilon 6P}{\pi dtS_{\text{m}}} \tag{3.4}$$

Combining equations 3.1 and 3.4 gives,

$$\varepsilon_{x\max} = \frac{\sigma_{\text{xmax}}}{S_{\text{m}}}(1+3\upsilon) \tag{3.5}$$

Therefore, stiffness of asphalt mixture specimen is derived from following equation.

$$S_{\text{m}} = \frac{\sigma_{\text{xmax}}}{\varepsilon_{x\max}}(1+3\upsilon) \tag{3.6}$$

The target strain is given before testing. A compressive force is applied to the specimen taking into account the target strain. As the target strain is constant, the applied vertical force is also constant. Consequently, elastic stiffness is derived from the stress and strain relationship. The stress distribution of specimen is presented in Figure 3.6.

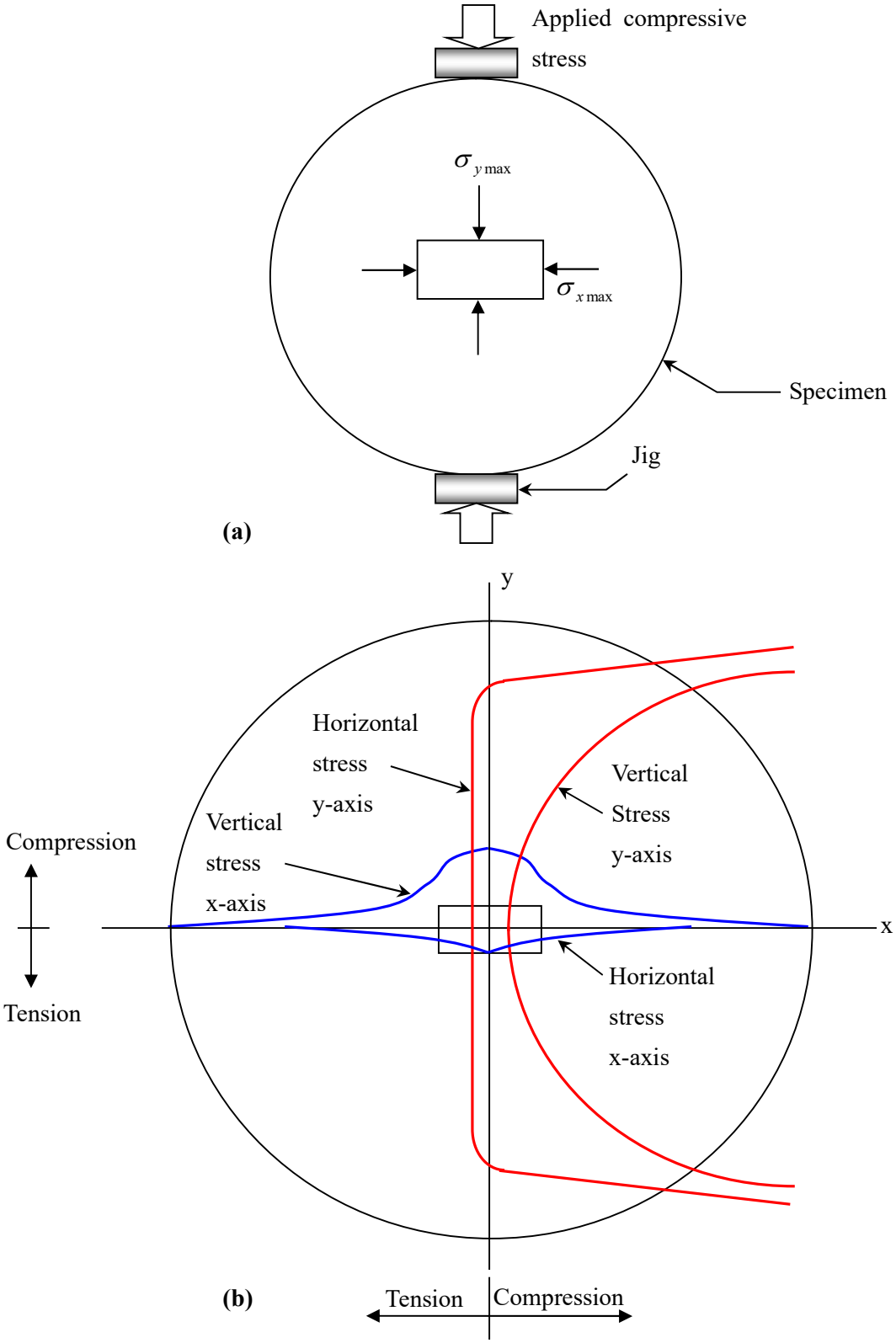

Figure 3.6 Stress distribution in the indirect tensile mode of test (after Read and Whiteoak 2003) (a) Testing state (b) Stress distribution

In case of the ITSM test, the stiffness modulus of specimen is calculated using following equation.

$$S_{\mathrm{m}} = \frac{P(c_5 - \upsilon c_6)}{\delta_{\mathrm{h}} t} \tag{3.7}$$

where S_{m} = Stiffness modulus, P = applied related load, ν = Poisson's ratio, δ_{h} = resilient total horizontal deformation, t = thickness of specimen, c_5 and c_6 = constants depending on specimen diameter and loading strip width.

In addition, schematic representation of the ITSM test is shown in Figure 3.7.

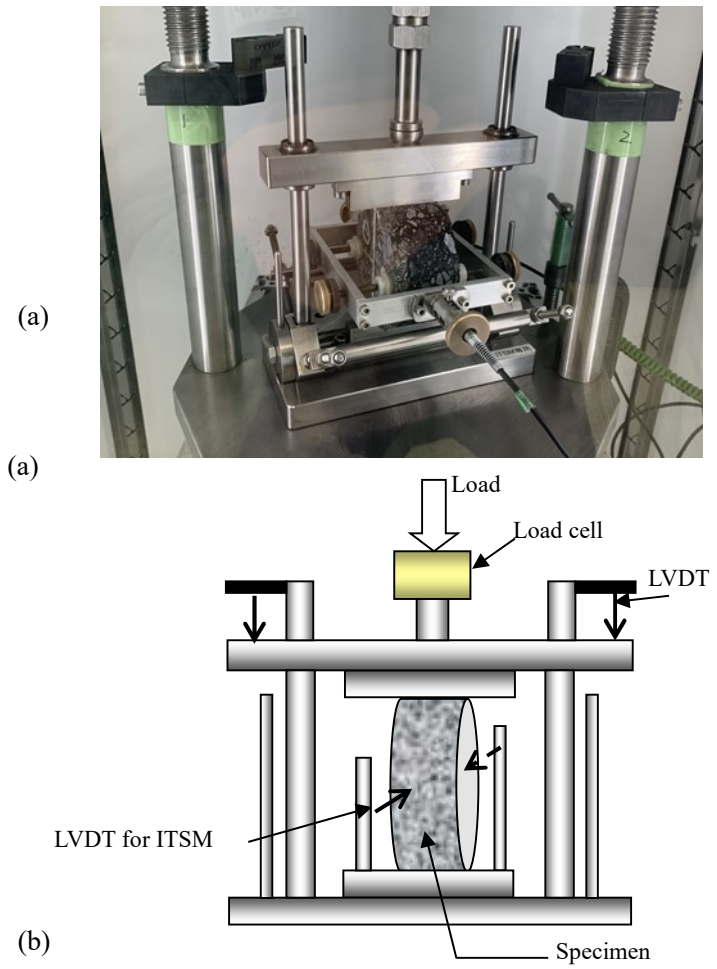

Figure 3.7 Indirect Tensile Stiffness Modulus (ITSM) test (a) Photographic image, (b) Schematic image

3.6.2 Indirect Tensile Fatigue Test

Fatigue properties of the asphalt mixture were assessed by the Indirect Tensile Fatigue Test (ITFT) in this research (see Figure 3.8). The test is performed under controlled stress conditions until vertical deformation indicated failure (BS EN 12697-24, 2012). The test was conducted as per BS EN12697-24 and the ITFT tests were carried out using the following test parameters:

- Test temperature: 20°C
- Loading condition: Controlled stress
- Loading rise time: 124 milliseconds
- Failure indication: 50% reduction from initial stiffness

Linear regression analysis of the ITFT results was conducted to determine the fatigue functions for the asphalt mixtures based on the following relationship:

$$N_f = a\,\varepsilon_0^{-b} \tag{3.8}$$

where N_f is the fatigue life, ε_0 is the initial tensile strain (microstrain) and a and b are experimentally determined coefficients.

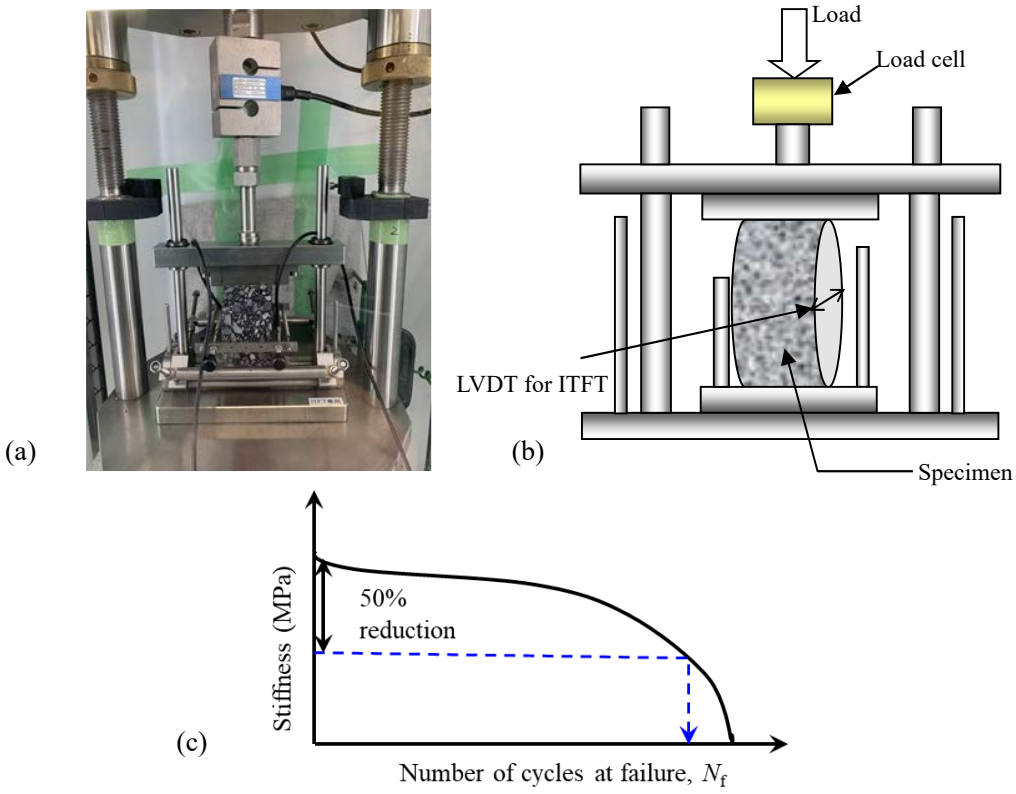

Figure 3.8 Indirect Tensile Fatigue Test (ITFT) (a) Photographic image, (b) Schematic image, (c) failure criteria

3.7 DYNAMIC SHEAR RHEOMETER (DSR)

A series of experiments for measuring the dynamic mechanical properties of binder were conducted using Dynamic Shear Rheometer (DSR) (see Figure 3.9). In this research, DSR tests were conduct for three types of assessments: stiffness, fatigue, and the relationship between complex shear modulus G^* and phase angle δ. In general, DSR is used to measure complex shear modulus G^* using bituminous specimens. In this tests, their complex modulus, G^*, and phase angle, δ were measures for frequencies of 0.1-10 Hz at eight temperatures (34°C, with 6°C increases). These results were also assessed through master curves of G^* and black diagram (i.e. relationship between G^* and δ).

To conduct experiments using bitumen, gap between parallel plates which is confining bitumen specimen, Gap between parallel plates must be kept at 2 mm for 8 mm plate and 1 mm for 25 mm plate. In terms of test types used in this research, master curve for each binder were mainly drawn from measurement results using 25 mm parallel plates with 1 mm gap. For binder fatigue tests, 8 mm parallel plates with 2 mm gap were applied. In addition, rheological assessment using G^* and phase angle were also carried out using 8 mm parallel plate with 2 mm gap. The results of these differences will be discussed in following chapters.

(a) 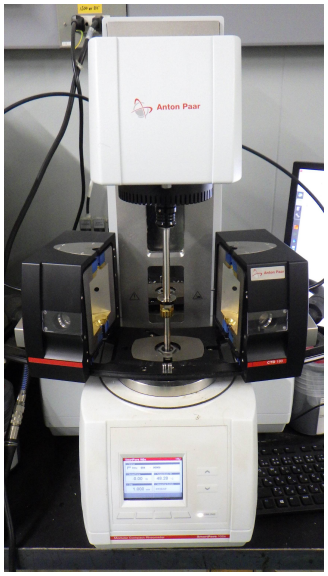

(b) 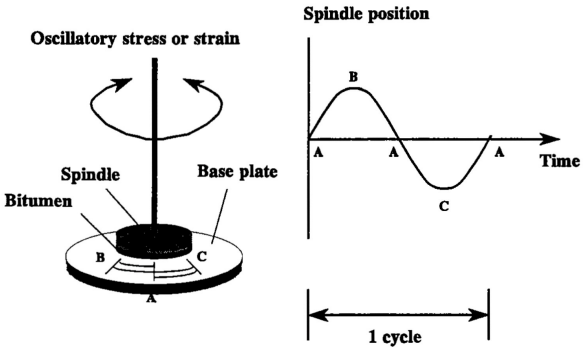

Figure 3.9 Dynamic Shear Rheometer (DSR) (a) picture, (b) Schematic image of DSR test (Airey 1997)

DSR test can be conducted with either stress-controlled or strain-controlled condition. For stress-controlled condition, target shear stress is applied to the bitumen specimen by giving torque force using the spindle, then the rotation of the spindle is measured and the applied shear stress is obtained through calculation. In case of strain-controlled condition, torque force is applied to reach target strain using the spindle and the applied shear stress is estimated through calculation (Airey 1997). Shear stress and strain applied to bitumen specimen are presented by following equations.

$$\tau = \frac{2T}{\pi r^3} \tag{3.9}$$

where τ is shear stress (Pa), T is torque (N.m), r is radius of parallel plates (m).

$$\gamma = \frac{\vartheta r}{h} \tag{3.10}$$

where γ is shear strain, ϑ is deflection angle, h is gap between two parallel plates (i.e. thickness of bitumen sample) (m).

Through the DSR test, complex shear modulus, G^*, is obtained through calculation. During the test, shear stress and strain are demonstrated as shown in Figure 3.10. In general, G^* is presented as a ration of shear stress to shear strain using following equation and figure (see Figure 3.10).

$$Complex\ shear\ modulus, G^* = \frac{Peak\ stress}{Peak\ strain} \tag{3.11}$$

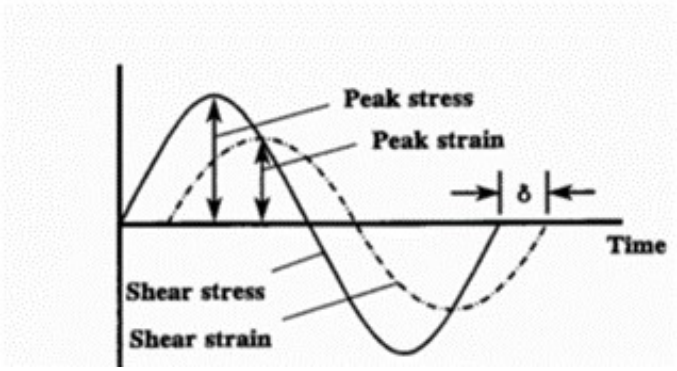

Figure 3.10 Definition of stiffness modulus in Dynamic Shear Rheometer (DSR) test (Airey 1997)

The complex shear modulus represents the resistance to deformation applied by torque force during DSR test. *G** is composed by storage modulus, *G*' which shows elastic behaviour, and loss modulus, *G*'' which demonstrates viscous behaviour (see Figure 3.11). This means that *G** is presented as vector of *G*' and *G*''. These two components are connected to *G** with phase angle, δ which indicates lag between peak stress and strain. The equation of these two components are as follows:

$$Strage\ modulus, G' = G^* cos\delta \tag{3.12}$$

$$Loss\ modulus, G'' = G^* sin\delta \tag{3.13}$$

This relationship is presented by the graph shown in Figure 3.11. This figure demonstrates the behaviour of bitumen during the test. The vertical axis shows viscous behaviour of bitumen while horizontal axis indicates its elastic behaviour. In this graph, phase angle, δ, is presented anti-clockwise meaning 0° is elastic behaviour and 90° is viscous behaviour. By presenting this relationship, the behaviour of bitumen can be graphically demonstrated.

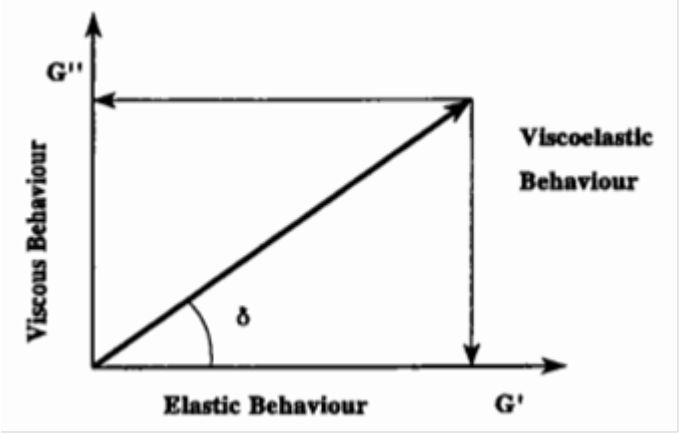

Figure 3.11 Behaviour of bitumen during Dynamic Shear Rheometer (DSR) test (Airey 1997)

3.8 SATS CONDITIONING PROCEDURE

In this research, the durability of the specimens were assessed using the Saturation Ageing Tensile Stiffness (SATS) conditioning (see Figure 3.12). This test was developed at the University of Nottingham and has been standardized by the UK Highway Agency (Collop *et al.* 2004, Choi 2005, Airey *et al.* 2005, 2007, Grenfell *et al*. 2011, 2012). The test features combined aging with moisture, temperature and pressure conditionings. The compacted specimens were placed in a pressurized vessel, and then conditioned at a predetermined moisture saturation level, temperature and pressure for 24 hours (Nicholls *et al*. 2011, DeCarlo *et al*. 2020). After that, the specimens were removed from the vessel. The detailed conditioning procedures are described as follows:

1. The dry mass of the specimen is measured.
2. The specimens are soaked in distilled water at 20°C and saturated by vacuum pressure at 65 kPa for 30 min.
3. The wet mass of the specimen is measured, then the percentage saturation is calculated as the “initial saturation”.
4. The specimens are placed in the vessel on the 1st to 3rd trays (see Figure 3.12 (b)). The top lid of the vessel is closed, then the vessel and water within are maintained at 85°C for at least two hours before inserting the specimens.
5. The saturated specimens are positioned in the vessel on the 1st to 3rd trays, then the lid of the vessel is closed and the air pressure is gradually raised to 0.5 MPa.
6. The test conditions are maintained at 85°C for 24 hours.
7. After 24 hours, the vessel temperature is reduced to 30°C, at which temperature it is cooled for 24 hours. After that, the air pressure is gradually decreased to atmospheric pressure, then the surface of the specimens is dried, and each specimen is weighed. The percentage saturation is calculated as the “retained saturation”.
8. The Indirect Tensile Stiffness Modulus (ITSM) is measured immediately after determining the mass of the specimen, which are then wrapped in plastic cling-film to retain their moisture content. After that, the Indirect Tensile Fatigue Test (ITFT) is conducted to examine the specimen after SATS conditioning.

After the SATS condition, the effect of the SATS condition is assessed through retained saturation and stiffness. In this study, the retained saturation and stiffness are calculated from following equations (Nicholls *et al*. 2010).

$$Retained\ saturation\ (\%) = \frac{M_{w2} - M_d}{\frac{M_d}{G_{mb}} - \frac{M_d}{G_{mm}}} \times 100 \tag{3.14}$$

where M_d is mass of dry specimen (g), M_{w2} is mass of wet specimen after the condition, G_{mb} is dry bulk density (g/cm^3), G_{mm} is maximum density (g/cm^3).

$$Retained\ stiffness\ (MPa) = \frac{S_{m\,after\ conditiong}}{S_{m\,before\ conditiong}} \tag{3.15}$$

(a)

(b)

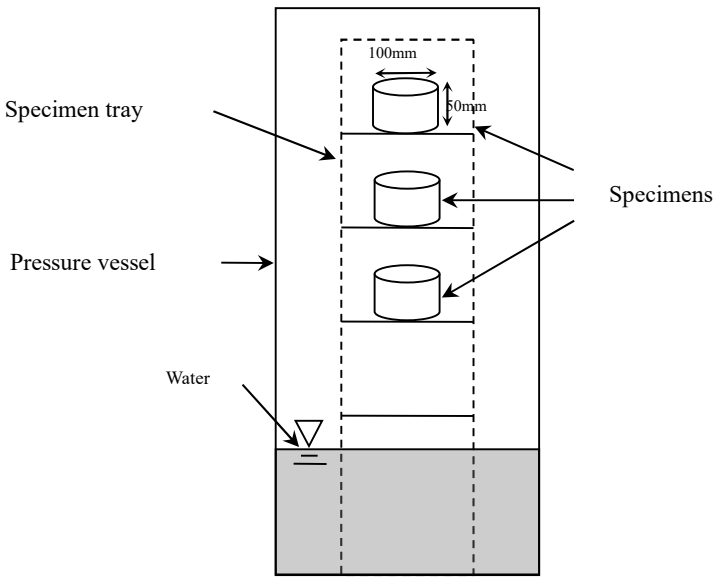

Figure 3.12 SATS condition vessel (a) Photograph, (b) Schematic of inside of vessel (after Airey 2005)

3.9 OUTLINE OF LABORATORY EXPERIMENTS

In this research, laboratory specimens (diameter: ϕ=100 mm, height: h =50 mm) were prepared from the ten types of mixtures (HMA, 30% RAP1, 60% RAP1, 30% RAP2, 60% RAP2, WMA, 30% RAP1-WMA, 60% RAP1-WMA, 30% RAP2-WMA and 60% RAP2-WMA). Then, the physical and mechanical properties of the mixtures as well as those of the binders extracted from the mixtures were assessed through various types of laboratory experiments as shown in Figures 3.7 to 3.12. In order to simulate the combined aging, Saturation Aging Tensile Stiffness (SATS) test was conducted on targeted laboratory specimens based on the EN 12697-45. Hereafter, the combined aging through the SATS tests will be referred to as SATS conditioning.

3.9.1 Flow of laboratory experiments

As in Figure 3.7, after the specimens were prepared, Indirect Tensile Stiffness Modulus (ITSM) tests were first performed on the specimens, in accordance with the BS EN 12697-26. Then the specimens were divided in two groups. The specimens in one group were subjected to the SATS conditioning. The detailed procedure of the SATS conditioning will be presented later. Following the SATS conditioning, ITSM tests were carried out on the specimens. After the ITSM tests were conducted, the stripping status of each specimen was quantitatively evaluated by conducting analysis of the cross-sectional profile of the specimen. Then, binders, i.e., aged binders were extracted from the specimens, followed by the DSR (Dynamic Shear Rheometer) tests. The binders were extracted from the specimens through the fractioning column with chromatographic as solvent by following EN 12697-4.

On the other hand, the specimens in the other group were not subjected to the SATS conditioning. After the ITSM tests were conducted, binders, i.e., unaged binders were extracted from the specimens. Finally, the rheological characteristics of extracted binders with and without the conditioning were also evaluated through Dynamic Shear Rheometer (DSR). The flow of laboratory experiments are shown in Figure 3.13.

3.9.2 Combined aging with SATS conditioning

As mentioned before, the SATS conditioning, which was the combined aging through the SATS tests, were applied to the targeted specimens. The SATS test was originally developed at the University of Nottingham (Airey 2002, 2003, Collop *et al*. 2004a, Collop, Choi and Airey 2004b, Choi 2005, Airey *et al*. 2005, 2007, Nicholls *et al*. 2006, Grenfell *et al*. 2011, 2012, 2015) and the test method has been standardized by the UK Highway Agency and it is currently standardized as EN 12697- 45. As described in Figure 3.12, the vessel in the SATS tests can give specimens combined aging of moisture, temperature and pressure. In this study, the SATS conditioning was carried out in accordance with EN 12697-45, but since the conditioning was particularly important for applying the combined aging to the specimens, the detailed procedure is described below.

Firstly, the dry mass of the targeted specimens were measured, then the specimens were soaked in distilled water at 20°C and saturated by vacuum pressure at -65 kPa for 30 min. Followingly, the wet mass of each specimen was measured so that the percentage saturation was calculated as the “initial saturation”. Meanwhile, keeping the top lid closed, the vessel with water inside was maintained at 85°C for at least two hours before inserting the specimens. After that, the saturated specimens were positioned in the vessel on the trays, then the lid of the vessel was closed again and the air pressure inside was gradually raised to 0.5 MPa. One of the reasons for setting the pressure to be 0.5 MPa instead of 2.1 MPa was to minimize the damage of each specimen by referring to previous studies. This trend is also confirmed in preliminary experiment in this research. For 2.1 MPa, 1.0 MPa in air pressure, dramatic drop in retained stiffness were confirmed in specimen, showing microcrack. However, in case of 0.5 MPa in the pressure, no visual damage was confirmed in specimens. Therefore, air pressure was set to 0.5 MPa in this study. The conditions were maintained at 85°C for 24 hours in accordance with the previous studies. After 24 hours, the vessel temperature was reduced to 30°C, at which the vessel was cooled for another 24 hours. Finally, the air pressure was gradually decreased to the atmospheric pressure, making the surface of the specimens dried, and each specimen was weighed. The percentage saturation was calculated as the “retained saturation”.

Immediately after measuring the mass of the specimens, each specimen was wrapped in plastic cling-film to retain the moisture content. Then, as described

before, indirect tensile stiffness modulus of the specimens were measured by conducting the ITSM tests. Consequently, fatigue properties of the specimens were examined with the ITFTs. In practice, the SATS conditioning has been conducted to assess the durability performance of asphalt mixture, especially focusing on stiffness. Thereby, the conditioning could be beneficial for the evaluation of moisture sensitivity on aggregates because the reduction in stiffness would be related to stripping. Meanwhile, it is also vital to assess the resiliency of RAP mixtures through the fatigue properties. Thereby, in this study, attempts were also made to evaluate the fatigue performance of mixtures those experienced the conditioning. It was expected that the use of high-quality aggregate in the mixtures and the low pressure of 0.5 MPa in the SATS conditioning might make it possible to investigate the fatigue performance of mixtures even after they experienced the conditioning. As a result, the residual service life of the HMA and WMA mixtures with and without RAP contents, experiencing the conditioning were successfully compared based on the ITFT results.

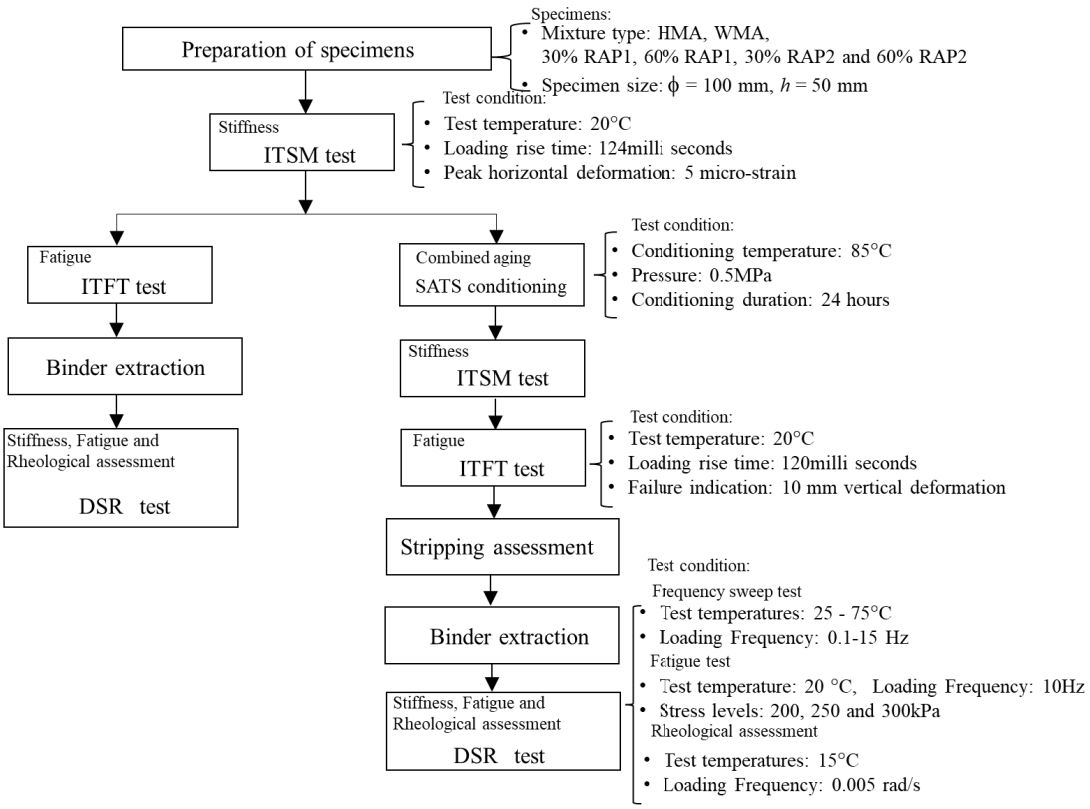

Figure 3.13 Flow of laboratory experiments

CHAPTER 4

Combined Aging Characteristics of HMA with RAP

4.1 INTRODUCTION

This chapter describes the assessment of Hot-Mixed Asphalt (HMA) and RAP mixtures with rejuvenator using the Saturation Aging Tensile Stiffness Test (SATS) conditioning. In particular, moisture and aging damage mechanism for RAP mixtures associated with rejuvenator are discussed. In this research, SATS conditioning were used to simulate combined aging situation on site, and two types of rejuvenator were investigated related to RAP binders and mixtures. In this experiment, 30% and 60% RAP mixtures were studied compared with HMA and those characteristics are addressed through stiffness modulus and fatigue properties obtained from Nottingham Asphalt Tester (NAT) and Dynamic Shear Rheometer (DSR).

4.2 BINDER PROPERTIES

To prepare RAP mixtures, the optimum ratio of rejuvenator to RAP binder extracted from waste reclaimed asphalt (RA) sources was investigated. Subsequently, RAP mixtures with 30 and 60% RAP ratio blended with the rejuvenators were produced. For comparison, HMA mixtures were prepared using a virgin binder and virgin aggregates.

4.2.1 Binder blending design

In this study, virgin and RA binders were prepared to design HMA and RAP mixtures. The virgin binder was 60/80 pen bitumen, whereas the RA binder was extracted from RA sources provided by a plant through a fractioning column with trichloroethylene as the solvent, according to the American Society for Testing and Materials (ASTM) D 1856-95a. The properties of the virgin and RA binders were examined through penetration tests, softening tests, and rotational viscosity tests from 150 °C to 120 °C according to ASTM D5-97, ASTM D 36, and ASTM D 4402-02, respectively. The test results are listed in Tables 4.1 to 4.2.

As shown in Table 4.1, the penetration of the RA binder is significantly lower than that of the virgin binder. The table also demonstrates that the softening point of the RA binder is much higher than that of the virgin binder. This trend is consistent with the viscosities observed for the virgin and RA binders. These results indicate that the RA binder was heavily aged under in-service conditions. Therefore, it was necessary to recover the RA binder by dosing it with rejuvenating agents for the production of RAP mixtures. In this study, two types of oil-based rejuvenators (Rejuvenators 1 and 2) were selected. The properties of these two rejuvenators are listed in Table 4.2.

Table 4.1 Properties of virgin and reclaimed asphalt (RA) binders

	Penetration at 25 °C (1/10 mm)	Softening point (°C)	Viscosity at 120°C (mPa.s)	Viscosity at 150°C(mPa.s)
Virgin binder	63	48.5	835.6	186.5
RA binder	12	80.5	21300	2035

Table 4.2 Properties of two types of rejuvenators

	Penetration at 25 °C (g/cm^3)	Dynamic viscosity (mm^2/s)	Ratio of viscosity with thin-film oven test (TFOT) to that without TFOT	Reduction rate of mass content with TFOT to that without TFOT (%)
Rejuvenator 1	0.948	48.5	1.10	-0.28
Rejuvenator 2	0.925	80.5	1.05	-1.37

It should be noted that Rejuvenator 1 exhibited a slightly higher density than Rejuvenator 2. However, it can be observed in the table that both rejuvenators exhibit similar viscosity characteristics. In terms of the saturation, aromatic, resin, and asphaltene (SARA) fraction in the rejuvenators, Rejuvenator 1 had high in aromaticity, whereas Rejuvenator 2 was rich in saturation. Because the two rejuvenators had different compositions, the SARA fraction of the RA binder also changed after blending.

Consequently, a binder blending design was conducted to obtain RAP binders that could meet the grade of 70 penetration, such that the penetration of the RAP binders became close to that of the virgin binder. First, the RA binder was mixed with each rejuvenator at rejuvenator ratios of 0, 15, and 20% (percentage by mass of the RA binder). Subsequently, a linear relationship between the penetration and rejuvenator ratio was obtained for the mixed binders. Based on these relationships, the optimum rejuvenator ratios for achieving a 70 pen grade were determined to be 18.3 and 21.5% for Rejuvenators 1 and 2, respectively. Finally, two types of blended binders were prepared with the optimum rejuvenator ratios of Rejuvenators 1 and 2.

Each blended binder with the optimum rejuvenator ratio was analyzed using a chromatographic method (ASTM-D2007). The results are shown in Figure 4.1, along with those obtained for the rejuvenators. The figure also shows the results obtained for the virgin and RA binders. As can be observed in the figure, the two blended binders, that is, the RA binders blended with Rejuvenators 1 and 2, showed differences, especially with respect to the aromatic and resin components. The blended binder with Rejuvenator 1 showed a higher percentage of resin relative to Rejuvenator 2, whereas the latter binder showed a higher percentage of aromatics. However, both binders showed a higher percentage of aromatics and a lower percentage of resin components than the RA binder. In addition, looking at chemical composition of rejuvenator, rejuvenator 1 is aroma-rich, whilst

rejuvenator 2 is saturate-rich. Therefore, it can be said that the mechanical properties of RAP mixture might be affected by those compositions.

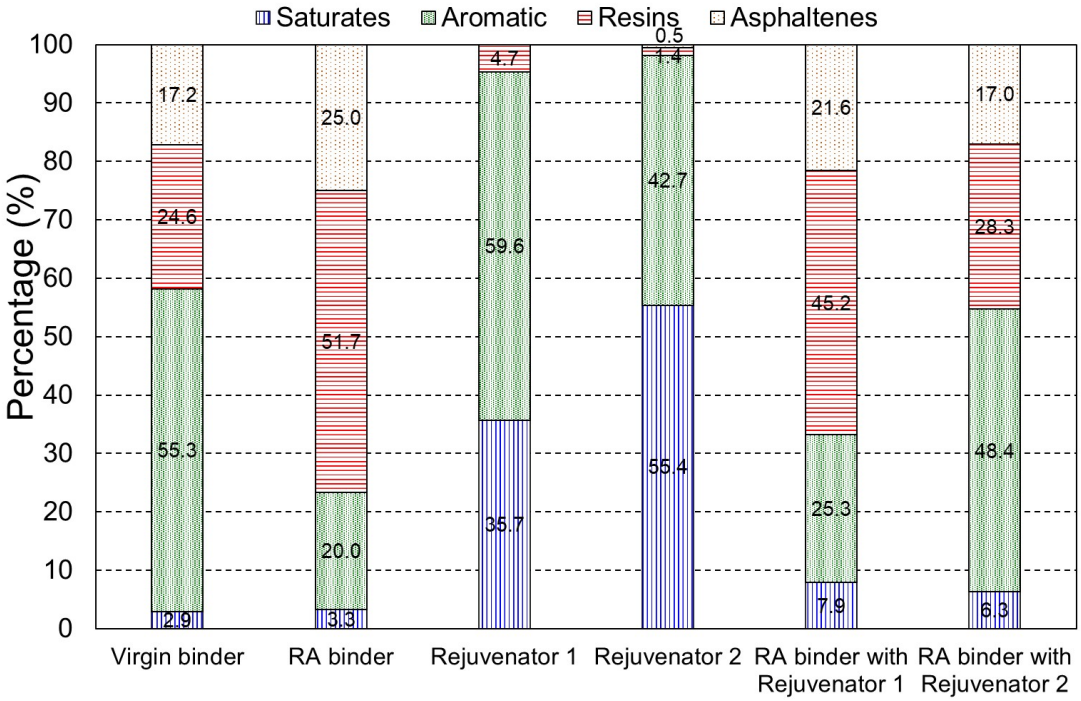

Figure 4.1 Chemical compositions of virgin binder, reclaimed asphalt (RA) binder, Rejuvenator 1, Rejuvenator 2, RA binder with Rejuvenator 1, and RA binder with Rejuvenator 2

4.2.2 Preparation of mixtures

Densely graded asphalt mixtures (AC 13) were prepared using rejuvenators, RAP aggregates, virgin aggregates, and virgin binder to assess the durability of the RAP mixtures. In this study, the mixing ratio of RAP aggregates to the total amount of aggregates was set to 30 or 60%. Four types of RAP mixtures were prepared by employing two types of rejuvenators and two types of RAP contents. Hereafter, the mixtures with 30 and 60% RAP ratio using Rejuvenator 1 are denoted as 30% RAP1 and 60% RAP1, respectively. Similarly, the mixtures with 30 and 60% RAP ratio using Rejuvenator 2 are denoted as 30% RAP2 and 60% RAP2. AC 13 was also prepared using a virgin binder and aggregates to assess the durability of the HMA mixtures. Both HMA and RAP mixtures were designed to meet the standard grading range for AC 13, and the binder content was determined using the Marshall design method.

In this study, the target penetration was set to 70 pens, and the optimum rejuvenator amount was determined by changing it to 0, 15, and 20% by weight of the RA binder. The ratio indicated in the 70 pen in the binder was selected from linear regression analysis. To manufacture each type of RAP mixture, the RAP aggregates were first mixed with each rejuvenator considering the optimum rejuvenator ratio. The blended aggregates were then placed in an oven at 130 °C for 3 h. After curing, the aggregates were mixed with a virgin binder and virgin aggregates, which had been heated at 160 °C. As aforementioned, the RAP aggregate content ratio was set to 30 or 60%. After mixing, the mixed aggregates were compacted at 140 °C to obtain the laboratory test specimens. The details of the binder tests results are presented in Tables 4.3 to 4.7.

The densities and air void contents of the five mixtures (HMA, 30% RAP1, 60% RAP1, 30% RAP2, and 60% RAP2) were measured after manufacturing the Marshall specimens. The densities and void contents of the RAP mixtures ranged from 2356 kg/m^3 to 2380 kg/m^3 and 5.5% to 5.6%, respectively, which were close to those of the HMA mixture. This suggests that all RAP mixtures were

successfully designed and ready for the laboratory experiment program, as presented in the next section.

Table 4.3 Properties of HMA binder

	Penetration at 25°C (1/10 mm)	Softening point (°C)	Viscosity at 120°C (mPa.s)	Viscosity at 150°C(mPa.s)
HMA	58	48	930.2	312.9

Table 4.4 Properties of 30% RAP1-HMA binder

	Penetration at 25°C (1/10 mm)	Softening point (°C)	Viscosity at 120°C (mPa.s)	Viscosity at 150°C(mPa.s)
30% RAP1-HMA	53	51.5	1248	262.9

Table 4.5 Properties of 30% RAP2-HMA binder

	Penetration at 25°C (1/10 mm)	Softening point (°C)	Viscosity at 120°C (mPa.s)	Viscosity at 150°C(mPa.s)
30% RAP2-HMA	49	51.5	1364	287.6

Table 4.6 Properties of 60% RAP1-HMA binder

	Penetration at 25°C (1/10 mm)	Softening point (°C)	Viscosity at 120°C (mPa.s)	Viscosity at 150°C(mPa.s)
60% RAP1-HMA	44	54	1602	320.7

Table 4.7 Properties of 60% RAP2-HMA binder

	Penetration at 25°C (1/10 mm)	Softening point (°C)	Viscosity at 120°C (mPa.s)	Viscosity at 150°C(mPa.s)
60% RAP2-HMA	48	54	1449	295.0

4.3 CHANGES IN MIXTURES PROPERTIES WITH AND WITHOUT SATS CONDITIONING

The properties of the five types of mixtures (HMA, 30% RAP1, 60% RAP1, 30% RAP2, and 60% RAP2) were evaluated through ITSM tests and ITFTs, as shown in Figures 3.5 to 3.6. In this section, the stiffness values obtained from ITSM tests are presented. The fatigue behaviors obtained from the ITFTs are presented in the subsequent section. Note that the fatigue behaviors of the HMA and RAP mixtures subjected to SATS conditioning were investigated to assess their residual service life after the damage from the conditioning.

4.3.1 Stiffness modulus

To investigate the changes in the stiffness of the mixtures with and without SATS conditioning, ITSM tests were conducted on specimens of five types of mixtures (HMA, 30% RAP1, 60% RAP1, 30% RAP2, and 60% RAP2). Table 4.8 summarizes the obtained stiffness and air void content values of the mixtures with and without SATS conditioning. The stiffness shown in the table is the average stiffness obtained from the three specimens for each mixture. The standard deviation values are listed in the table. As shown, without SATS conditioning, the average stiffness of the RAP mixtures was lower than that of the HMA mixture, although the RAP 1 and RAP 2 binders were adjusted to 70 pen grade with the rejuvenators. This indicates that the stiffness of the RAP mixtures can differ from that of the HMA mixture, even if the penetration of the binder and grading of the RAP mixtures are adjusted to be close to those of the HMA mixture. The RAP mixtures showed a stiffness lower than that of the HMA mixture probably because of the rheological properties of the RAP binders, as shown in Figure 4.8. As discussed in following section, the G^* of the RAP binders becomes lower than that of the virgin binder as the phase angle decreases. This will be discussed in more detail in section 4.5

Figure 4.2 (a) shows the retained stiffness ratio, that is, the ratio of stiffness with SATS conditioning to that without SATS, as calculated from the stiffness of an identical specimen with and without SATS conditioning. The ratio of the HMA mixture was significantly lower than 1.0, whereas the ratios of the RAP mixtures were higher than those of the HMA mixtures. Moreover, the ratios obtained for the 60% RAP1 and 60% RAP2 mixtures were higher than those for the 30% RAP1 and 30% RAP2 mixtures, respectively.

In Figure 4.2 (b), the retained stiffness ratio is plotted against the retained saturation of each specimen. As shown, the ratio decreases with an increase in the retained saturation, suggesting that the decrease in the mixture stiffness caused by SATS conditioning is strongly related to the increase in the retained saturation. In the figure, the RAP mixtures show higher retained stiffness ratios with lower retained saturations compared to the HMA mixtures, indicating that the RAP mixtures will degrade less against combined aging than the HMA mixture in terms of stiffness. This trend became more significant with an increase in the RAP content, irrespective of the rejuvenator type. In terms of retained saturation, all mixtures were placed between 20 to 80%.

Table 4.8 Stiffness of the mixtures with and without SATS conditioning

(HMA and RAP mixtures)

	HMA		30% RAP1		60% RAP1		30% RAP2		60% RAP2	
	Without	With	Without	With	Without	With	Without	With	Without	With
Average air voids (%)	3.7		4.2		4.0		3.7		3.7	
Average stiffness (MPa)	2688	2025	2011	1964	2080	2285	2229	2084	2073	2067
Std Dev. Stiffness (MPa)	174	231	105	371	95	104	142	290	87	113
CoV Stiffness (%)	6	11	5	19	5	5	6	14	4	5

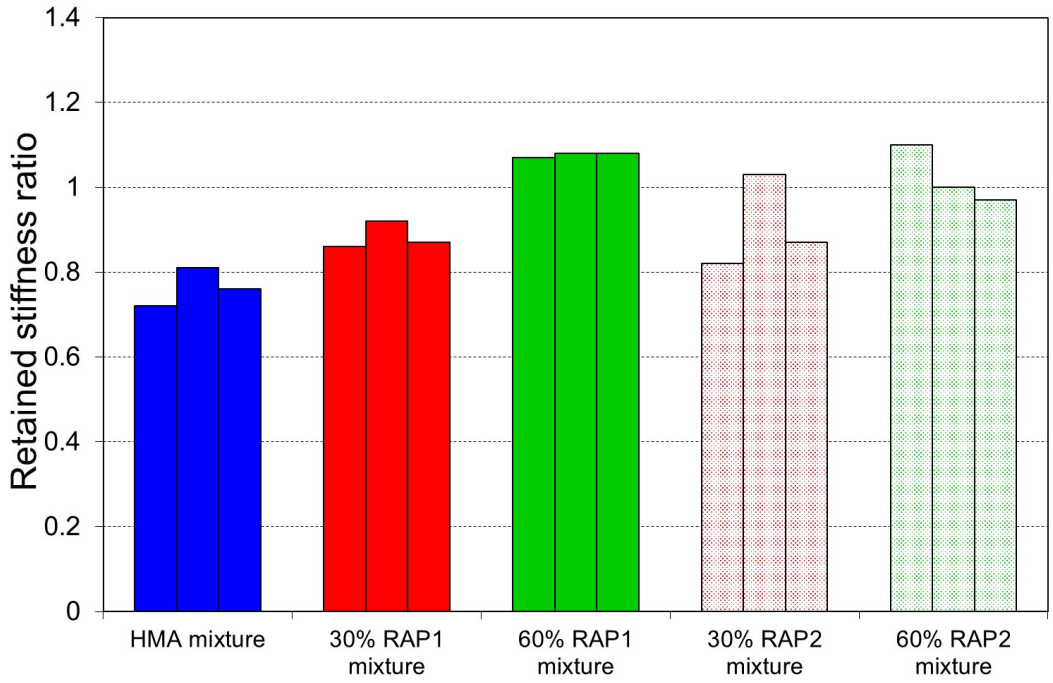

(a)

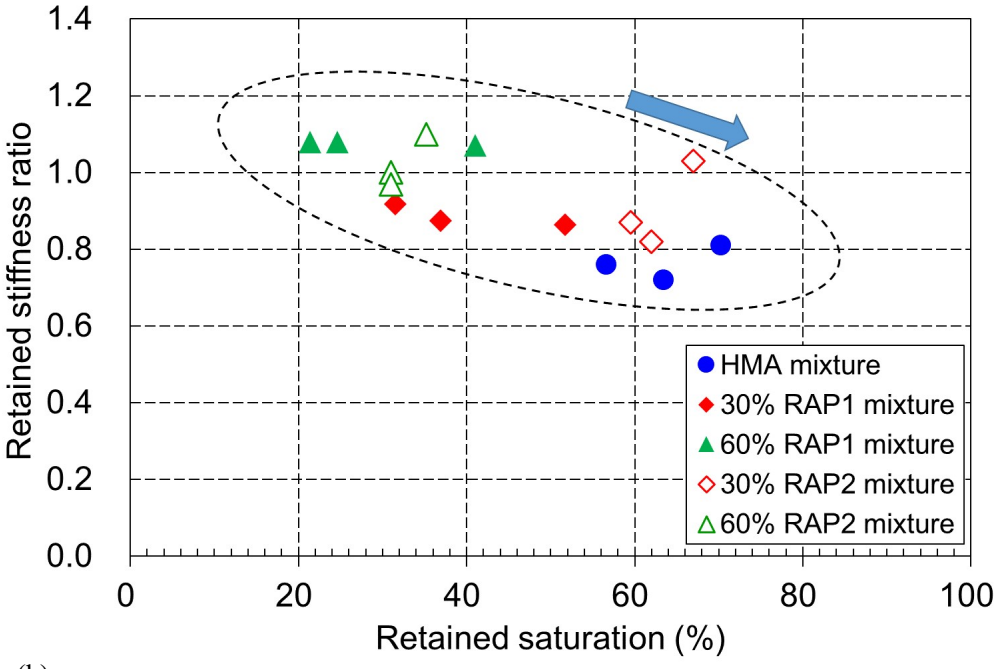

(b)

Figure 4.2 Retained stiffness ratio from ITSM tests (HMA and RAP mixtures)
(a) Retained stiffness ratio for each mixture, (b) Relationships between the retained stiffness ratio and retained saturation for each mixture

4.3.2 Fatigue behavior and residual service life

Fatigue characterists of the five mixtures with and without SATS conditioning were evaluated through the ITFTs, following the test conditions shown in Figure 4.3. Cocurullo *et al*. (2008) examined fatigue characteristics of asphalt mixture specimens by assuming its vertical deformation as changes in stiffness modulus through ITFT. In their ITFTs, changes in specimen diameter was normalised by dividing it into its initial diameter (normalised creep stiffness = (specimen diameter-vertical deformation)/specimen diameter). The calculated value was called "normalised creep stiffness" and the relationship between the normalised creep stiffness and fatigue characteristics was studied through the experiment. In the experiments, 50% stiffness reduction was defined as fatigue failure point in each specimen (see Figure 4.3). This research also examined the fatigue characteristics of RAP-WMA mixture, following their assumption.

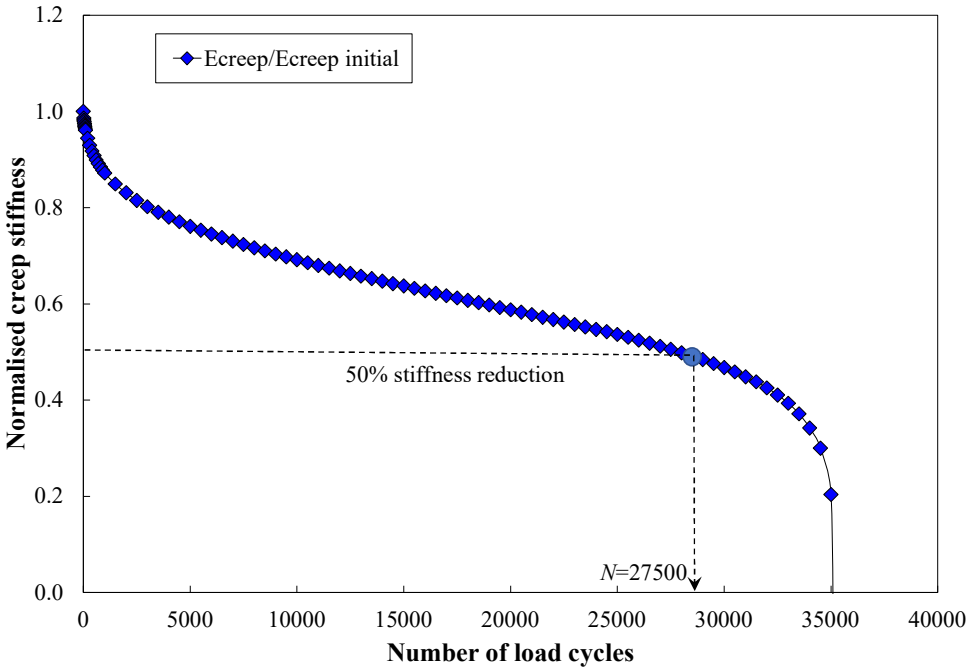

Figure 4.3 Difference in fatigue failure criteria (HMA and RAP mixtures)

Figures 4.4 and 4.6 present the results from the ITFTs conducted on the HMA and RAP mixtures without SATS conditioning, and Figures 4.5 and 4.7 demonstrate those with SATS conditioning. The relationships among the initial strain, stress level and the number of cycles to failure are shown in the figures. The number of cycles to failure was determined in accordance with BS EN 12697-24, as shown in Figure 3.8.

As shown in Figure 4.4, both the RAP 1 and RAP 2 mixtures show longer fatigue cycles than the HMA mixture, despite their initial strains being nearly the same as that of the HMA mixture. This observation is different from that observed for the fatigue properties of binders (refer to Figure 4.14). This suggests that the adhesion state of the binder and aggregates significantly influences the fatigue properties of the mixtures. In addition, the fatigue cycles of the RAP mixtures increased when the RAP ratio increased from 30 to 60% for both the RAP1 and RAP2 mixtures. This suggests that the service life of the RAP mixtures increased as the chances of adhesion between the RAP aggregates and binders increased.

Comparing the results in Figures 4.4, notably, the RAP mixtures with SATS conditioning demonstrate a longer residual service life compared to the HMA mixture with SATS conditioning (see Figures 4.5). Similar to the case without SATS conditioning, this tendency was more pronounced when the RAP ratio was increased from 30 to 60% for both RAP1 and RAP2 mixtures. It can also be observed that the number of cycles at failure of the RAP mixtures with SATS conditioning is reduced relative to that without SATS conditioning. However, the initial strain of the RAP mixtures did not change significantly with or without SATS conditioning. This agrees with the fact that the retained stiffness ratios of the RAP mixtures were relatively close to 1.0, as shown in Figure 4.2 (b).

Figure 4.5 also demonstrates that the RAP1 mixtures showed differences in the initial strains between the 30 and 60% RAP ratio, whereas the RAP 2 mixtures

showed similar strains even when the RAP ratio were different. This difference may be attributed to the difference in the air void content between the RAP1 and RAP2 mixtures, as shown in Table 4.8. The RAP1 mixtures showed a decrease in the air void content as the RAP aggregate content increased, whereas the RAP2 mixtures showed the same air void content between 30 and 60% RAP contents. Because the RAP1 mixtures included higher resin components, their compaction performance became worse than that of the RAP2 mixtures, and higher air voids were attained in the RAP1 mixtures. This suggests that the difference in the type of rejuvenator affects the compaction performance of the RAP mixtures, resulting in different fatigue behaviors.

In case of results summarized with stress level, significant results can be seen in Figures 4.5 and 4.7. In case of the test results without SATS conditioning, both RAP1 and RAP2 mixtures demonstrate similar fatigue life with HMA mixture. However, for the test results with the conditioning, the results showed clear difference between HMA and RAP mixtures in fatigue curve. RAP mixtures demonstrated longer fatigue life than that of HMA mixture. This trend was confirmed both in RAP1 and RAP2 mixtures. This result suggest that high RAP mixtures have longer fatigue cycles than that of HMA mixture.

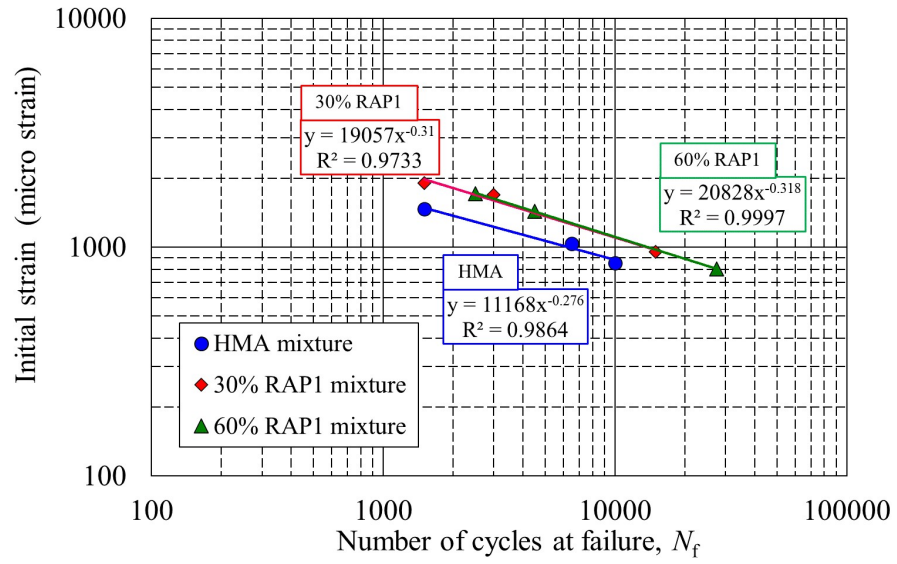

(a)

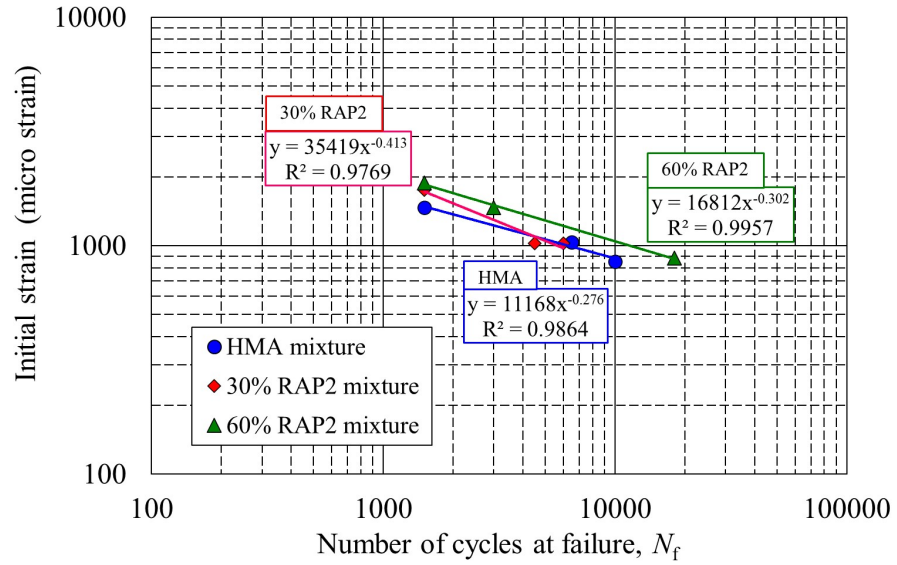

(b)

Figure 4.4 Relationships between the initial strain and number of cycles at failure of the mixtures from ITFTs without SATS conditioning (a) HMA & RAP1 mixtures, (b) HMA & RAP2 mixtures

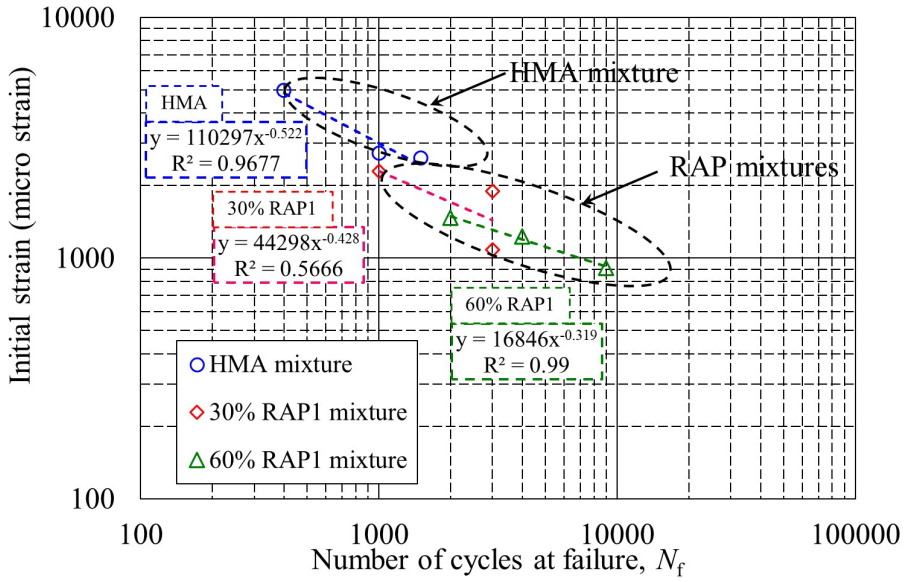

(a)

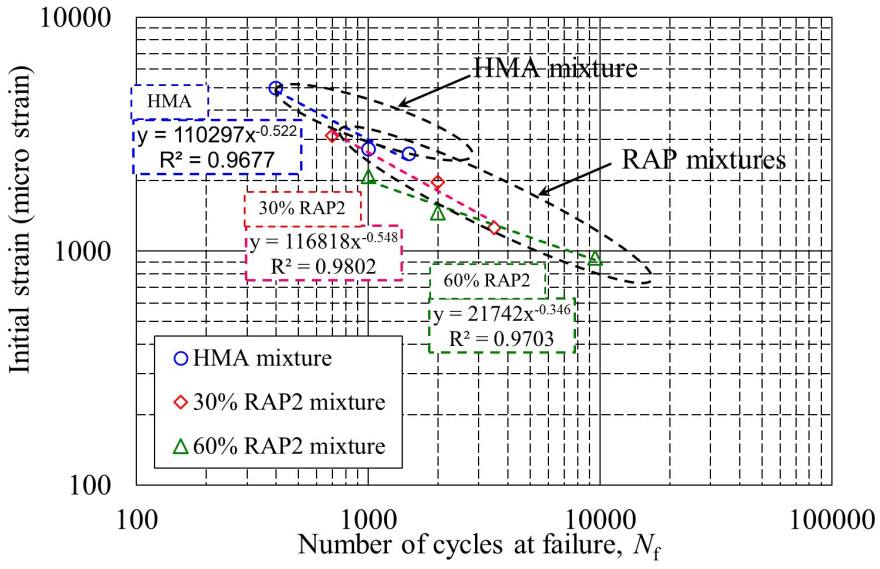

(b)

Figure 4.5 Relationships between the initial strain and number of cycles at failure of the mixtures from ITFTs with SATS conditioning (a) HMA & RAP1 mixtures, (b) HMA & RAP2 mixtures

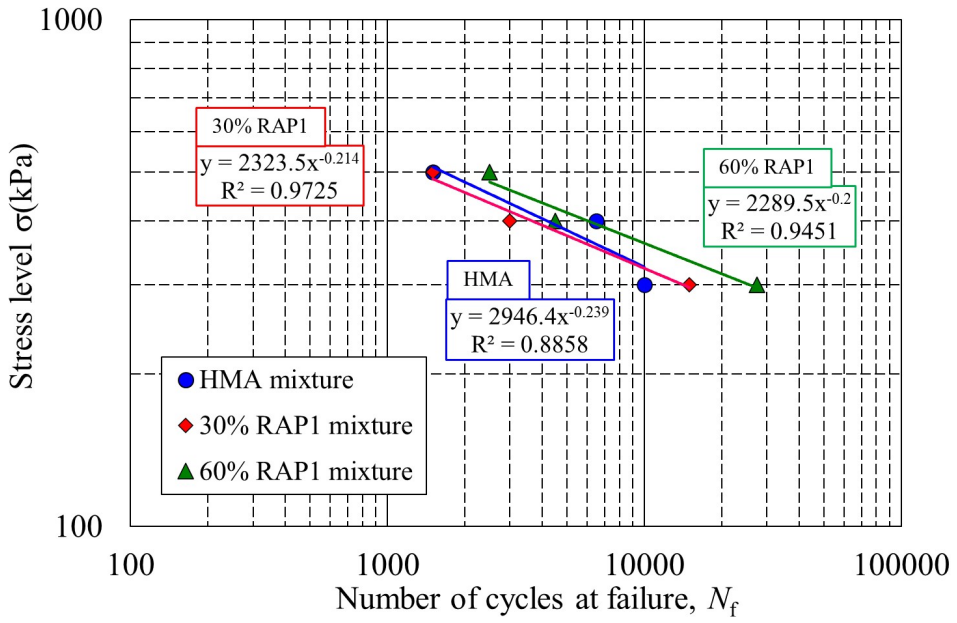

(a)

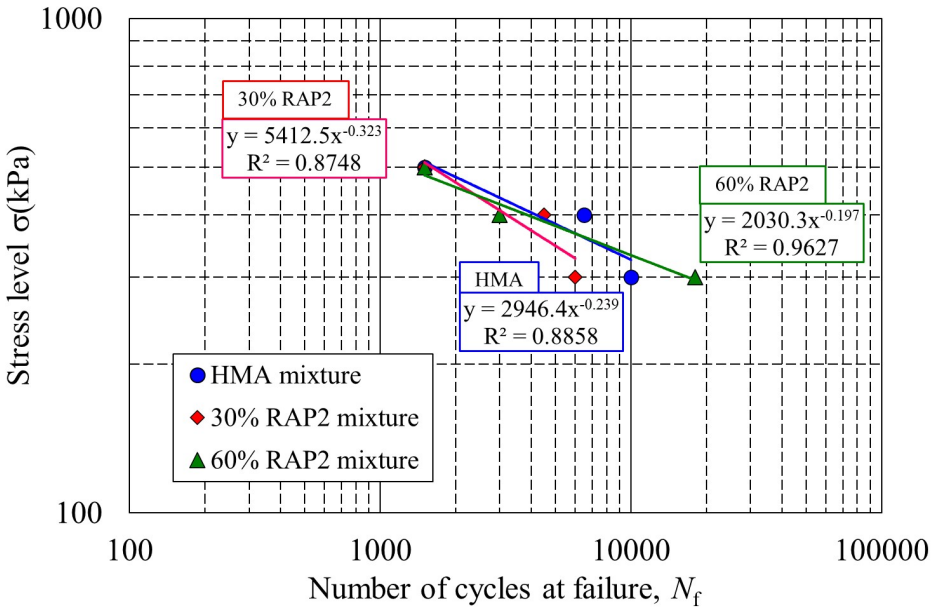

(b)

Figure 4.6 Relationships between the stress level and number of cycles at failure of the mixtures from ITFTs with SATS conditioning (a) HMA & RAP1 mixtures, (b) HMA & RAP2 mixtures

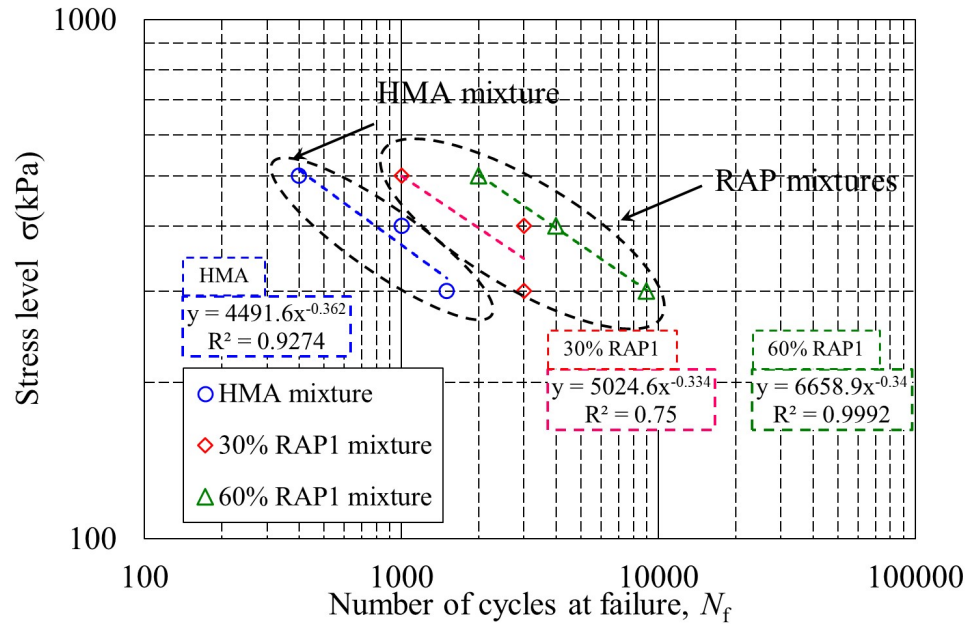

(a)

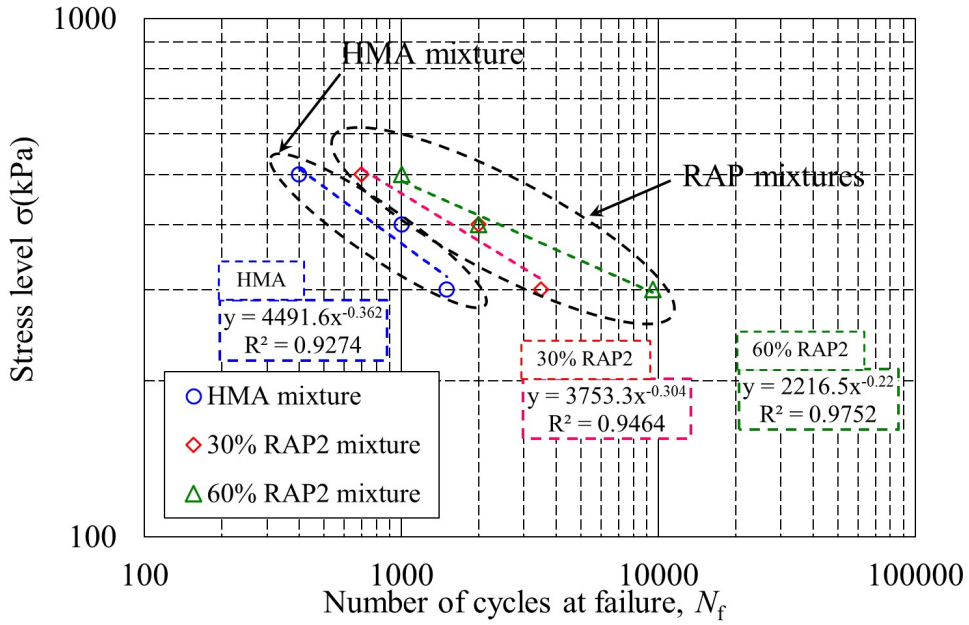

(b)

Figure 4.7 Relationships between the stress level and number of cycles at failure of the mixtures from ITFTs with SATS conditioning (a) HMA & RAP1 mixtures, (b) HMA & RAP2 mixtures

4.3.3 Mixture failure pattern

In order to understand the fatigue characteristics of HMA and RAP mixtures in more detail, the fatigue results of the five specimens were analysed in this study. Figure 4.8 shows the fatigue failure patterns for HMA and RAP mixtures with SATS conditioning, based on ITFT results conducted at 500kPa. As can be seen in the results, the differences in RAP ratio and rejuvenators were confirmed from each failure mode. RAP mixtures showed longer fatigue life, when compared with that of HMA mixtures. This result is more pronounced when RAP ratio was increased from 30% to 60%, and the same trend can be seen in RAP1 and RAP2 specimens.

Meanwhile, looking at differences in rejuvenators, RAP1 mixtures demonstrated longer fatigue life, when compared with that of RAP2 mixtures. As described in the previous section, despite the fact that RAP 1 specimen showed slight difference in air void contents compared to RAP 2 specimens, it indicated longer fatigue life. In addition, this trend is more pronounced as RAP contents increase. This might highlight influence of rejuvenator for the mechanical properties of RAP mixtures. Therefore, it seems that this result implies the differences in rejuvenators in the fatigue life of RAP mixtures.

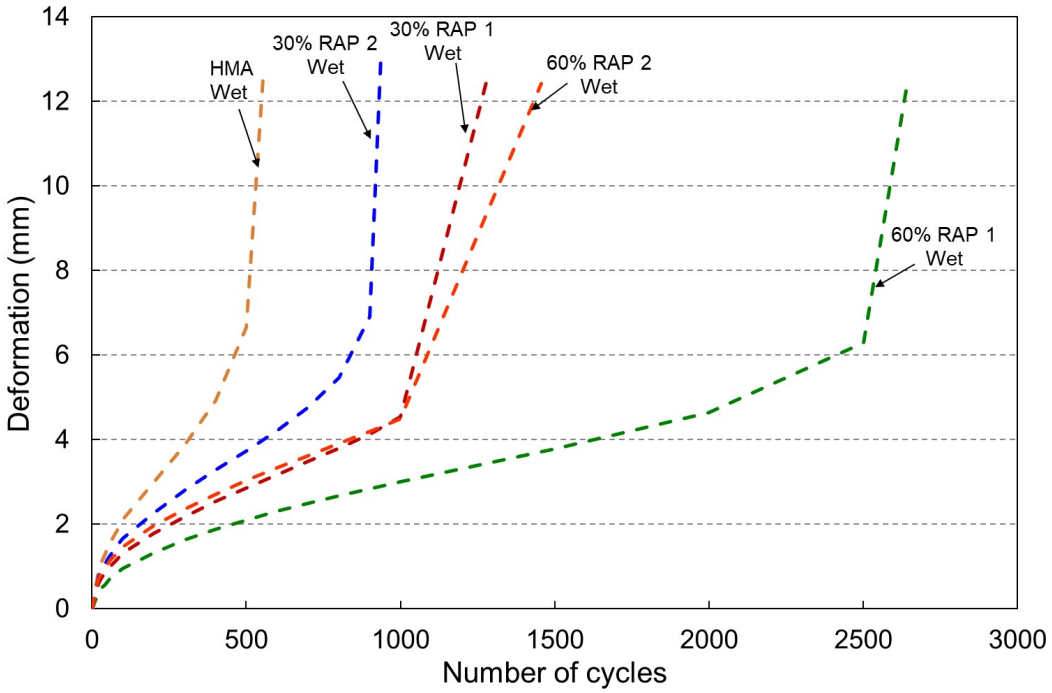

Figure 4.8 Fatigue relationships for HMA and RAP mixtures with SATS conditioning (Stress level: 500 kPa)

4.4 STRIPPING CHARACTERISTICS OF THE MIXTURES WITH SATS CONDITIONING

As shown in Figure 3.13, the stripping status of the HMA and RAP mixtures with SATS conditioning was examined after the ITFTs. Each mixture specimen was divided into two cross-sections, and the stripping areas were measured through analysis following the Japanese standard of the immersed wheel tracking test, B004. The stripping ratio of each specimen was defined as the area of the stripping aggregate divided by the cross-sectional area. Consequently, an average stripping ratio was obtained for each mixture (Plastic film depicting mesh was placed on the cross-section, then stripped area was counted, and stripping ratio was calculated).

Figure 4.9 shows the average stripping ratio of the mixtures with the SATS conditioning. As a result, the average ratio of the HMA mixture showed approximately 8% whereas those of RAP mixtures indicated less than 4%. Moreover, the stripping resistance increased as the RAP content increased. The 30 and 60% RAP1 mixtures demonstrated 1.1 and 0.8% whilst those of RAP2 mixtures illustrated 3.4 and 0.6%, respectively. Although it seems that the differences in rejuvenator might influence the stripping resistance of mixtures, the obtained results demonstrate that the RAP mixtures have better stripping resistance than the HMA mixture. Similar to the findings obtained for the fatigue characteristics, the results indicate that the stripping resistance of the mixtures increases as the chances of adhesion between the RAP aggregates and RAP binders increases.

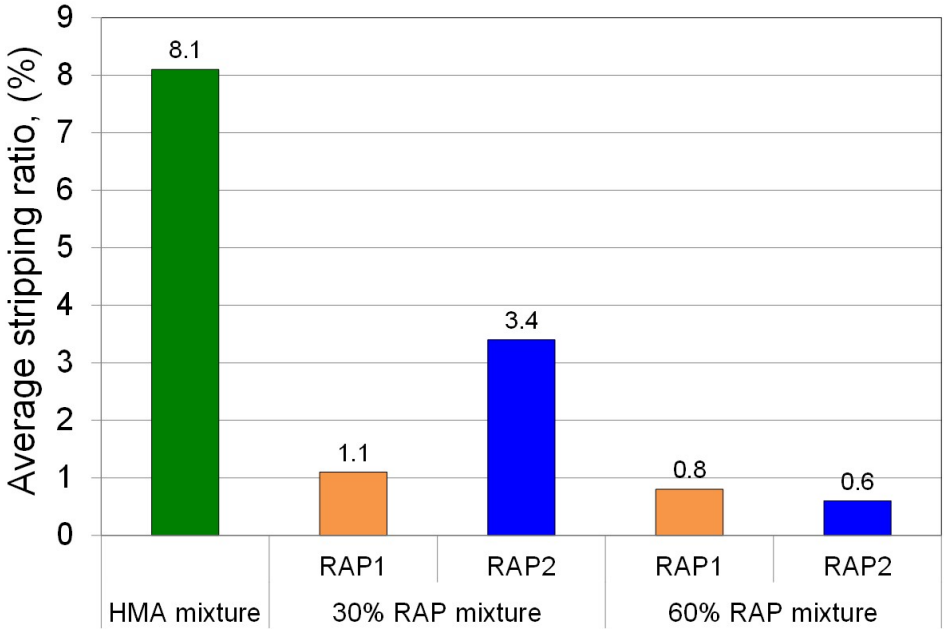

Figure 4.9 Average stripping ratio of the mixtures with the SATS conditioning (HMA and RAP mixtures)

4.5 CHANGES IN PROPERTIES OF BINDERS WITH AND WITHOUT SATS CONDITIONING

As shown in Figure 3.13, the asphalt binders were extracted from the laboratory specimens of the mixtures to investigate the binder properties with and without SATS conditioning. The binders were extracted from specimens of five types of mixtures (HMA, 30% RAP1, 60% RAP1, 30% RAP2, and 60% RAP2). The properties of the extracted binders were evaluated via frequency sweep and fatigue tests using DSR. In this section, first, the results obtained from the frequency sweep tests are presented; the fatigue test results are then presented in the subsequent section.

4.5.1 Stiffness modulus

From the frequency sweep tests, the complex modulus G^* and phase angle δ of each binder were evaluated for a range of frequencies of 0.1–10 Hz at eight temperatures from 34 °C to 78 °C in 6 °C increments. These results were assessed using the master curves of G^* and black diagrams.

Figure 4.10 presents the master curves of G^* for the binders extracted from the specimens without and with SATS conditioning, respectively. The master curves were obtained at a reference temperature of 34 °C. In general, old binders tend to increase G^* compared to virgin binders. However, as shown in Figure 4.10 (a), the master curves obtained for each binder were almost similar. This suggests that the rejuvenators successfully worked when mixed with the RAP aggregates and that the master curves of the binders of the RAP mixtures could be similar to that of the HMA mixture. Comparing the results in Figure 4.8, it can be observed that there is no significant change in the properties of each binder with SATS conditioning. This is probably because a low pressure (0.5 MPa) and a curing period of 24 h were set in the SATS conditioning in this study.

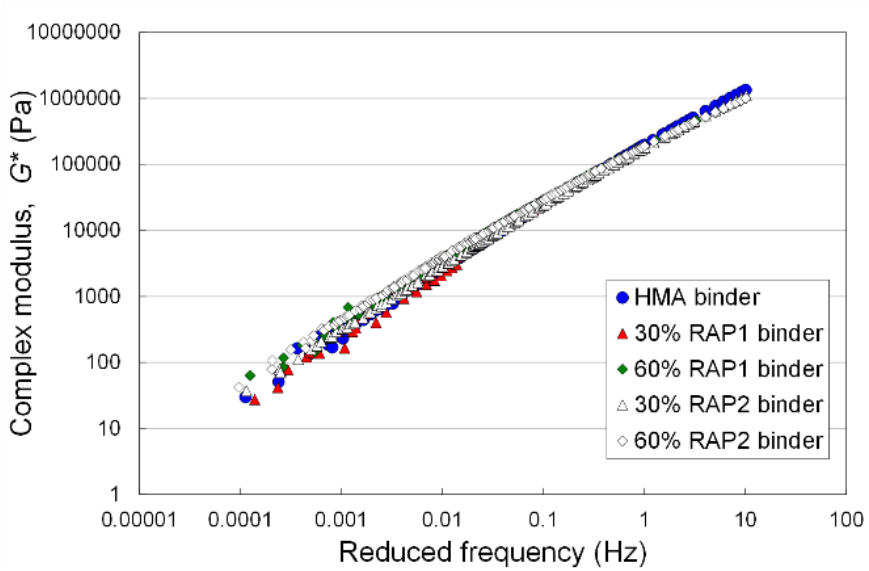

(a)

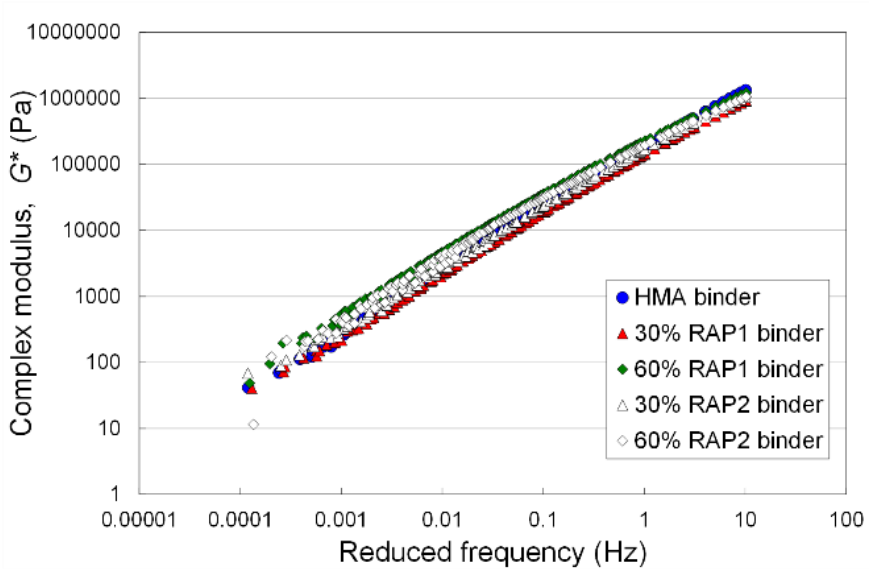

(b)

Figure 4.10 Dynamic shear rheometer (DSR) master curve of binders extracted from five types of mixture at a reference temperature of 34°C (a) Without SATS conditioning, (b) With SATS conditioning

To understand the detailed rheological properties of the binders, the relationship between G^* and δ is represented by a black diagram. Figure 4.11 show the black diagrams for the five extracted binders with and without the SATS conditioning, respectively, using the results measured at a temperature of 34 °C. The results shown in the figures reveal that there is no significant difference in the G^* - δ relationship of each binder with or without SATS conditioning. It was also found that the G^*– δ relationships shifted towards a lower phase angle as the RAP content increased from 0 (i.e. HMA) to 60%. This trend can be observed in both RAP 1 and RAP 2 binders, with or without SATS conditioning.

As shown in Figure 4.12, detailed analyses were conducted on the changes in the binder properties with and without SATS conditioning, based on the ratio of G^* with SATS conditioning ($G^*_{conditioned}$) to G^* without SATS ($G^*_{unconditioned}$), as obtained at 10 Hz for each type of mixture. In the figure, the ratios are plotted against the temperature. It can be observed that the ratio of each binder is nearly 1.0, at all temperatures. It also appears that there is little change in binder stiffness with and without SATS conditioning. However, carefully examining the details, the binder extracted from the 30% RAP1 mixture showed ratios lower than 1.0, whereas the binder from the 60% RAP1 mixture demonstrated higher ratios than those from the HMA and RAP 2 mixtures. Different trends in the effects of SATS conditioning on the RAP1 and RAP2 binders were also observed for the results obtained at other frequencies. Although details of the reason (s) for the different trends need to be studied in the future, the difference may be attributed to the difference in the chemical compositions of the binders. As shown in Figure 4.1, both the virgin binder and the RA binder with Rejuvenator 2 show similar components in the SARA fractions. However, the RA binder with Rejuvenator 1 had a different chemical composition in the SARA fraction compared with those of the virgin binder and the RA binder with Rejuvenator 2.

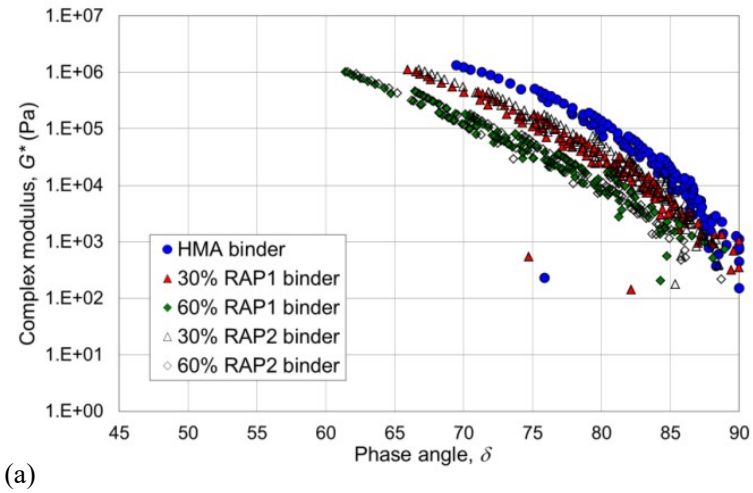

(a)

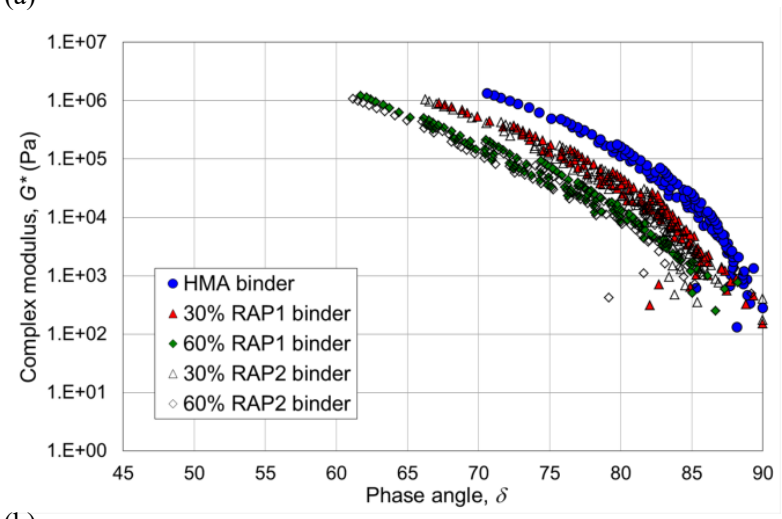

(b)

Figure 4.11 Black diagram of binders extracted from five types of mixture obtained from the frequency sweep test using DSR (a) Without SATS conditioning, (b) With SATS conditioning

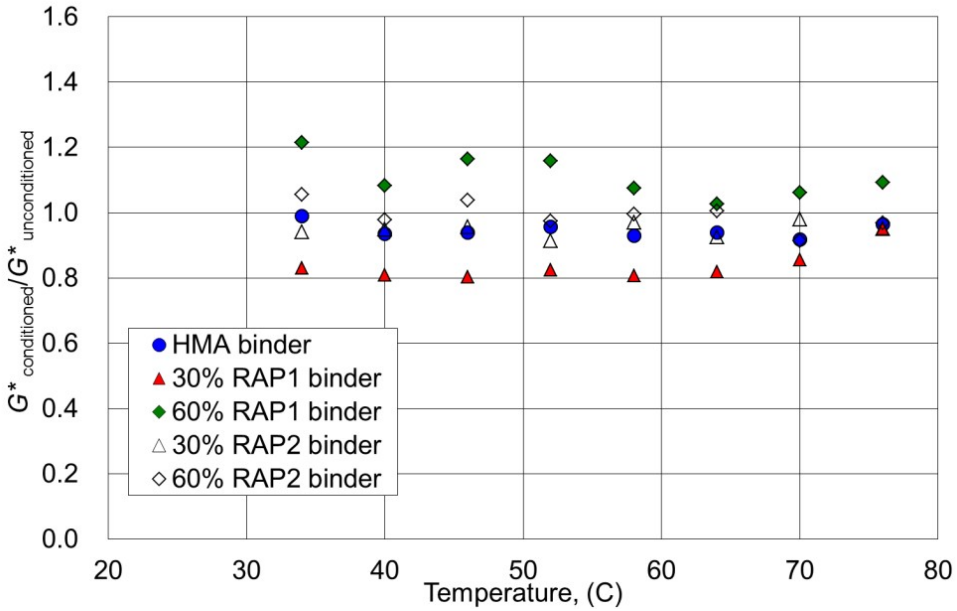

Figure 4.12 Ratio of $G^*_{conditioned}$ with the SATS conditioning to the $G^*_{unconditioned}$ without the SATS conditioning obtained at 10 Hz for each type of mixture

4.5.2 HMA fatigue behaviour with 50% reduction in complex modulus *G**

To understand fatigue characteristics of the binders extracted from the five types of the mixtures with and without the combined aging, fatigue tests were also performed on the binders using the DSR. As shown in Figure 3.9, the tests were conducted under stress control.

To determine the number of cycles at the fatigue failure in the tests, failure criterion shown in Figure 4.13 was used. Figure 4.13 shows an example of the relationship between the complex modulus *G** and number of cycles, N obtained from the test. The number of cycles at the fatigue failure of each binder was determined as the number of cycles to reach 50% reduction in initial complex modulus *G**.

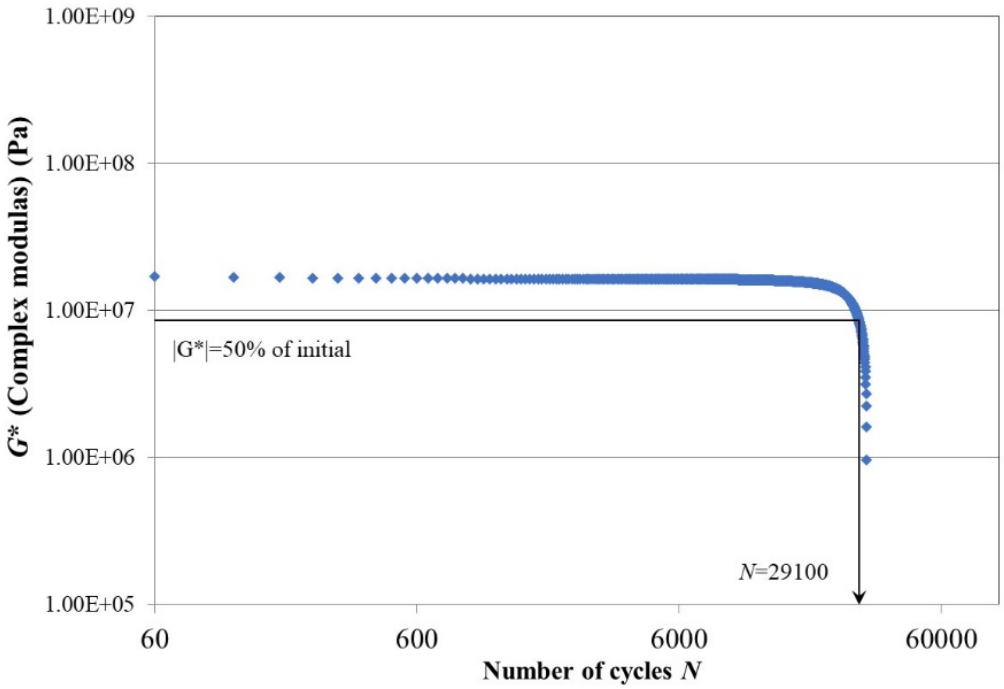

Figure 4.13 Failure criterion using complex modulus to determine the number of cycles at the fatigue failure (HMA and RAP binders)

Figures 4.14 to 17 show the test results obtained for the binders without the SATS conditioning and for those with the SATS conditioning, respectively. Firstly, high correlation between the initial strain and the number of cycles at failure was observed in each fatigue test result. It is found in Figure 4.14 that the relationships between the initial strain and the number of loading cycles at failure of the RAP binders without the SATS conditioning are located in the upper left side of that of the HMA binder. This indicates that the RAP binders were less durable against fatigue compared to the HMA binder. It is also found that there is a tendency that the fatigue life of the RAP binders without the SATS conditioning was decreased with the increase in the RAP ratio irrespective of the rejuvenator types.

Meanwhile, Figure 4.15 shows that the difference in the effect of the SATS conditioning on the fatigue behaviour between the RAP1 and RAP2 binders. The binder from the 30% RAP1 mixture reduced fatigue life whereas that from the 60% RAP1 binder showed little change in the failure life after the conditioning. The RAP2 binders did not show any significant changes in fatigue behaviour for the 30% RAP contents through the conditioning, whilst it demonstrated larger initial strain with the shorter failure life for the 60% RAP contents after the conditioning.

These results suggest that the G^* ratio ($G^*_{conditioned}/G^*_{unconditioned}$) is harmonized with fatigue test results. As can be seen in Figure 4.10, 60% RAP1-HMA binder showed slight increase in the G^* ratio whilst that of WMA binder indicated significant drop in the ratio. 30% RAP1, 30% RAP2 and 60% RAP2 binders also showed changes in the G^* ratio with and without the SATS conditioning. The same trend can be seen in fatigue test results. In particular, 60% RAP1 binder showed increase in failure cycles whereas HMA binder demonstrated significant reduction in failure life, with and without the condition. Other binders also exhibited changes in failure cycles after the condition. Therefore, it implies that both the G^* ratio and the fatigues results are harmonizing.

In addition, it is speculated that the types of rejuvenator also affects these results. The RAP1 is resin based binder, whereas both virgin and RAP2 are asphaltenes based binder as shown in Figure 4.1. Therefore, this implies that RAP1 binder might be strong against combined aging, whilst HMA and RAP2 binders would be

less durable for the aging. However, further investigation needs to be conducted through mixture test result.

In case of test results summarized with stress level, the results demonstrated clear difference among HMA, RAP1 and RAP2 binders. For results obtained from without SATS conditioning, fatigue curve results showed difference in each RAP ratio. This trend was confirmed both in RAP1 and RAP2 binders. However, as to the results provided from with the conditioning, significant differences can be seen between RAP1 and RAP2 binders. For RAP1 binder, fatigue curve for 30% and 60% RAP binders showed similarity in the results. However, for RAP2 binder, fatigue cycles for those binder showed parallel curve in the results. These results might demonstrate differences in rejuvenator types. Therefore, chemical composition of rejuvenator and rejuvenated binders might affect rheological property of those binders.

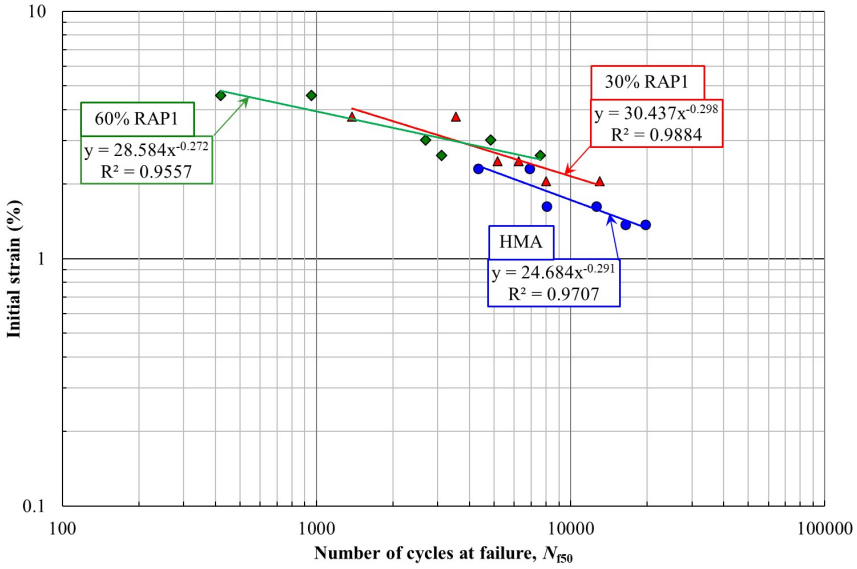

(a)

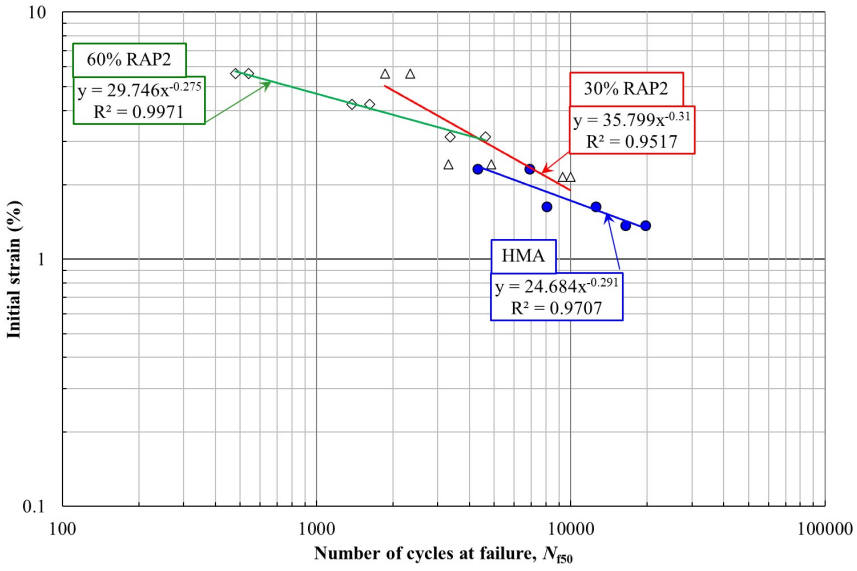

(b)

Figure 4.14 Relationships between the initial strain and the number of cycles at failure from the binder fatigue tests without SATS conditioning (a) HMA & RAP1 binders (b) HMA & RAP2 binders

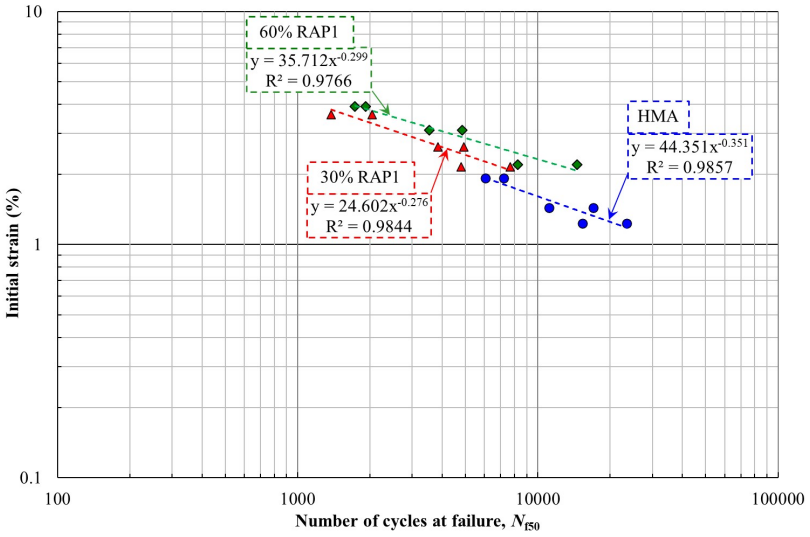

(a)

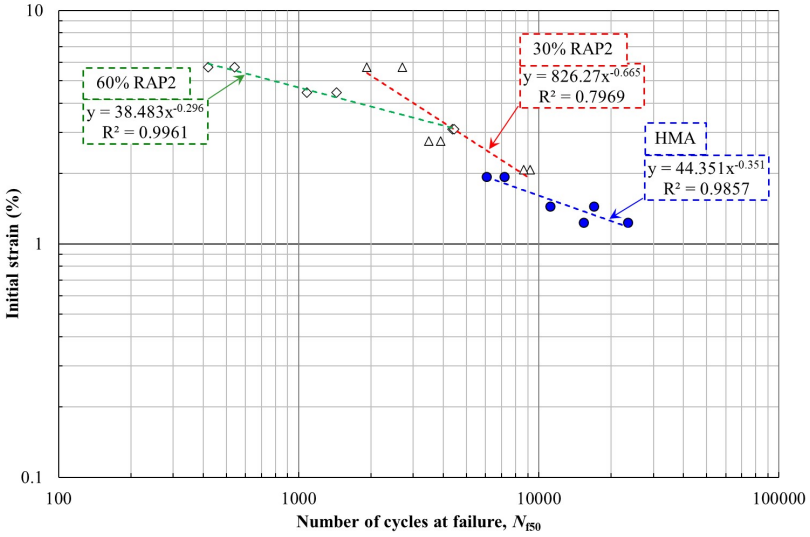

(b)

Figure 4.15 Relationships between the initial strain and the number of cycles at failure from the binder fatigue tests with SATS conditioning (a) HMA & RAP1 binders (b) HMA & RAP2 binders

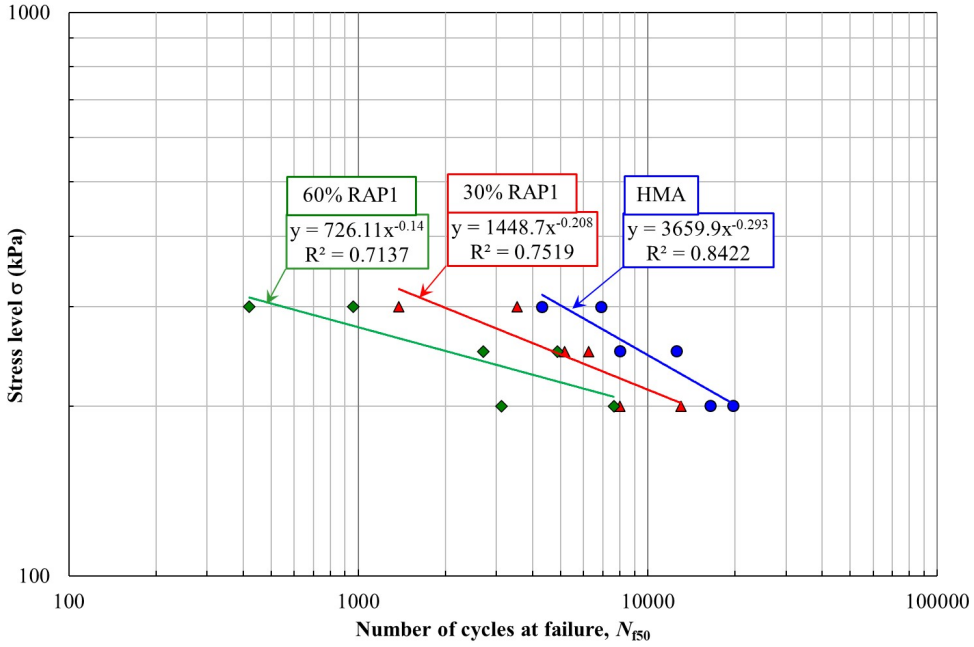

(a)

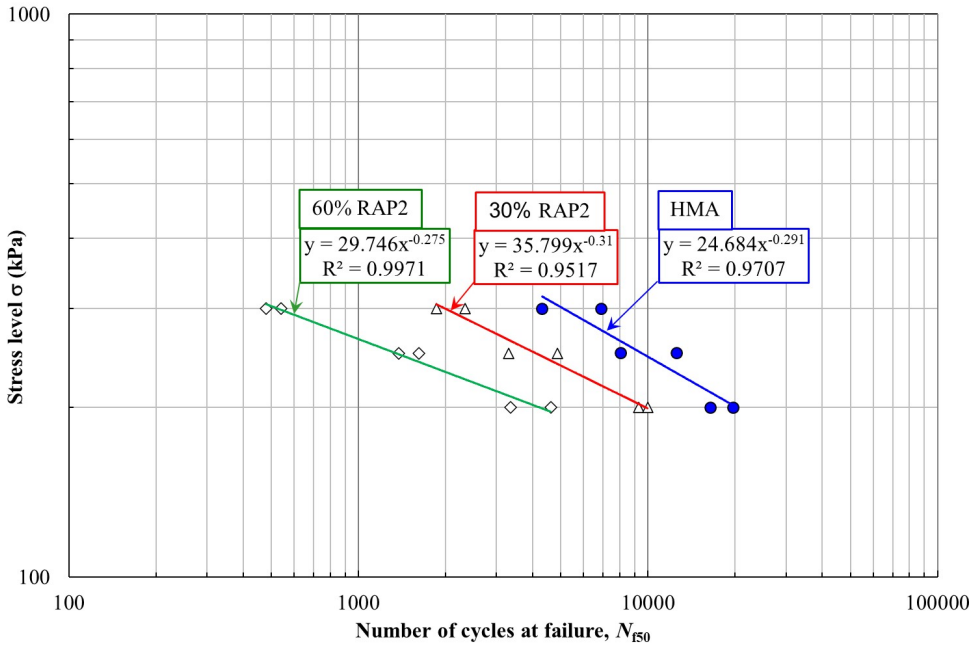

(b)

Figure 4.16 Relationships between the stress level and the number of cycles at failure from the binder fatigue tests without SATS conditioning (a) HMA & RAP1 binders (b) HMA & RAP2 binders

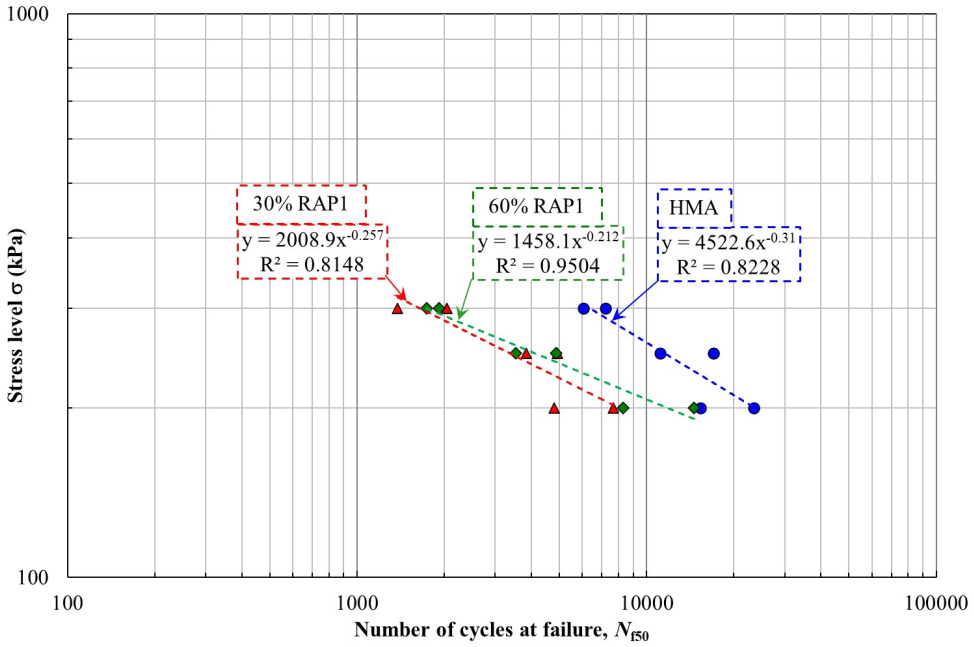

(a)

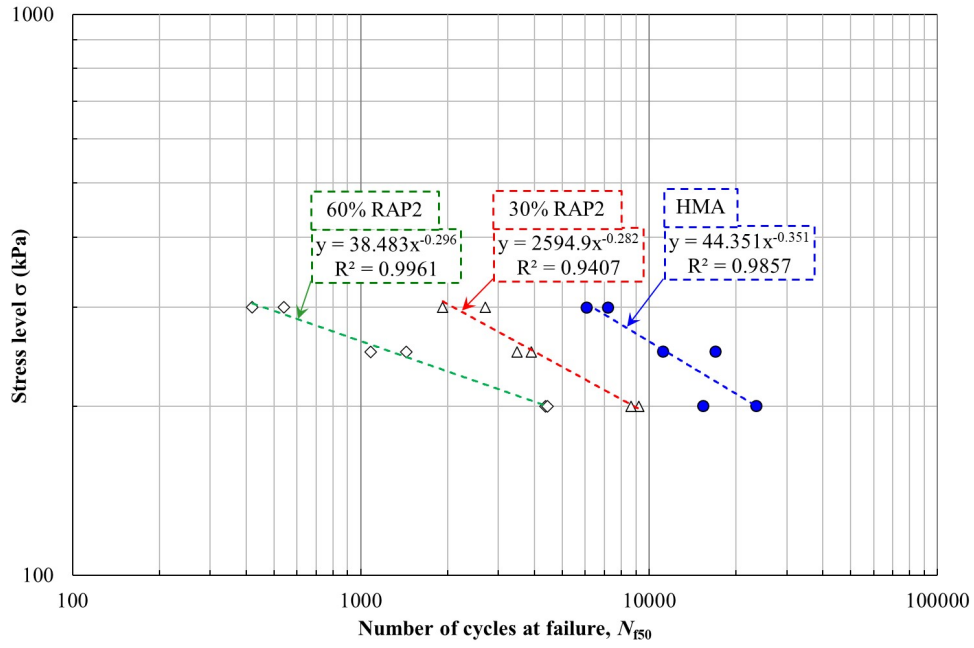

(b)

Figure 4.17 Relationships between the stress level and the number of cycles at failure from the binder fatigue tests with SATS conditioning (a) HMA & RAP1 binders (b) HMA & RAP2 binders

4.6 FATIGUE BEHAVIOUR OF HMA AND RAP BINDERS WITH 20% REDUCTION IN DISSIPATED ENERGY

To understand the fatigue characteristics of the binders extracted from the specimens of five types of mixtures with and without combined aging, fatigue tests were also performed on the binders using DSR. As shown in Figure 3.13, the tests were conducted under stress-control conditions.

The failure criterion shown in Figure 4.18 is used to determine the number of cycles at fatigue failure. Figure 4.18 shows an example of the relationship between the dissipated energy ratio (*DER*) and the number of cycles obtained from the test. The *DER* is defined as follows:

$$DER=\frac{\sum_1^N W_i}{W_N}, \tag{4.1}$$

where W_N is the dissipated energy in cycle N, W_i is the dissipated energy in cycle i, and $\sum_1^N W_i$ is the total sum of the dissipated energy up to cycle N. W_i can be obtained as follows:

$$W_i = \pi\sigma_i\varepsilon_i sin\varphi_i \tag{4.2}$$

where σ_i is the stress level in cycle i, ε_i is the strain level in cycle i, and φ_i is the phase angle in cycle i.

In general, cracks propagate when the actual *DER* decreases by 20% relative to the *DER* in the non-destructive state, as represented by the straight line in Figure 4.18. Thus, the number of cycles at failure (N_f) was determined when the actual *DER* decreased by 20%.

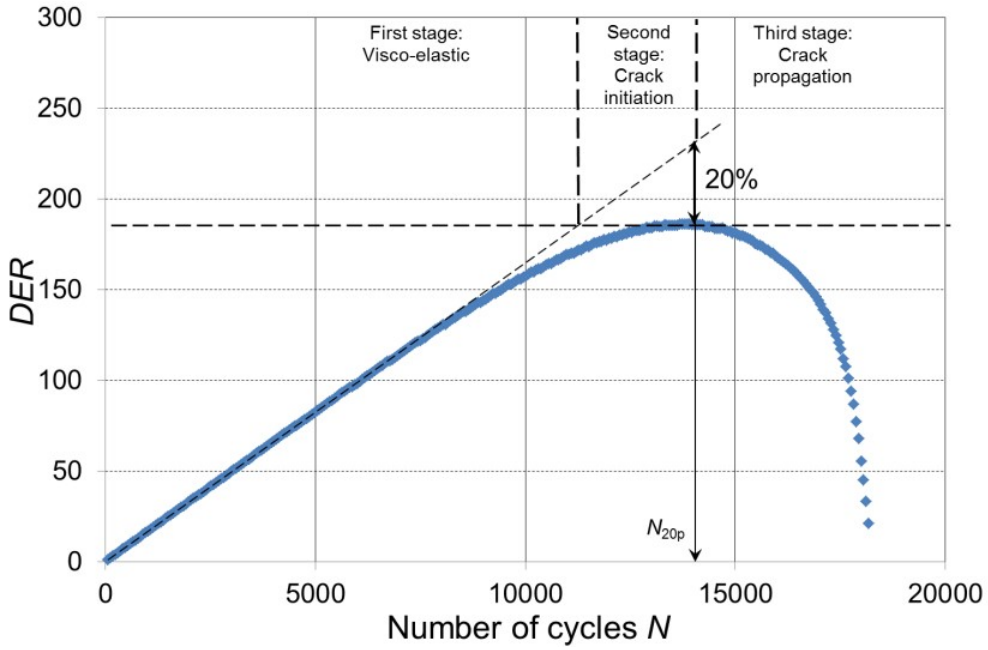

Figure 4.18 Failure criterion using dissipated energy ratio (*DER*) to determine the failure state in the fatigue test using DSR (HMA binder)

Figures 4.19 and 4.20 show the test results obtained for the specimens without SATS conditioning and those with SATS conditioning. In Figure 4.19 (a) and (b), the relationships between the initial *DER* and the number of loading cycles at failure of the RAP binders without SATS conditioning are located on the upper left side of those of the HMA binder. This indicates that RAP binders are less durable against fatigue than HMA binders. In addition, there is a tendency for the fatigue life of the RAP binders without SATS conditioning to decrease with an increase in the RAP content, irrespective of the rejuvenator type. These observations are consistent with those shown in Figure 4.19.

Comparing the results in Figure 4.19, it can be observed that the changes in the fatigue behaviors of the binders from SATS conditioning are insignificant (see Figure 4.20). However, a more detailed analysis revealed differences in the effects of SATS conditioning on the fatigue behaviors of RAP1 and RAP2 binders. The RAP 2 binders did not show any significant differences in fatigue behaviors with and without SATS conditioning. Notably, the HMA binder also showed little difference in fatigue behaviors with and without SATS conditioning. However, the binder from the 30% RAP1 mixture showed a slight reduction in fatigue life, whereas that from the 60% RAP1 mixtures showed a slight increase in failure life when experiencing SATS conditioning. These trends are consistent with those observed in Figure 4.20.

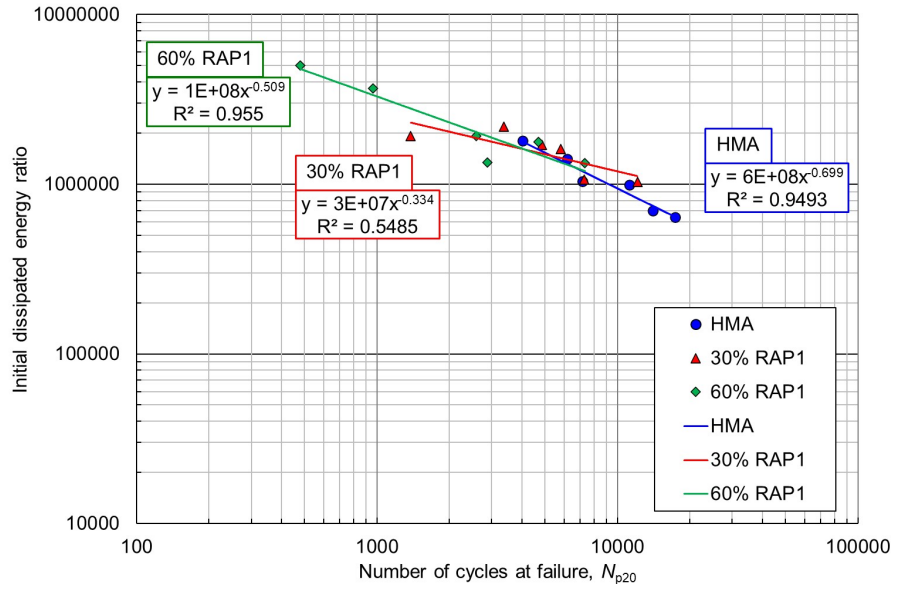

(a)

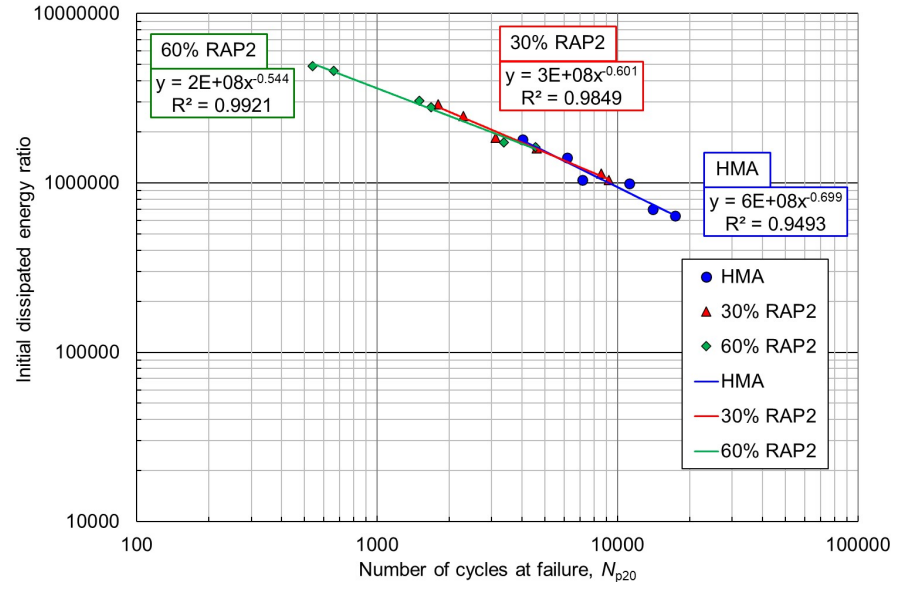

(b)

Figure 4.19 Relationships between the initial dissipated energy ratio and the number of cycles at failure from the binder fatigue tests without SATS conditioning (a) HMA & RAP1 binders, (b) HMA & RAP2 binders

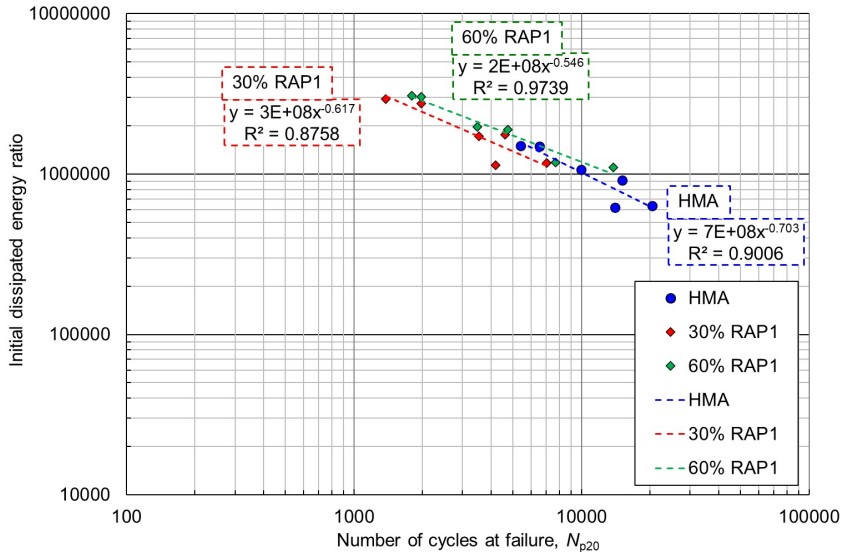

(a)

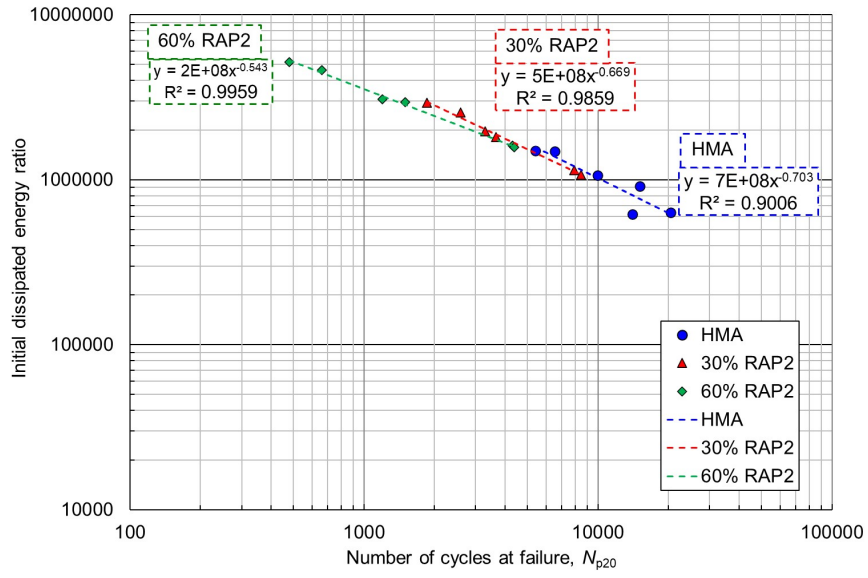

(b)

Figure 4.20 Relationships between the initial dissipated energy ratio and the number of cycles at failure from the binder fatigue tests with SATS conditioning (a) HMA & RAP1 binders, (b) HMA & RAP2 binders

4.7 SUMMARY

To assess the durability of RAP mixtures, the mechanical and physical properties of RAP mixtures with 30 and 60% RAP ratio blended with two types of oil-based rejuvenator agents (denoted as 30% RAP1, 60% RAP1, 30% RAP2, and 60% RAP2 mixtures, respectively), both with and without SATS conditioning, were experimentally investigated. For comparison, the properties of the HMA mixtures were investigated in the same way. In the experiments, SATS conditioning was used to simulate combined aging. The following conclusions were obtained from the test results.

1. Significant trends were observed in the changes in the properties of the HMA and RAP mixtures with SATS conditioning. The ITSM test results demonstrated that the RAP mixtures with rejuvenators did not show a reduction in retained stiffness, whereas the HMA mixtures showed a significant drop in stiffness with SATS conditioning. In addition, in the ITFTs, the RAP mixtures with rejuvenators showed a longer residual service life than the HMA mixture after the damage from SATS conditioning. These trends were more pronounced for higher RAP content. In addition, detailed analyses showed that there were differences in the fatigue behaviors of RAP mixtures with different rejuvenators. These differences might be attributed to differences in the compaction performances of the RAP mixtures with different rejuvenators, which could (in turn) be due to the different components of the chemical properties of the RAP binders.
2. The RAP mixtures with rejuvenators showed a lower stripping ratio with SATS conditioning than that of the HMA mixture. This trend became more pronounced as RAP content increased. All the experimental results suggested that the adhesion states of the binder and aggregates caused a difference in durability between the HMA mixture and RAP mixtures with SATS conditioning.
3. Asphalt binders were extracted from the laboratory specimens of five types

of the mixtures (HMA, 30% RAP1, 60% RAP1, 30% RAP2 and 60%), in order to investigate the binder properties with and without the SATS conditioning. The properties of the extracted binders were evaluated through frequency sweep tests and fatigue tests using DSR. The results demonstrated that there was no significant change in the properties of each binder with the SATS conditioning. This was probably due to the fact that the low pressure of 0.5 MPa and the curing period of 24 hours set by the SATS conditioning in this study. However, the detailed analyses of the test results showed that there were differences in the stiffness and the fatigue results among the RAP binders with different rejuvenators with the SATS conditioning. The different trends in the effects of the SATS conditioning on the RAP1 and RAP2 binders might be attributed to the difference in the chemical composition of the binders, which were brought by different rejuvenators.

CHAPTER 5

Combined Aging Characteristics of WMA with RAP

5.1 INTRODUCTION

This chapter examines the assessment of WMA and RAP-WMA mixtures associated with rejuvenator using the Saturation Aging Tensile Stiffness Test (SATS) conditioning. Two types of rejuvenator were investigated related to RAP binders and mixtures. In this experiment, 30% and 60% RAP mixtures were studied compared with WMA and those characteristics are addressed through stiffness modulus and fatigue properties obtained from Nottingham Asphalt Tester (NAT) and Dynamic Shear Rheometer (DSR). The moisture and aging damage mechanism for RAP mixtures are examined related to mixture and binder results.

5.2 PREPARATION OF MIXTURES

In this study, five types of WMA mixtures were prepared for laboratory experiments: fresh WMA mixture, and WMA mixtures with 30% and 60% RAP ratio blended with two types of rejuvenator agents. The mixture design is the same as that of HMA mixture. WMA additive (i.e. wax) was added to each virgin binder. The dosage amount of the additive is three percent of total binder (i.e. virgin and RAP binders). After blending virgin binder with the additive, the blended binder was added to hot aggregates during manufacture process. Then the aggregates and binder were mixed in laboratory mixer. After manufacturing specimen, the density and air voids of specimen were measured. In addition, binder properties after

manufacturing specimen were also analyzed through binder tests (see Tables 5.1 to 5.5). These results show differences in each binder, and the detailed analysis results were discussed in following sections.

Table 5.1 Properties of WMA binder without SATS conditioning

	Penetration at 25°C (1/10 mm)	Softening point (°C)	Viscosity at 120°C (mPa.s)	Viscosity at 150°C(mPa.s)
WMA	39	59.5	837.3	188.3

Table 5.2 Properties of 30% RAP1-WMA binder without SATS conditioning

	Penetration at 25°C (1/10 mm)	Softening point (°C)	Viscosity at 120°C (mPa.s)	Viscosity at 150°C(mPa.s)
30% RAP1-WMA	46	56.5	1006	223.8

Table 5.3 Properties of 30% RAP2-WMA binder without SATS conditioning

	Penetration at 25°C (1/10 mm)	Softening point (°C)	Viscosity at 120°C (mPa.s)	Viscosity at 150°C(mPa.s)
30% RAP2-WMA	46	54.5	948.1	209.3

Table 5.4 Properties of 60% RAP1-WMA binder without SATS conditioning

	Penetration at 25°C (1/10 mm)	Softening point (°C)	Viscosity at 120°C (mPa.s)	Viscosity at 150°C(mPa.s)
60% RAP1-WMA	46	54.5	1361	280.8

Table 5.5 Properties of 60% RAP2-WMA binder without SATS conditioning

	Penetration at 25°C (1/10 mm)	Softening point (°C)	Viscosity at 120°C (mPa.s)	Viscosity at 150°C(mPa.s)
60% RAP2-WMA	53	54	1193	246.2

5.3 CHANGES IN PROPERTIES OF MIXTURES THROUGH THE CONDITIONING

Properties of five types of the mixtures (WMA, 30% RAP1-WMA, 60% RAP1-WMA, 30% RAP2-WMA and 60% RAP2-WMA) were evaluated through ITSM tests and ITFTs as shown in Figures 3.7 to 3.8. In this chapter, first, the stiffness obtained from the ITSM tests are presented, meanwhile the fatigue properties obtained from ITFTs will be presented in the subsequent section. It should be noted that the fatigue behaviors of the mixtures experiencing the SATS conditioning were investigated to assess their residual service life remained after the damage from the conditioning.

5.3.1 Stiffness modulus

To investigate the change in the stiffness of the mixtures with and without the SATS conditioning, the ITSM tests were conducted on the five types of the mixtures (WMA, 30% RAP1-WMA, 60% RAP1-WMA, 30% RAP2-WMA and 60% RAP2-WMA). The testing condition was depicted in Figure 3.7. Table 5.6 demonstrates the obtained stiffness and the air void content of the mixtures with and without the SATS conditioning. It should be noted that the stiffness shown in the table was the average of the stiffness obtained from three specimens for each mixture. The standard deviation and covariation values are also shown in the table. As in the table, for the condition without the SATS conditioning, the average stiffness of the RAP-WMA mixtures were lower than that of WMA mixture, although the RAP 1 and RAP 2 binders were adjusted to be the 70 pen grade with the rejuvenators before adding the wax. The fact indicated that stiffness of RAP-WMA mixtures can differ from that of WMA, even if the penetration of binder and the grading of the RAP mixtures are adjusted to be close to those of the WMA mixture. The reason why the RAP-WMA mixtures showed the stiffness lower than that of the WMA mixture may be linked to the rheological properties of the RAP-WMA binders which is presented in Figure 5.11. Further discussion will be conducted in following sections.

Table 5.6 Stiffness of the mixtures with and without SATS conditioning (WMA and RAP-WMA mixtures)

	WMA		30% RAP1		60% RAP1		30% RAP2		60% RAP2	
	Without	With	Without	With	Without	With	Without	With	Without	With
Average air voids (%)	4.7		5.0		5.3		4.9		4.9	
Average stiffness (MPa)	2952	2423	2469	2694	2147	2527	2551	2235	2063	2261
Std Dev. Stiffness (MPa)	298	128	146	52	120	82	35	265	75	18
CoV Stiffness (%)	10	5	6	2	6	3	1	12	4	1

In Figures 5.1 (a) and (b), the retained stiffness ratio (i.e., the ratio of stiffness with the SATS conditioning to that without the SATS) was plotted against the retained saturation for each specimen. It is found that the ratio decreases with the increase in the retained saturation, suggesting that the decrease in the mixture stiffness caused by the SATS conditioning is strongly related to increase in the retained saturation. In the figure, the RAP-WMA mixtures showed the higher retained stiffness ratios with lower retained saturations compared to the WMA mixtures, indicating that the RAP-WMA mixtures would degrade less against the combined aging than the WMA mixture, in terms of stiffness. Furthermore, with regard to retained saturation, it appears that changes in retained stiffness occurs at around 50% in the saturation. This trend is more pronounced for the WMA and 30% RAP2-WMA mixtures showing significant drop in the retained stiffness ratio at around 0.8. Therefore, there seems to be existed phase change point for the WMA and RAP-WMA mixtures in the retained saturation. In terms of retained saturation, all mixtures were plotted between 20 to 80%, as shown in the previous chapter.

With regard to rejuvenator, it appears that rejuvenator type would affect both retained stiffness ratio and saturation. For RAP1-WMA mixture, both 30% and 60% contents were retained at 1.0 or higher. Since these mixtures have high in resin components in RAP binder as shown in Figure 4.1, this might be the effect of rejuvenator added. The same trend as the RAP1-WMA mixture can be seen in 60% RAP2-WMA mixture. In this case, it seems that RAP aggregates might be influenced in the stiffness of 60% RAP2-WMA mixture after the conditioning. However, there seems significant drop in 30% RAP2 -WMA mixture. Because virgin binder is still dominated in the 30% RAP2 mixture, the specimen might show similar ratio to that of WMA mixture. In addition, RA binder with rejuvenator 2 indicates similar components to virgin binder, the specimens may be influenced by the effect of the combined aging. Therefore, further investigations were made in fatigue test results.

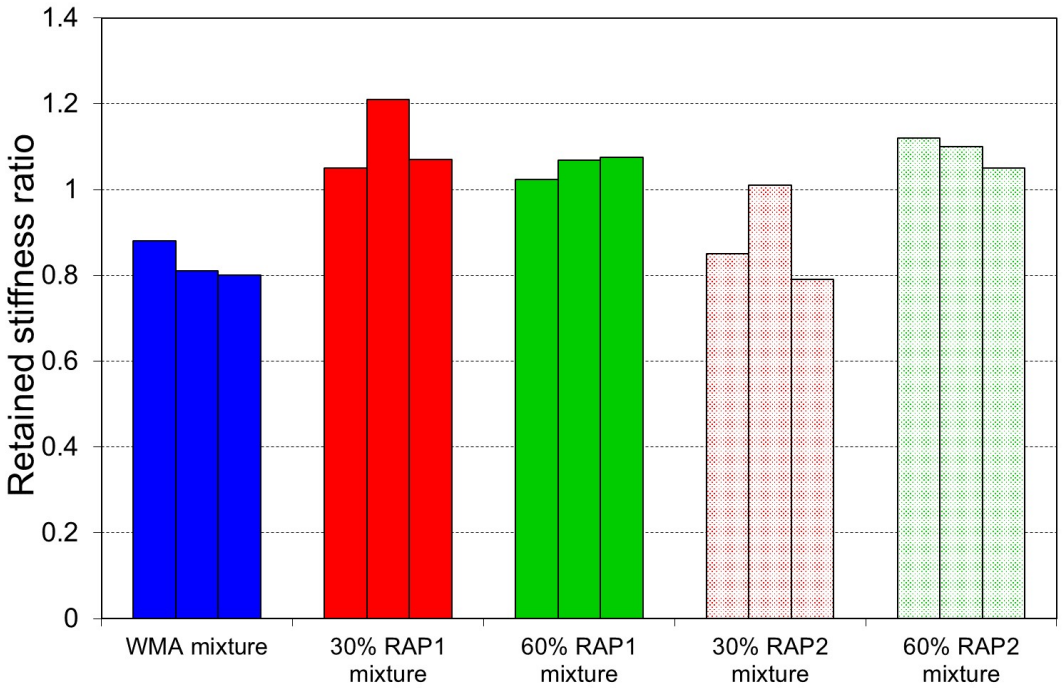

(a)

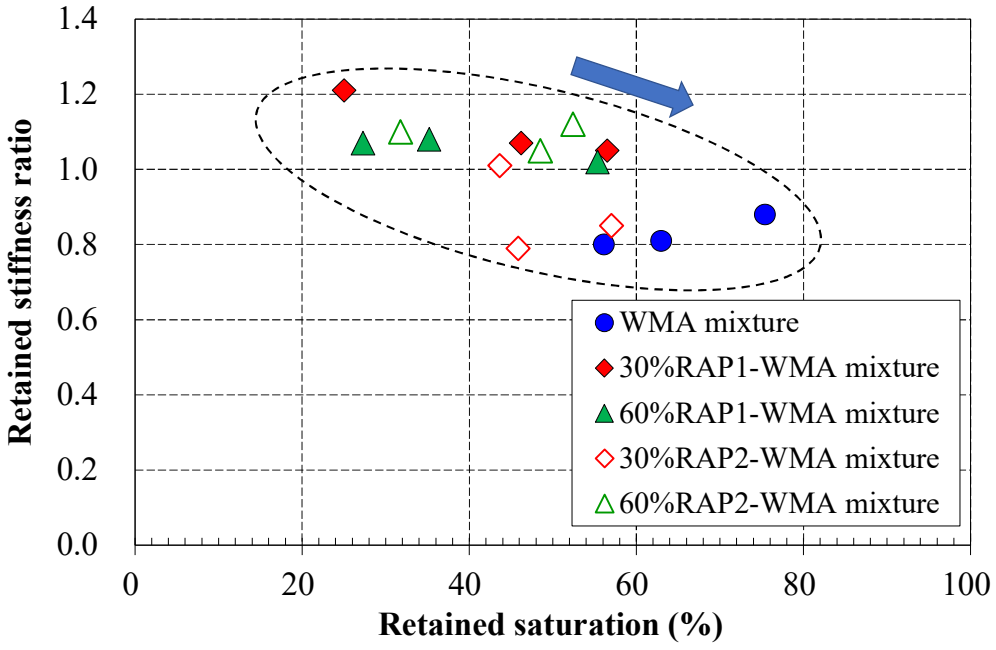

(b)

Figure 5.1 Relationships between the retained stiffness ratio and retained saturation for each WMA mixture

5.3.2 Fatigue behavior and residual service life

Fatigue characterists of the five mixtures with and without SATS conditioning were evaluated through the ITFTs, following the test conditions shown in Figure 3.8. As shown in the previous chapter, the fatigue characteristics of WMA mixture were examined by assuming its vertical deformation as changes in stiffness modulus through ITFT. In this casee, changes in specimen diameter was also normalised by dividing it into its initial diameter (normalised creep stiffness = (specimen diameter-vertical deformation)/specimen diameter). The calculated value was called "normalised creep stiffness" and the relationship between the normalised creep stiffness and fatigue characteristics was studied through the experiment. In the experiments, 50% stiffness reduction was defined as fatigue failure point in each specimen (see Figure 5.2). This research also examined the fatigue characteristics of RAP-WMA mixture, following this assumption.

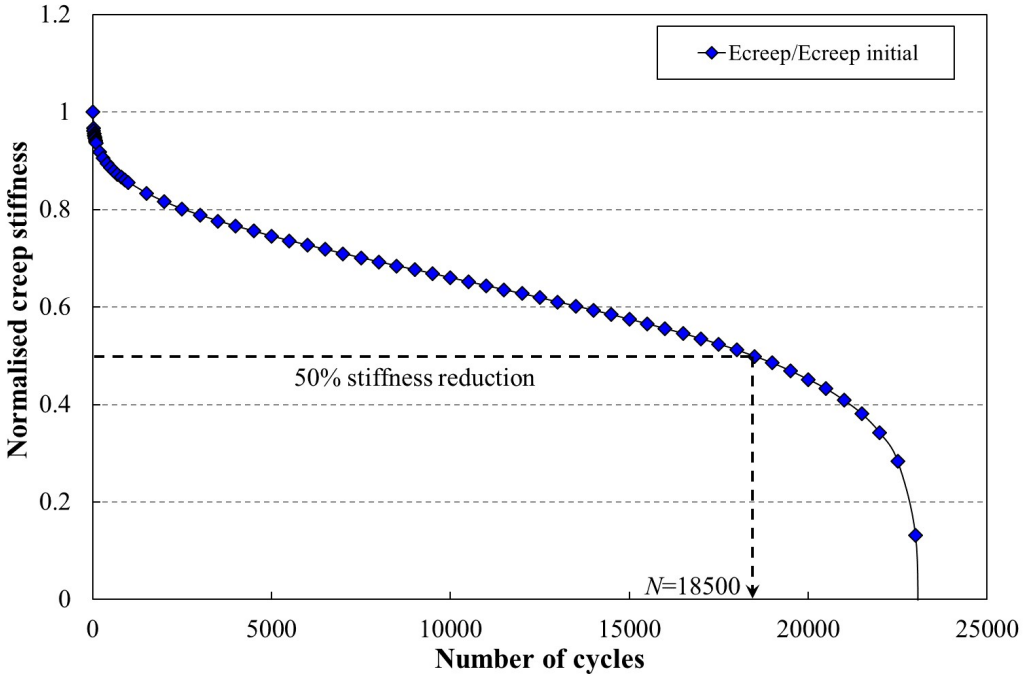

Figure 5.2 Difference in fatigue failure criteria (WMA and RAP-WMA mixtures)

Figures 5.3 and 5.5 present the results of the ITFTs conducted on the WMA and RAP-WMA mixtures without SATS conditioning and Figures 5.4 and 5.6 show those with the SATS conditioning. The relationships among the initial strain, the stress level and the number of cycles at failure are shown in the figures. It was found in Figure 5.3 that both the RAP 1-WMA and RAP 2-WMA mixtures showed longer fatigue cycles compared to the WMA mixture, despite showing the initial strain nearly same as that of the WMA mixture. The observation was different from that observed for the fatigue properties of the binders (see Figures 5.13 to 16). The fact suggests that the adhesion state of the binder and aggregates might have a significant influence on the fatigue properties of the mixtures.

In Figures 5.4 and 5.6, the RAP-WMA mixtures with the SATS conditioning demonstrated a longer residual service life compared to the WMA mixture with SATS conditioning. It can be also seen that the number of cycles at failure of the WMA mixtures with the SATS conditioning was reduced relative to that without the SATS conditioning. However, looking at Figure 5.4, the initial strain of the RAP-WMA mixtures did not change significantly with or without SATS conditioning, except for 30% RAP2-WMA mixture. However, the results showed the differences in RAP1-WMA and RAP2-WMA mixtures, in terms of initial strain and failure life. This agrees with the fact that the retained stiffness ratios of the RAP-WMA mixtures are relatively close to 1.0, as shown in Figure 5.1. Similar trend to this result can be seen in stress level results shown in Figure 5.6.

These results implies that the retained stiffness ratio and the fatigue result are harmonizing after the SATS conditioning. As shown in Figure 5.1, 30% RAP1-WMA, 60% RAP1-WMA and 60% RAP2-WMA mixtures remained similar stiffness with and without the SATS condition, showing 1.0 in retained stiffness ratio, whilst 30% RAP2-WMA and WMA mixtures indicated reduction in the stiffness ratio, showing 0.8 after the condition. Similar trend to the retained stiffness ratio can be seen in fatigue results as shown in Figures 5.4 and 5.6. RAP1-WMA and 60% RAP2-WMA mixtures did not show significant changes in

initial strain with and without the condition, 30% RAP2-WMA and WMA mixtures indicated changes in the initial strain with the condition. Furthermore, the initial strain of 30% RAPs-WMA mixture were closed to that of WMA mixtures after the condition. These results suggest the fatigue results showed similarity in the retained stiffness ratio, thus it can be said that both the retained stiffness and the fatigues results are harmonizing in WMA and RAP-WMA mixtures.

In case of results summarized with stress level, remarkable results can be found in Figures 5.5 and 5.7. In case of the test results without SATS conditioning, both RAP1 and RAP2 WMA mixtures demonstrate similar fatigue life with WMA mixture. However, for the test results with the conditioning, the results showed clear difference between WMA and RAP WMA mixtures in fatigue curve. RAP WMA mixtures demonstrated longer fatigue life than that of WMA mixture. This trend was confirmed both in RAP1 and RAP2 WMA mixtures. The same trend was confirmed in HMA and RAP mixtures, shown in the previous chapter. Therefore, this result suggests that high RAP WMA mixtures have longer fatigue cycles than that of WMA mixture. In addition, these results also suggest that the effect of wax used in this study did not give negative effect on fatigue life of RAP WMA mixtures.

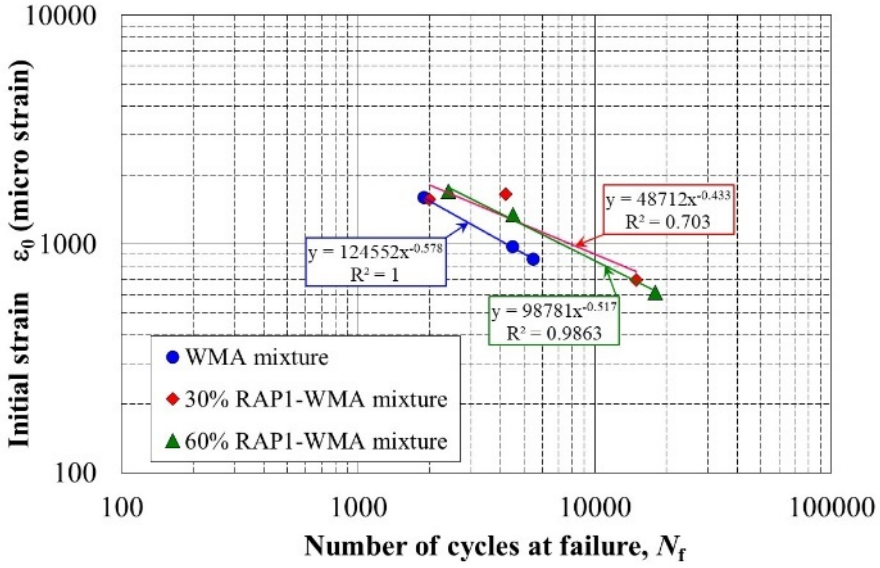

(a)

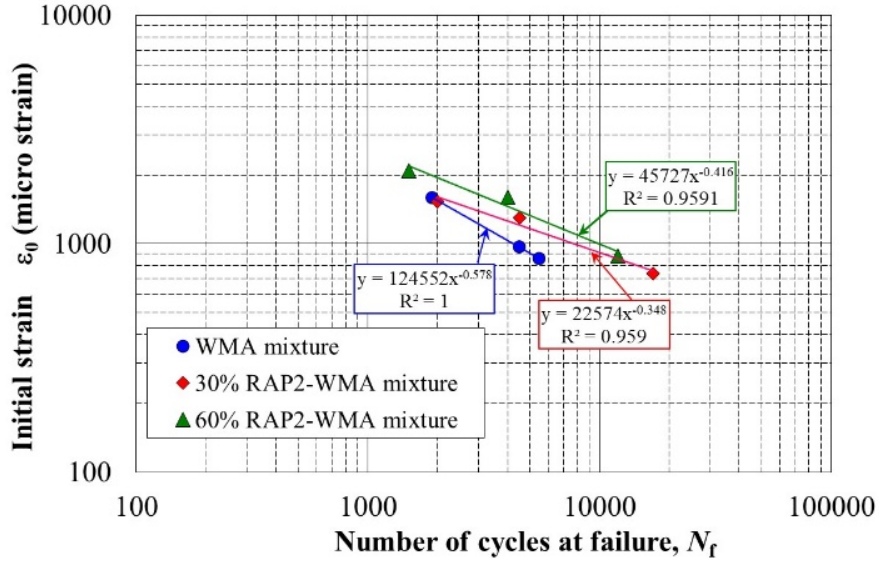

(b)

Figure 5.3 Relationships between the initial strain and the number of cycles at failure of the mixtures without SATS conditioning from ITFTs-50% reduction (a) WMA & RAP1 mixtures, (b) WMA & RAP2 mixtures

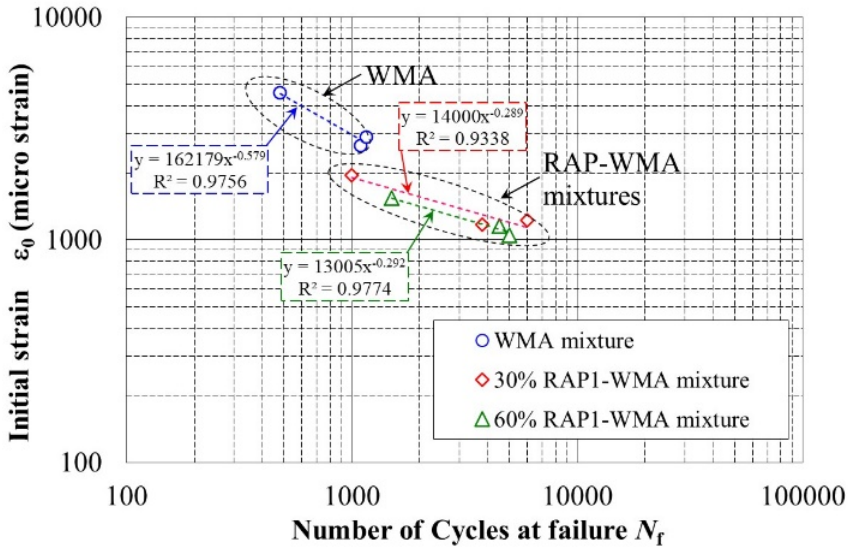

(a)

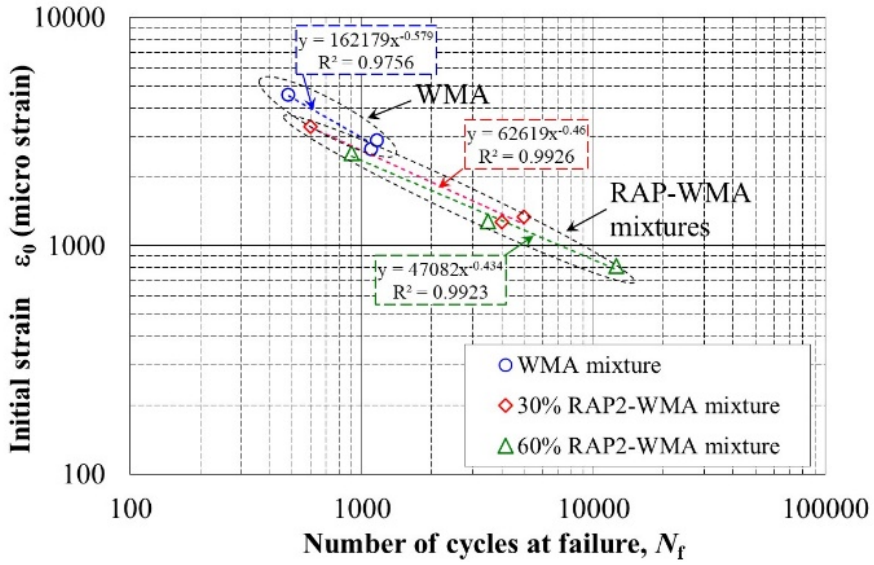

(b)

Figure 5.4 Relationships between the initial strain and the number of cycles at failure of the mixtures with SATS conditioning from ITFTs-50% reduction (a) WMA & RAP1 mixtures, (b) WMA & RAP2 mixtures

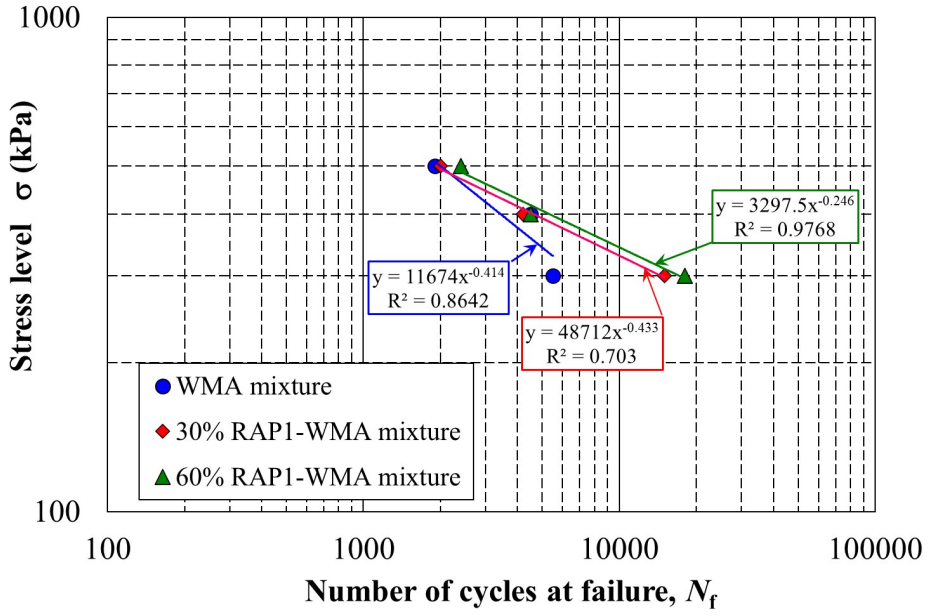

(a)

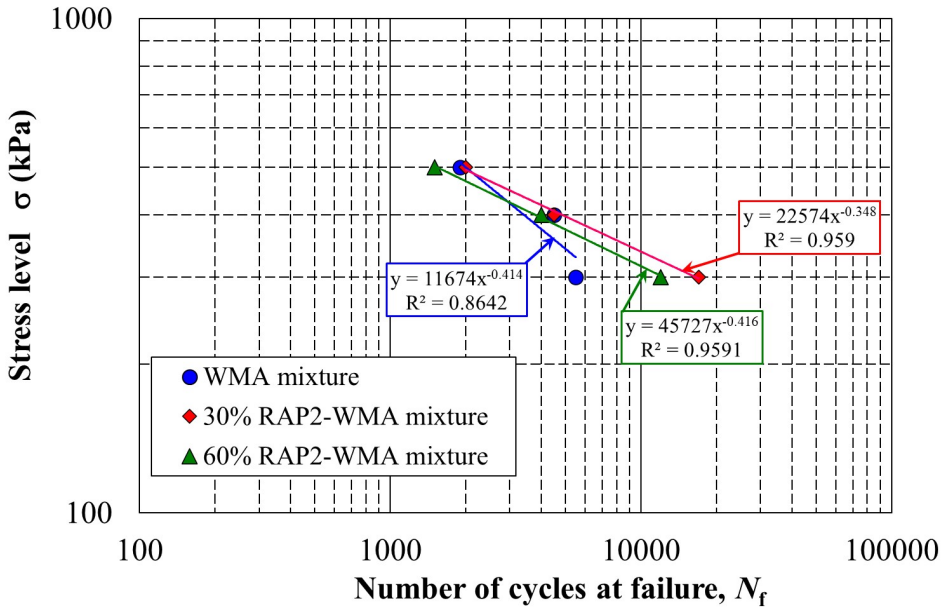

(b)

Figure 5.5 Relationships between the stress level and the number of cycles at failure of the mixtures without SATS conditioning from ITFTs-50% reduction (a) WMA & RAP1 mixtures, (b) WMA & RAP2 mixtures

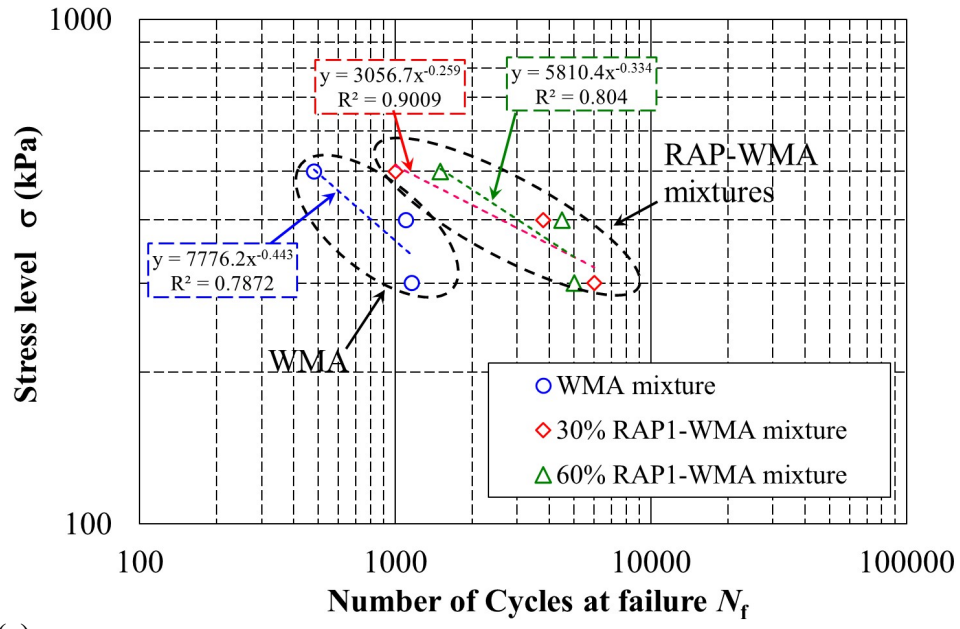

(a)

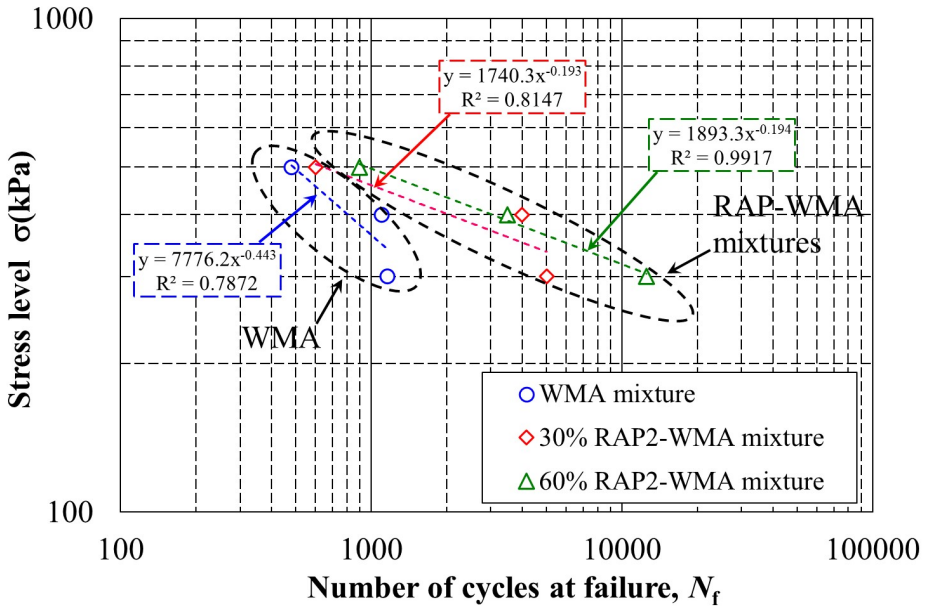

(b)

Figure 5.6 Relationships between the stress level and the number of cycles at failure of the mixtures with SATS conditioning from ITFTs-50% reduction (a) WMA & RAP1 mixtures, (b) WMA & RAP2 mixtures

5.3.3 Mixture failure pattern

To understand the fatigue characteristics of WMA and RAP-WMA mixtures from failure pattern perspective, the fatigue results of the five specimens were analysed in this study. The same analysis at that of HMA and RAP mixture was conducted in this section. Figure 5.7 shows the fatigue failure patterns for WMA and RAP-WMA mixtures with SATS conditioning, based on ITFT results conducted at 500kPa. As can be seen in the results, the differences in RAP ratio and rejuvenators were shown in each failure mode. RAP mixtures showed longer fatigue life, when compared with that of WMA mixtures. This result is more pronounced when RAP ratio was increased from 30% to 60%, and the same trend can be seen in RAP1-WMA and RAP2-WMA specimens.

Meanwhile, looking at differences in rejuvenators, RAP1-WMA mixtures demonstrated longer fatigue life, when compared with that of RAP2-WMA mixtures. As described in the previous section, despite the fact that RAP 1 specimen showed slight difference in air void contents compared to RAP 2 specimens, it indicated longer fatigue life. In addition, more remarkable trends were seen as RAP contents increase. This might indicate influence of rejuvenator for the mechanical properties of RAP-WMA mixtures. Therefore, it seems that this result might suggest the differences in rejuvenators, in the fatigue life of RAP-WMA mixtures.

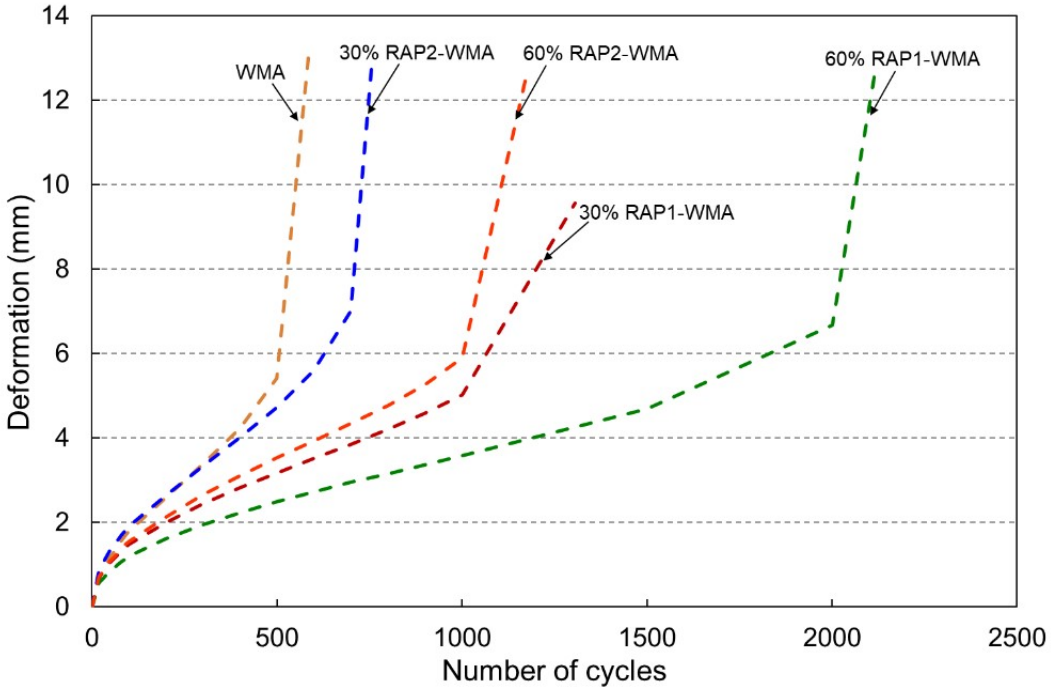

Figure 5.7 Fatigue relationships for WMA and RAP-WMA mixtures with SATS conditioning (Stress level: 500 kPa)

5.4 STRIPPING CHARACTERISTICS OF THE MIXTURES WITH THE SATS CONDITIONING

Stripping characteristics of WMA and RAP-WMA mixtures were also examined after the conditioning. After measuring retained stiffness, each specimen was divided into two-cross-sections, then the stripping area were assessed through analysis, in accordance with the Japanese standard of immersed wheel tracking test, B004 (Plastic film depicting mesh was placed on the cross-section, then stripped area was counted, and stripping ratio was calculated).

In terms of the results, the same trend as that of HMA and RAP mixture was seen in this section. As can be confirmed in Figure 5.8, the results suggest that the average stripping ratio of WMA mixture was higher than RAP mixture showing approximately 12% in WMA and less than 8% in RAP mixtures. In particular, the 30% and 60% RAP1 mixtures shows 1.1% and 1.8%, whereas those of RAP2 mixtures indicated 7.3% and 1.6%, respectively.

This result might be harmonized with retained stiffness shown in Figure 5.1. For RAP1-WMA mixtures, the results demonstrated that the retained stiffness shown in 30% and 60% RAP1-WMA remained at around 1.0. Meanwhile, RAP2-WMA mixtures reveal that the retained stiffness was dropped as RAP contents decreased from 60% to 30%. These results shows the same trend as the stripping characteristics obtained from the previous chapter. Therefore, this result implies that the stripping resistance of the mixtures might be related to retained stiffness of mixtures.

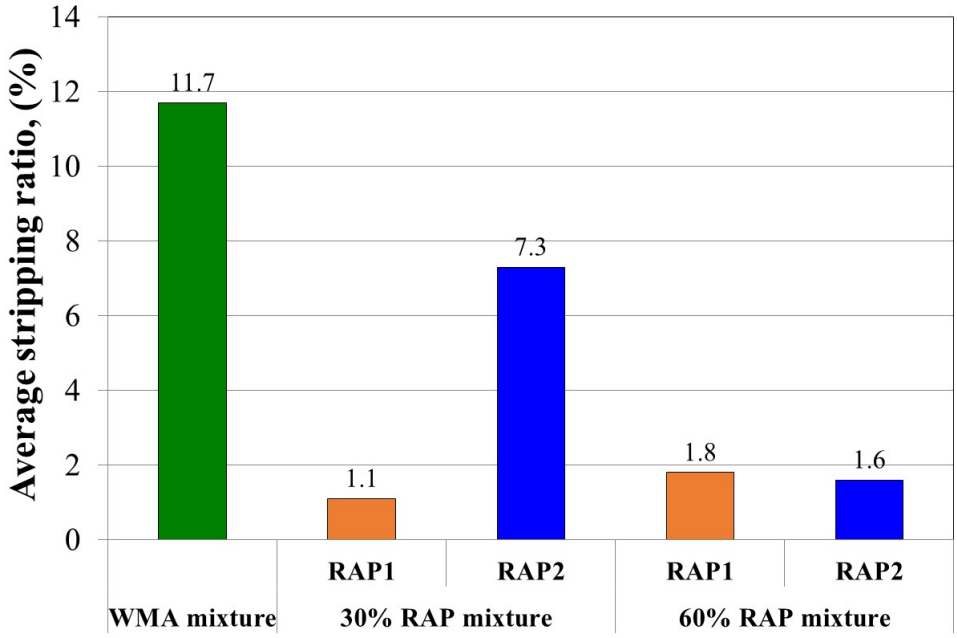

Figure 5.8 Average stripping ratio of WMA and RAP-WMA mixtures with the SATS conditioning (WMA and RAP-WMA mixtures)

5.5 CHANGES IN BINDER PROPERTIES THROUGH THE SATS CONDITIONING

To examine the mechanical properties of asphalt binders, the binders were extracted from the five asphalt mixture specimens with and without SATS conditioning. The binders' properties were evaluated through frequency-sweep tests, and fatigue test using Dynamic Shear Rheometer, DSR. The complex modulus and fatigue properties of the binders were examined through the tests.

5.5.1 Complex modulus

In the DSR tests, complex moduli, G^* and phase angles, δ of the binders were measured for the range of frequencies of 0.1-10 Hz at eight temperatures from 34 °C to 78 °C in 6 °C increments. These results were also assessed through master curves of G^* and black diagram.

Figure 5.9 shows master curves of binders extracted from the five types of mixture with and without SATS conditioning at a reference temperature of 34 °C. As can be seen in Figure 5.9 (a), the five binders showed slight differences in the G^* master curve. The WMA binder (i.e. the binder extracted from the WMA mixtures) indicates highest G^* value whereas the 60% RAP1-WMA binder (i.e. the binder extracted from the 60% RAP1-WMA mixture) demonstrated the lowest value amongst the five binders. This trend was consistent at all reduced frequency. However, the differences disappeared with SATS conditioning as in Figure 5.9 (b). Figure 5.9 (b) demonstrates that the five binders showed similar complex moduli at all reduced frequency. In particular, the complex moduli of the WMA binder were clearly reduced at all frequency by SATS conditioning. This indicated that the changes in binder properties by SATS conditioning were pronounced for the WMA binder.

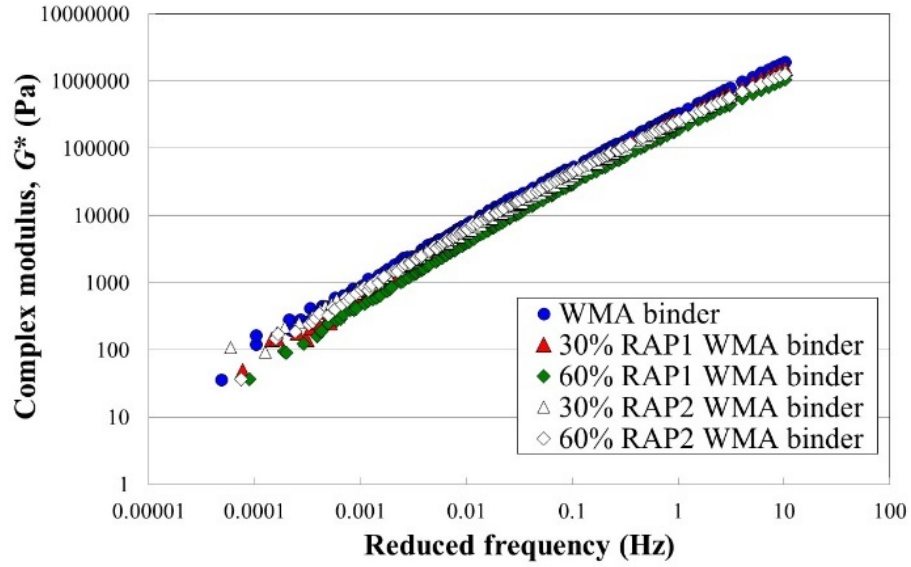

(a)

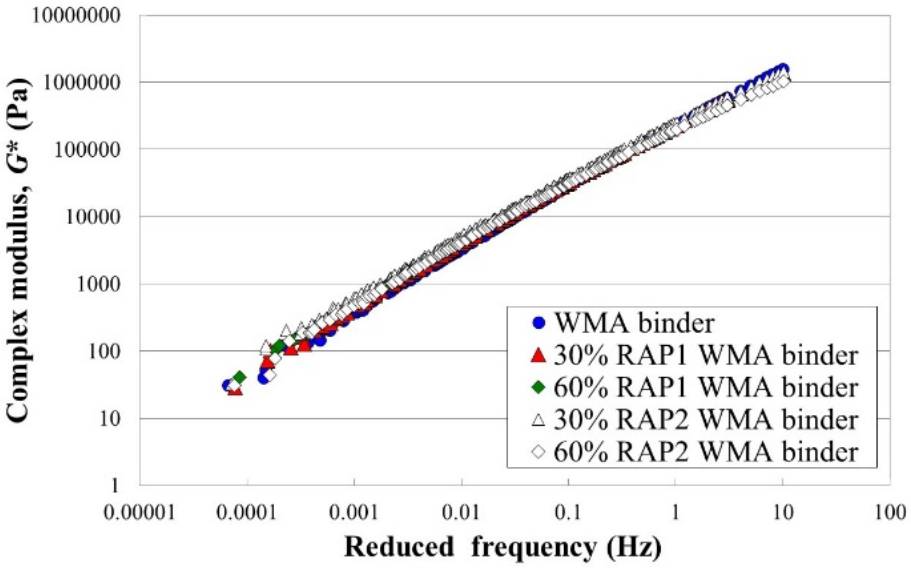

(b)

Figure 5.9 DSR Master curve of binders extracted from five types of mixture at a reference temperature of 34°C (a) Without SATS conditioning, (b) With SATS conditioning

In order to examine the binders' properties in more detail, the frequency–sweep test results were assessed through black diagram. Figure 5.10 presents the black diagram of the five binders with and without SATS conditioning. As shown in Figure 5.10 (a), both the WMA binder and the 30% RAP2-WMA binder (i.e. the binder extracted from the 30% RAP2-WMA mixture) demonstrated lower phase angle than the other three binders. Similar results to this behavior were seen in Qin *et al*. (2015) and Wang *et al*. (2018). Therefore, it can be said that this trend might be seen especially in wax modified binders.

However, of interest, Figure 5.10 (b) showed that the diagram of the WMA binder was shifted towards higher phase angle, whilst there were no dramatic changes in other four binders with the SATS conditioning. In case of WMA mixture production in laboratory, the wax is fully mixed with virgin binder, then WMA mixture is manufactured by mixing the WMA binder with aggregates. However, for RAP -WMA mixtures, the wax is mixed with lesser virgin binder contents than that of WMA mixture because RAP mixture already contains rejuvenated RAP binder. Assuming that the wax is influenced only for blended virgin binder, lesser effect is confirmed for RAP-WMA binders. Therefore, it is speculated that the WMA binder might be influenced by the effect of combined aging so that the wax additive blended with virgin binder might be dissipated after the conditioning.

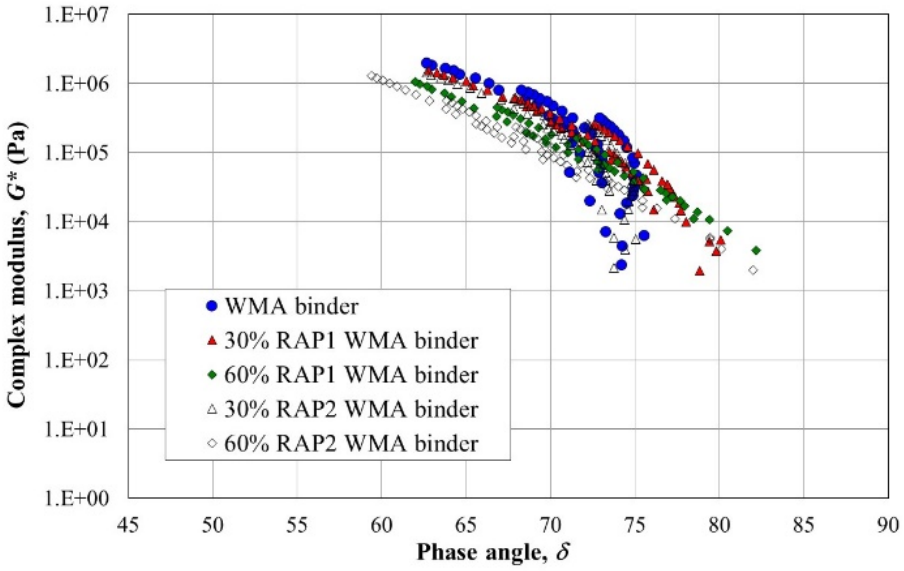

(a)

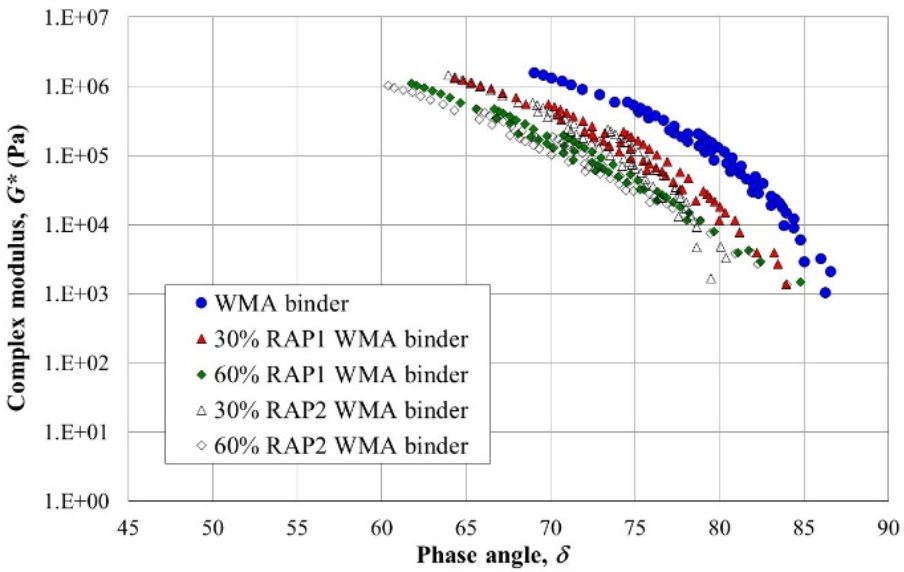

(b)

Figure 5.10 Black diagram of binders extracted from five types of mixture obtained from the frequency sweep test using DSR (a) Without SATS conditioning, (b) With SATS conditioning

Changes in the binder properties with and without SATS conditioning were examined in more detail, based on the ratio of G^* with the SATS conditioning, $G^*_{conditioned}$ to G^* without the SATS, $G^*_{unconditioned}$, as obtained at 10 Hz for each type of binders. As can be seen in Figure 5.11, the WMA binder showed a significant drop in G^* because the ratio indicates less than 0.8 from 34 to 76 °C. Meanwhile, the RAP1-WMA and RAP2-WMA binders showed different trend in the ratio. The RAP1-WMA binders indicate increase in the ratio toward 1.0, whilst the RAP2-WMA binders shows reduction in the ratio with the increase in the RAP contents. The difference in the trend may be induced by the difference in the chemical composition of the binders. As described in Figure 4.1, the RA binder with Rejuvenator 2 demonstrates similar chemical composition to the virgin binder in the SARA fraction, whereas the RA binder with Rejuvenator 1 shows different compositions from the virgin binder. In addition, the wax may influence the properties of virgin and RA binders. Therefore, the details of the reasons for the different trends need to be invested in future studies.

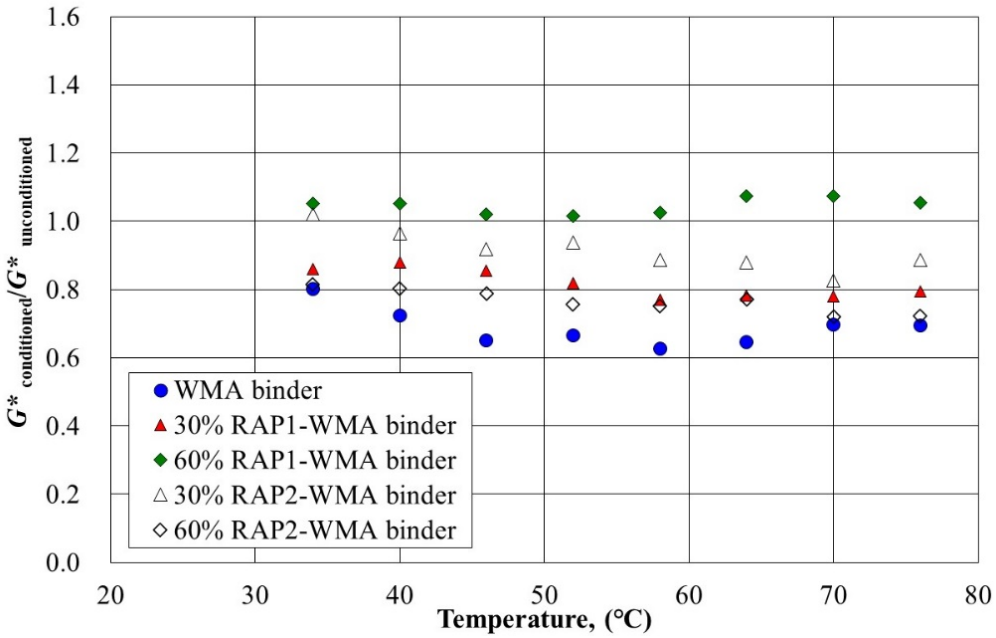

Figure 5.11 Ratio of $G^*_{conditioned}$ with the SATS conditioning to the $G^*_{unconditioned}$ without the SATS conditioning obtained at 10Hz for each type of mixture

5.5.2 WMA Fatigue behaviour with 50% reduction in complex modulus *G**

To understand fatigue characteristics of the binders extracted from the five types of the mixtures with and without the combined aging, fatigue tests were also performed on the binders using the DSR. As shown in Figure 3.13, the tests were conducted under stress control.

To determine the number of cycles at the fatigue failure in the tests, failure criterion shown in Figure 5.12 was used. Figure 5.12 shows an example of the relationship between the complex modulus *G** and number of cycles, *N* obtained from the test. The number of cycles at the fatigue failure of each binder was determined as the number of cycles to reach 50% reduction in initial complex modulus *G**.

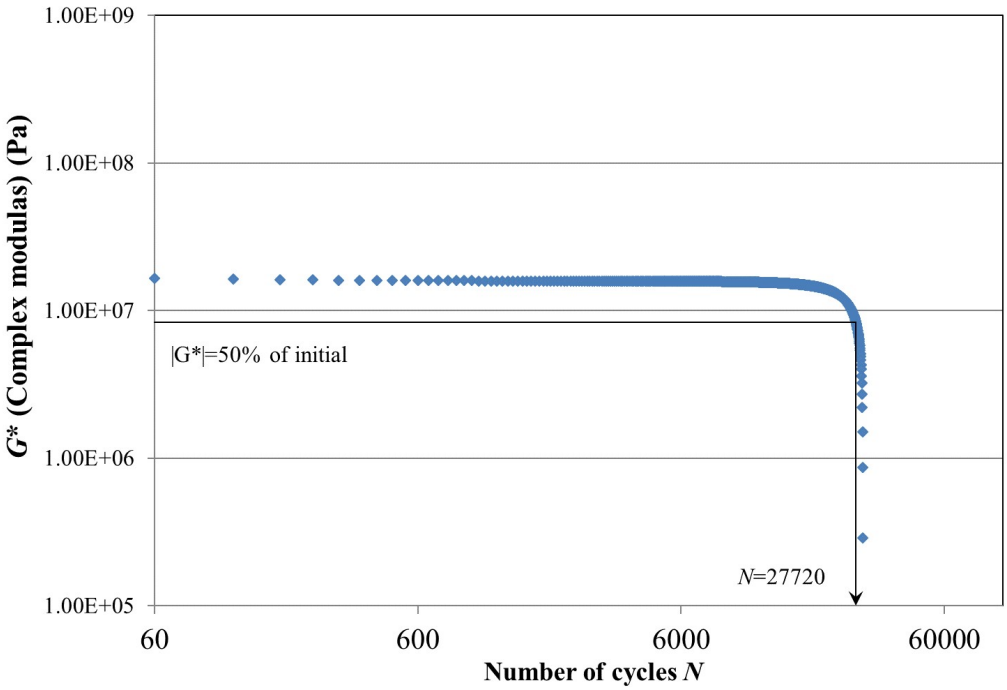

Figure 5.12 Failure criterion using complex modulus to determine the number of cycles at the fatigue failure (WMA and RAP WMA binders)

Figures 5.13 to 16 show the test results obtained for the binders without the SATS conditioning and for those with the SATS conditioning, respectively. Firstly, high correlation between the initial strain and the number of cycles at failure was observed in each fatigue test result. It is found in Figure 5.13 that the relationships between the initial strain and the number of loading cycles at failure of the RAP-WMA binders without the SATS conditioning are located in the upper left side of that of the WMA binder. This indicates that the RAP binders were less durable against fatigue compared to the WMA binder. It is also found that there is a tendency that the fatigue life of the RAP binders without the SATS conditioning was decreased with the increase in the RAP content irrespective of the rejuvenator types. The same trend as this result is also shown in Figure 5.15.

Meanwhile, Figure 5.14 shows that the difference in the effect of the SATS conditioning on the fatigue behaviour between the RAP1 and RAP2 binders. The binder from the 30% RAP1-WMA mixture reduced fatigue life whereas that from the 60% RAP1-WMA binder showed little change in the failure life after the conditioning. The RAP2-WMA binders did not show any significant changes in fatigue behaviour for the 30% RAP contents through the conditioning, whilst it demonstrated larger initial strain with the shorter failure life for the 60% RAP contents after the conditioning. The same trend as this result is also shown in Figure 5.16.

These results suggest that the G^* ratio ($G^*_{conditioned}/G^*_{unconditioned}$) is harmonized with fatigue test results. As can be seen in Figure 5.11, 60% RAP1-WMA binder showed slight increase in the G^* ratio whilst that of WMA binder indicated significant drop in the ratio. 30% RAP1-WMA, 30% RAP2-WMA and 60% RAP2-WMA binders also showed changes in the G^* ratio with and without the SATS conditioning. The same trend can be seen in fatigue test results. In particular, 60% RAP1-WMA binder showed increase in failure cycles whereas WMA binder demonstrated significant reduction in failure life, with and without the condition.

Other binders also exhibited changes in failure cycles after the condition. Therefore, it implies that both the G^* ratio and the fatigues results are harmonizing.

In addition, it is speculated that the types of rejuvenator also affects these results. The RAP1 is resin based binder, whereas both virgin and RAP2 are asphaltenes based binder as shown in Figure 4.1. Therefore, this implies that RAP1 binder might be strong against combined aging, whilst WMA and RAP2 binders would be less durable for the aging. However, further investigation needs to be conducted through mixture test result.

In case of test results summarized with stress level, the results demonstrated clear difference among WMA, RAP1 and RAP2 WMA binders. For results obtained from without SATS conditioning, fatigue curve results showed difference in each RAP ratio. This trend was confirmed both in RAP1 and RAP2 WMA binders. However, as to the results provided from with the conditioning, significant differences can be seen between RAP1 and RAP2 WMA binders. For RAP1 WMA binder, fatigue curve for 30% and 60% RAP binders showed similarity in the results. However, for RAP2 WMA binder, fatigue cycles for those binder showed parallel curve in the results. These results might demonstrate differences in rejuvenator types. This trend was also seen in HMA and RAP binders. Therefore, chemical composition of rejuvenator and rejuvenated binders might affect rheological property of those binders.

In terms of the wax effect, it was though that wax remained in mixture and binder did not give negative effect on fatigue life, since similar test results to HMA and RAP binders were seen in the test results.

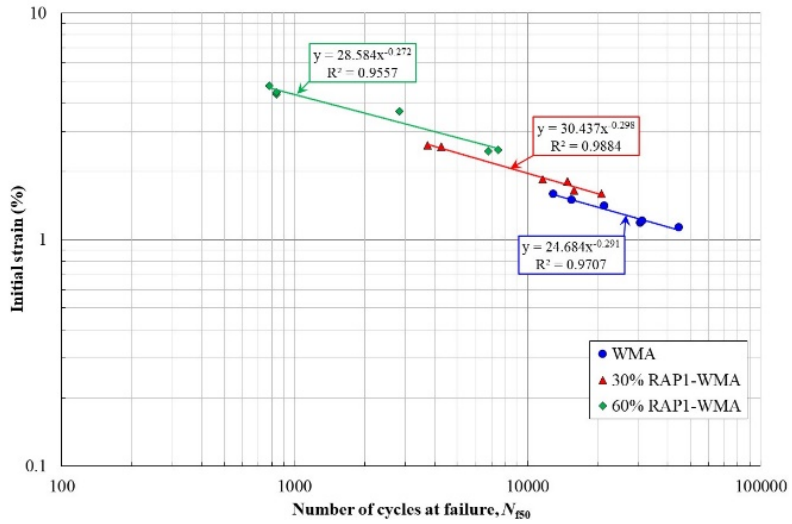

(a)

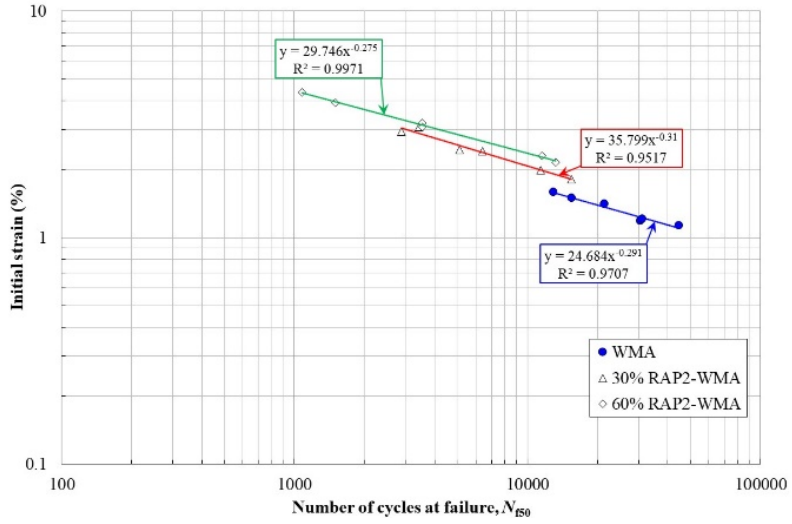

(b)

Figure 5.13 Relationships between the initial strain and the number of cycles at failure from the binder fatigue tests without SATS conditioning (a) WMA & RAP1 WMA binders (b) WMA & RAP2 binders

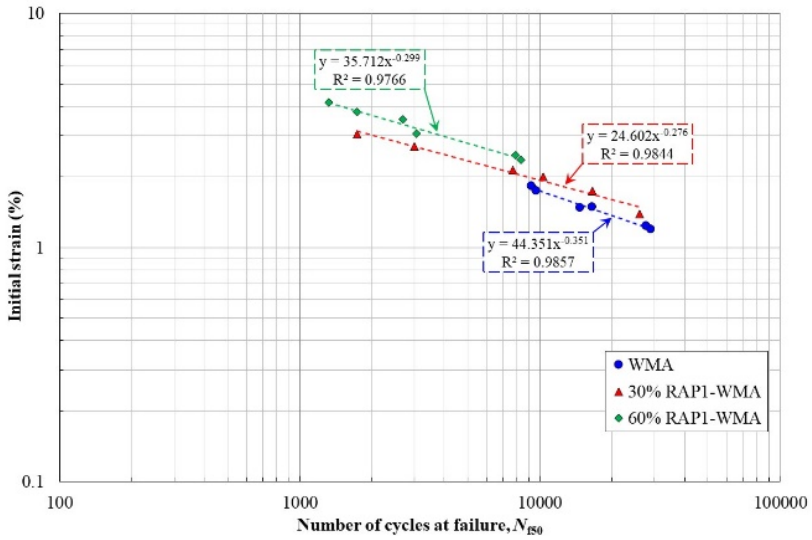

(a)

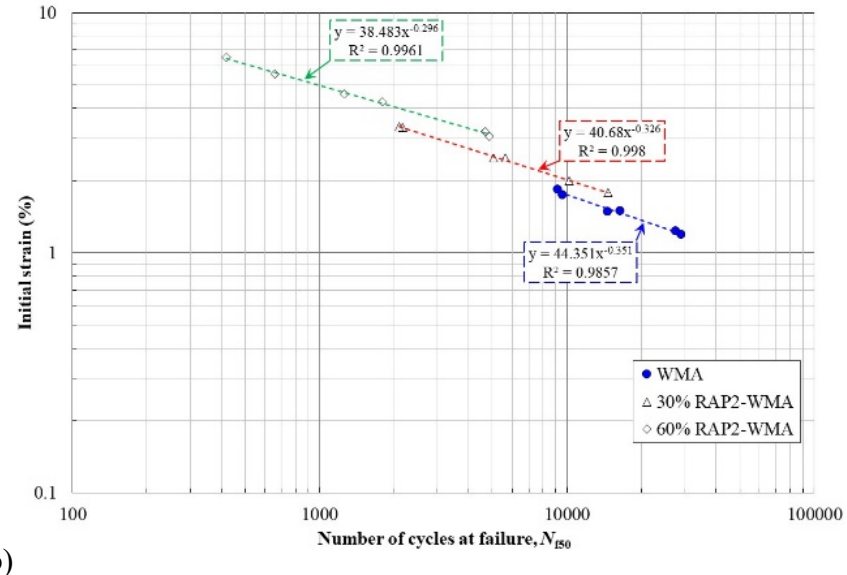

(b)

Figure 5.14 Relationships between the initial strain and the number of cycles at failure from the binder fatigue tests with SATS conditioning (a) WMA & RAP1 binders (b) WMA & RAP2 binders

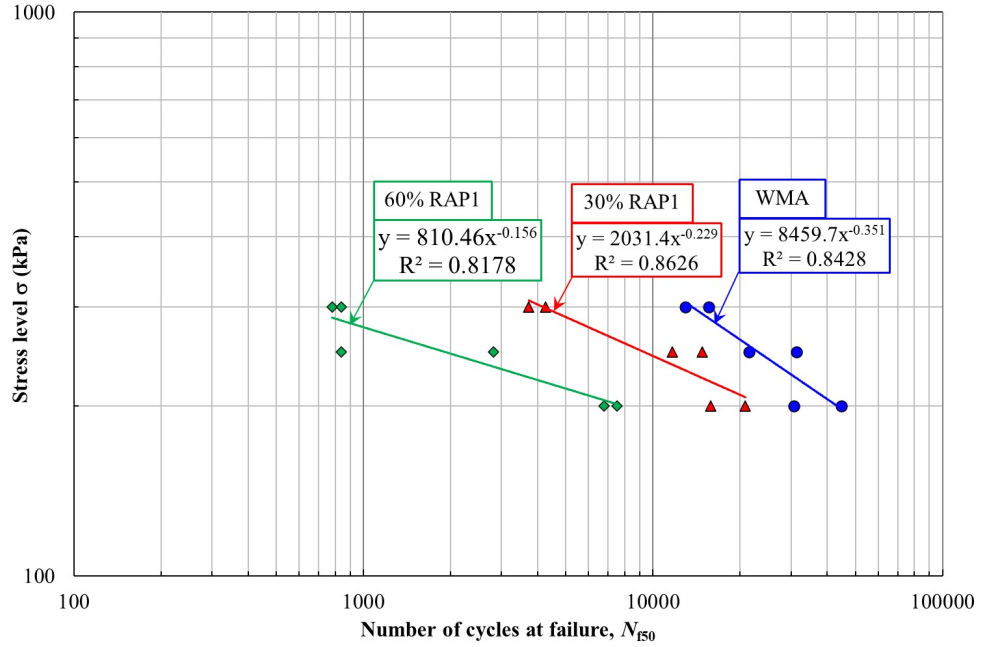

(a)

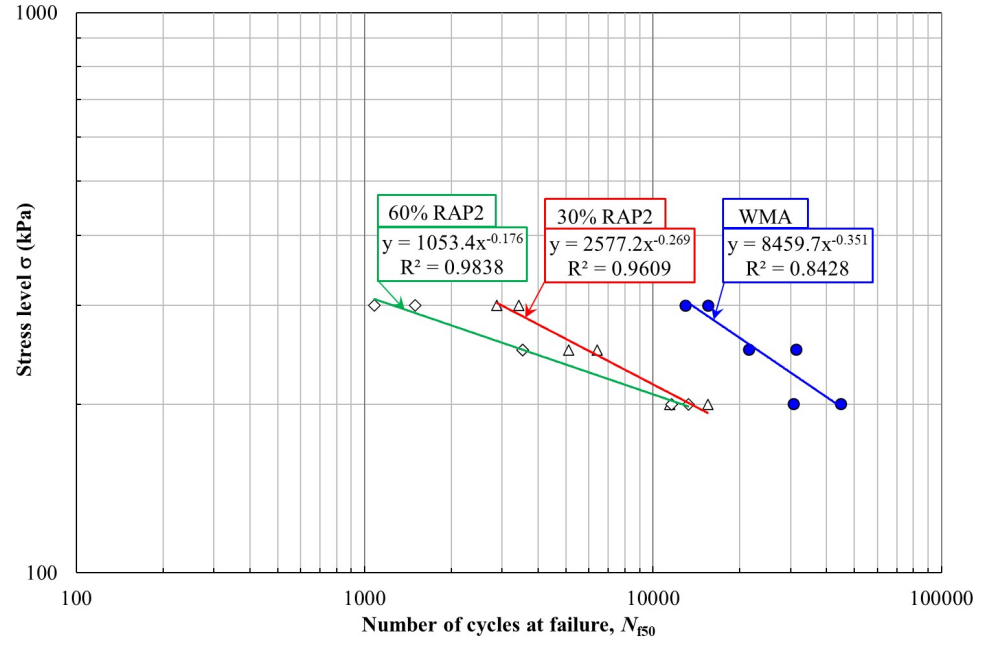

(b)

Figure 5.15 Relationships between the stress level and the number of cycles at failure from the binder fatigue tests without SATS conditioning (a) WMA & RAP1 binders (b) WMA & RAP2 binders

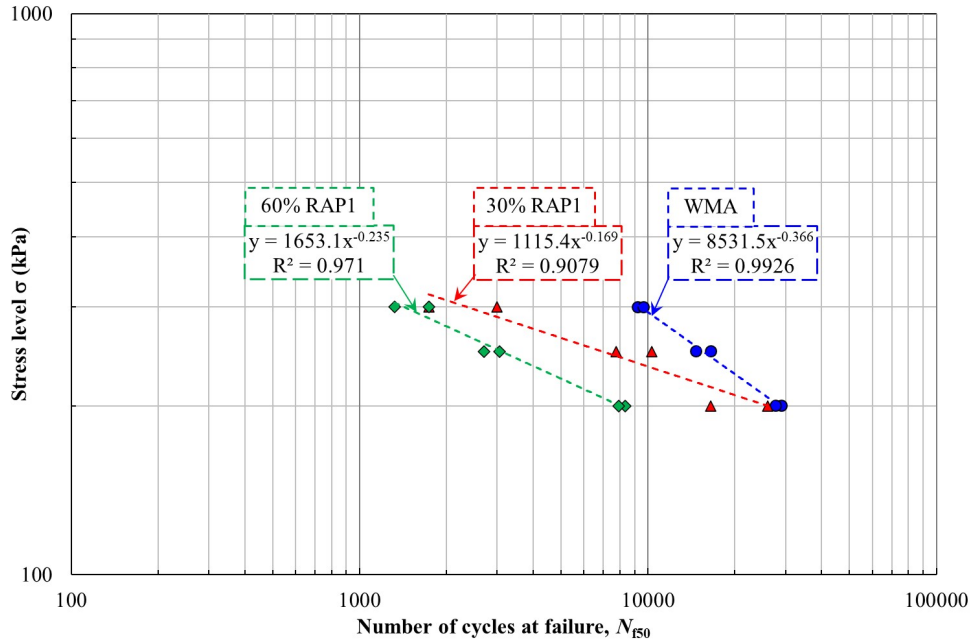

(a)

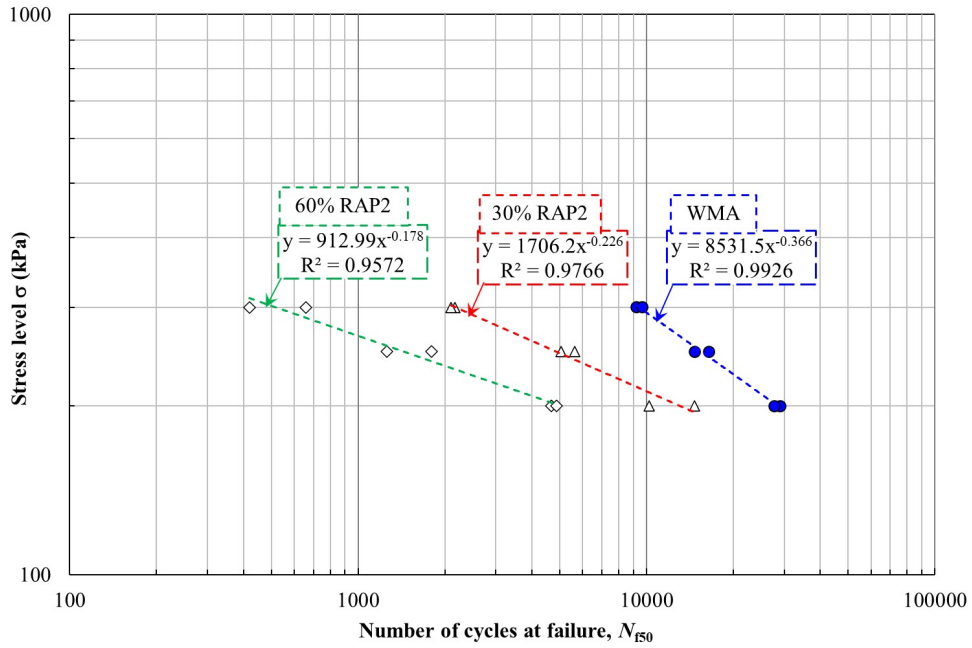

(b)

Figure 5.16 Relationships between the stress level and the number of cycles at failure from the binder fatigue tests with SATS conditioning (a) WMA & RAP1 binders (b) WMA & RAP2 binders

5.6 FATIGUE BEHAVIOUR OF WMA AND RAP WMA BINDERS WITH 20% REDUCTION IN DISSIPATED ENERGY

In order to analyze the fatigue characteristics of the binders extracted from the specimens of five types of mixtures with and without combined aging, fatigue tests were also performed on the binders using DSR. The same test procedure as that of HMA and RAP binders were conducted in this chapter (see Figure 3.13).

The failure criterion shown in Figure 5.17 is also used to detect the number of cycles at fatigue failure. Figure 5.17 shows an example of the relationship between the dissipated energy ratio (*DER*) and the number of cycles obtained from WMA binder. As shown in the previous chapter, the *DER* is defined as follows:

$$DER=\frac{\sum_1^N W_i}{W_N}, \tag{5.1}$$

where W_N is the dissipated energy in cycle N, W_i is the dissipated energy in cycle i, and $\sum_1^N W_i$ is the total sum of the dissipated energy up to cycle N. W_i can be obtained as follows:

$$W_i = \pi\sigma_i\varepsilon_i sin\varphi_i \tag{5.2}$$

where σ_i is the stress level in cycle i, ε_i is the strain level in cycle i, and φ_i is the phase angle in cycle i.

Figures 5.18 and 5.19 show the test results obtained for the specimens without SATS conditioning and those with SATS conditioning. In Figure 5.18 (a) and (b), the relationships between the initial *DER* and the number of loading cycles at failure of the RAP binders without SATS conditioning are located on the upper left side of those of the WMA binder. This indicates that RAP binders are less durable against fatigue than WMA binders. In addition, there is a tendency for the fatigue life of the RAP binders without SATS conditioning to decrease with an increase in the RAP content, irrespective of the rejuvenator type.

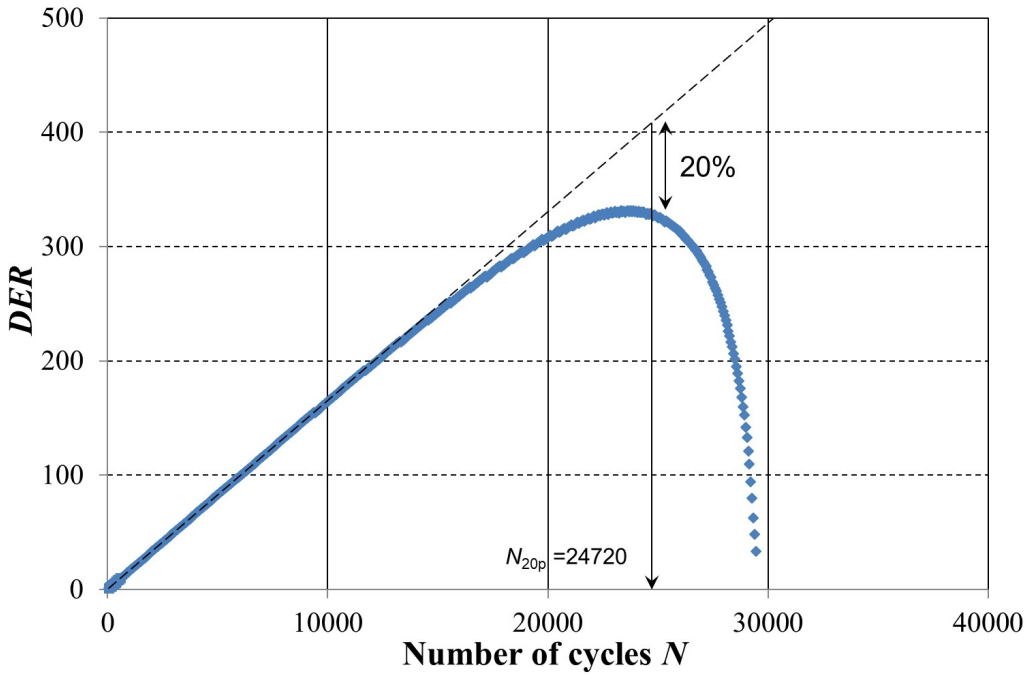

Figure 5.17 Failure criterion using dissipated energy ratio (*DER*) to determine the failure state in the fatigue test using DSR (WMA binder)

These observations are consistent with those shown in Figure 5.18.

Comparing the results in Figure 5.18, it can be observed that the changes in the fatigue behaviors of the binders from SATS conditioning are insignificant (see Figure 5.19). However, a more detailed analysis revealed differences in the effects of SATS conditioning on the fatigue behaviors of RAP1 and RAP2 binders. The RAP 2 binders did not show any significant differences in fatigue behaviors with and without SATS conditioning. Notably, the HMA binder also showed little difference in fatigue behaviors with and without SATS conditioning. However, the binder from the 30% RAP1 mixture showed a slight reduction in fatigue life, whereas that from the 60% RAP1 mixtures showed a slight increase in failure life when experiencing SATS conditioning. These trends are consistent with those observed in Figure 5.19.

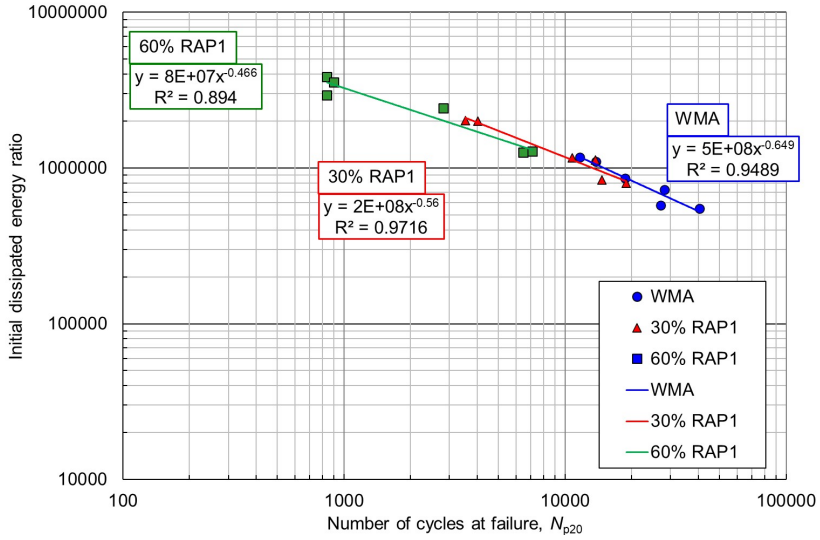

(a)

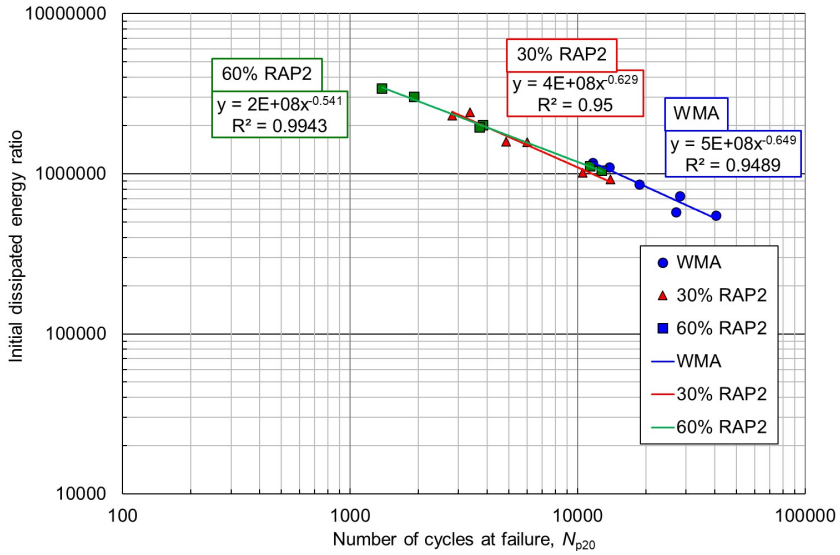

(b)

Figure 5.18 Relationships between the initial dissipated energy ratio and the number of cycles at failure from the binder fatigue tests without SATS conditioning (a) WMA & RAP1 binders, (b) WMA & RAP2 binders

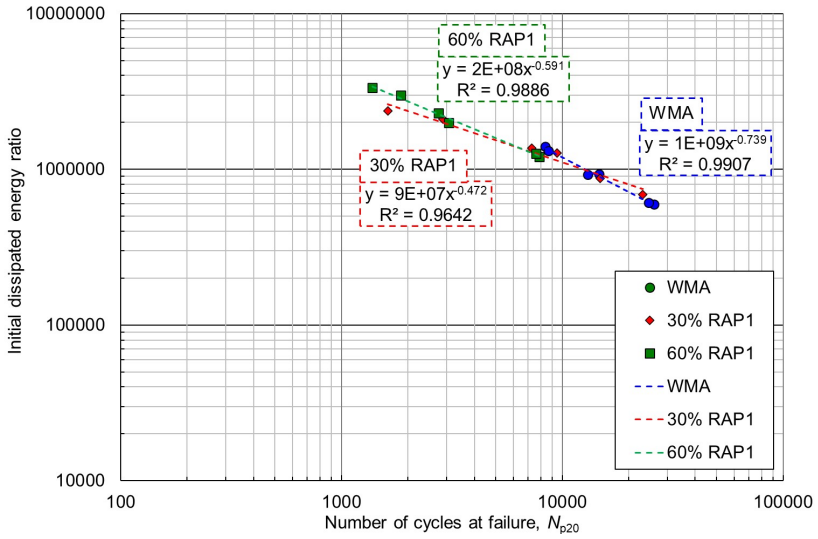

(a)

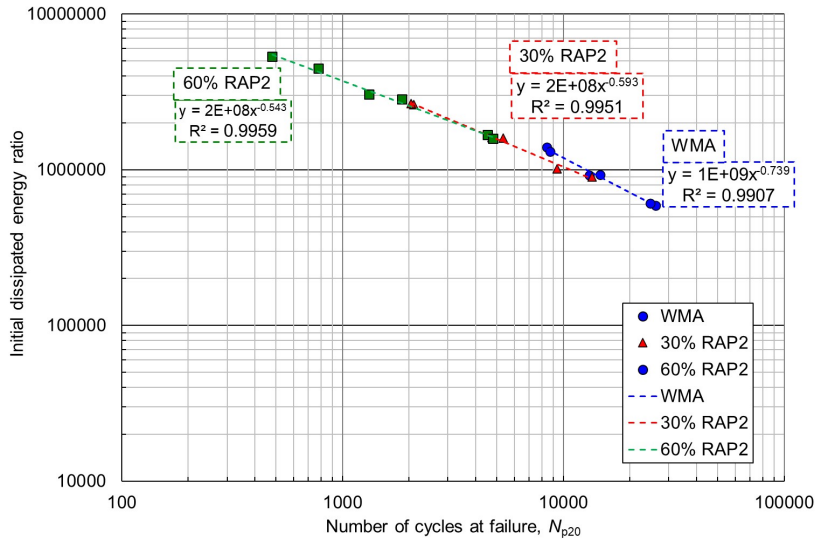

(b)

Figure 5.19 Relationships between the initial dissipated energy ratio and the number of cycles at failure from the binder fatigue tests (a) WMA & RAP1 binders, (b) WMA & RAP2 binders

5.7 SUMMARY

In order to evaluate the durability of RAP-WMA mixtures, mechanical and physical properties of RAP-WMA mixtures having 30 % and 60 % RAP contents blended with two types of rejuvenator agents (Rejuvenator 1 and 2), with and without combined aging, were experimentally investigated. For comparison, properties of WMA mixtures prepared from virgin binder and virgin aggregates, with and without combined aging, were also investigated. Saturation Aging Tensile Stiffness (SATS) conditioning were used to simulate the combined aging. Properties of the binders extracted from the RAP and the WMA mixtures were also examined. As a result, following findings were derived from the test results.

1. In terms of mixture properties, the SATS conditioning reveals that retained stiffness and fatigue test results are harmonized after the conditioning. 30% RAP1-WMA, 60% RAP1-WMA and 60% RAP2-WMA mixtures remained similar stiffness with and without the SATS conditioning, whereas WMA and 30% RAP2-WMA demonstrated reduction in stiffness with the condition.
2. Similar trend can be seen in fatigue results. RAP1-WMA and 60% RAP2-WMA mixtures did not show significant changes in initial strain with and without the condition, 30% RAP2-WMA and WMA mixtures indicates changes in the initial strain with the condition. In addition, the initial strain of 30% RAP2-WMA mixture were closed to that of WMA mixtures after the condition. In addition, the results summarized by stress level revealed that RAP-WMA mixture has longer fatigue life than that of WMA mixture.
3. With regard to stripping characteristics of mixtures, average stripping ratio is also corelated to retained stiffness and fatigue results. RAP1-WMA mixtures remained lower stripping ratio in 30% and 60% RAP ratios, whilst RAP2-WMA mixtures were shifted as RAP contents increase. Since similar trend can be seen in the retained stiffness and fatigue test results, stripping ratio is also harmonizing with these results.
4. With respect to binder properties, the G^* ratio ($G^*_{conditioned}/G^*_{unconditioned}$) is harmonized with fatigue test results. As can be seen in Figure 5.9, 60%

RAP1-WMA binder showed slight increase in the G^* ratio whilst that of WMA binder indicated significant drop in the ratio. 30% RAP1-WMA, 30% RAP2-WMA and 60% RAP2-WMA binders also showed changes in the G^* ratio with and without the SATS conditioning. The same trend can be seen in fatigue test results. In particular, 60% RAP1-WMA binder showed increase in failure cycles whereas WMA binder demonstrated significant reduction in failure life, with and without the condition. Other binders also exhibited changes in failure cycles after the condition. Therefore, it implies that both the G^* ratio and the fatigues results are harmonizing.

5. In terms of binder property, black diagram obtained from DSR test suggest that the WMA binder might be influenced by the effect of combined aging so that the wax additive blended with virgin binder might be dissipated after the conditioning, since test results of the binders were shifted toward high in phase angle. In addition, there seems no negative effect in fatigue curve of WMA and RAP WMA binders, compared to that of HMA and RAP binders. Therefore, the effect of wax could be neglected if wax was remained in binder.

CHAPTER 6

Durability Assessment based on Rheological Property

6.1 INTRODUCTION

As described in previous chapters, both mixture and binder were examined through the combined aging protocol for the four types of mixtures: HMA, RAP, WMA and RAP-WMA mixtures. However, as discussed in previous sections, the damage mechanism for mixture and binder are not clearly understood, especially for stripping. In addition, those relationship with rejuvenators also need to analyse in more detail. In order to examine these characteristics, rheological assessments were conducted through extracted binders. Furthermore, two-staged extractions were carried out to examine adhesion and cohesion properties of binders with rejuvenators. The aim of this chapter is to describe rheological assessments of extracted binders.

6.2 EVALUATION USING GLOVER-ROWE (G-R) PARAMETER

In order to evaluate the rheological differences among binders in more detail, the Glover-Rowe (G-R) parameter was used to evaluate the durability of the extracted binder with SATS conditioning. In general, the G-R parameter is calculated from values of complex modulus, ($|G^*|$) and phase angle (δ) by the equation (6.1), and the performance of binder is captured at a frequency of 0.005 rad/s and a temperature of 15°C as a DSR test condition (Glover *et al*. 2005, Rowe *et al*. 2014).

$$G - R = \frac{|G*|(cos\delta^2)}{sin\delta} \quad (6.1)$$

Figure 6.1 demonstrates black diagram with the DSR test results plotted. In general, the two curves are drawn in the black diagram representing block (significant) cracking and no-block (initial) cracking at 450kPa and 180kPa, respectively. Black cracking shows significant cracking whilst no block cracking indicates initial cracking for binder measured. In this research, by plotting the DSR test results obtained from G-R parameter testing condition in the black diagram, the state of extracted binder can be identified in the diagram. From the measurement results, it can be seen that virgin binder is plotted at around 80°, showing larger phase angle region. Meanwhile, RA binder is located at around 55°, showing initial damage of binders.

6.2.1 HMA evaluation using Glover-Rowe (G-R) parameter

In terms of the extracted binders with SATS condition, the five types of the extracted binders (i.e. HMA, 30% RAP1, 60% RAP2, 30% RAP2, 60% RAP2) were assessed in the black diagram. As can be seen from the figure, the result captures the differences of RAP ratio and rejuvenator. These results show the decrease in phase angle as RAP contents increase from HMA to 60% RAP1 and RAP2. Despite the fact that the penetration grade is adjusted to 70 pen using rejuvenator, each binder demonstrate different phase angle, showing similar complex modulus value. This trend is confirmed both in RAP1 and RAP2 binders. Therefore, it can be said that the properties of RAP binder is different in RAP contents, even if the penetration grade is adjusted using rejuvenator.

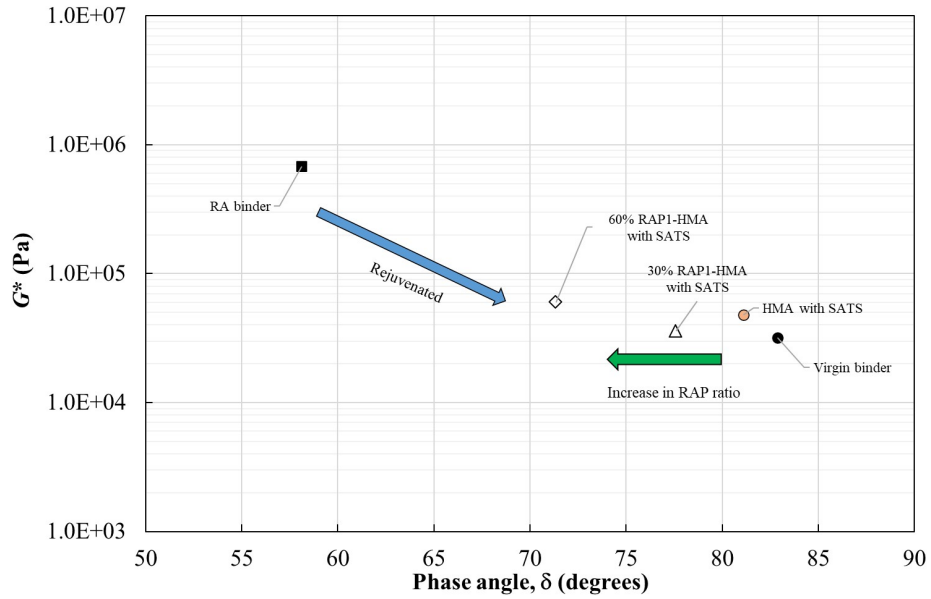

(a)

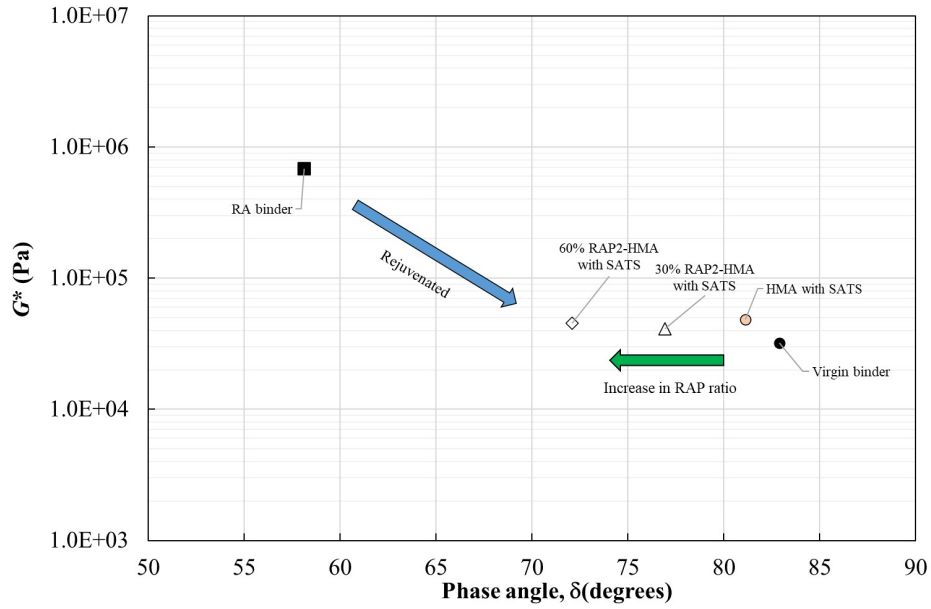

(b)

Figure 6.1 G-R parameter for the five extracted binders with the SATS conditioning (a) RAP1 binders, (b) RAP2 binders

6.2.2 WMA evaluation using Glover-Rowe (G-R) parameter

In terms of the extracted binders with SATS condition, the five types of the extracted binders (i.e. WMA, 30%RAP1, 60%RAP2, 30%RAP2, 60%RAP2) were assessed in the black diagram. As can be seen from Figure 6.2, the result captures the differences of RAP ratio and rejuvenator. These results show the decrease in phase angle as RAP contents increase from WMA to 60% RAP1 and RAP2. Of interest, the effect of wax was not seen in the results after the conditioning because similar G^*value can be seen in WMA, 30% RAP and 60% RAP, changing phase angle. This trend was confirmed in both Rejuvenator 1 and 2. Therefore, there seems no effect on wax modification with rejuvenator in WAM and RAP WMA mixtures after the condition.

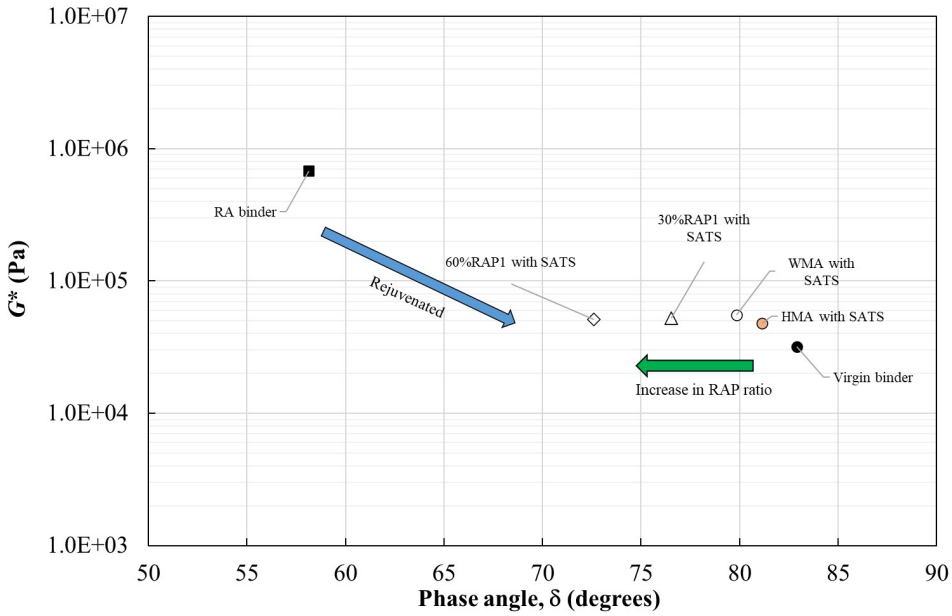

(a)

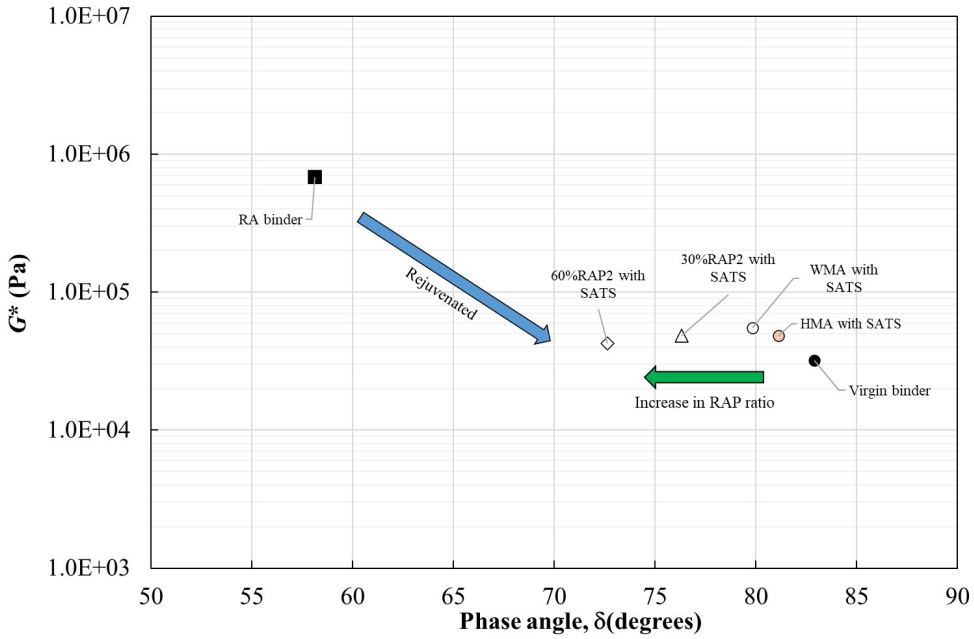

(b)

Figure 6.2 G-R parameter for the five extracted binders with the SATS conditioning (a) RAP1 binders, (b) RAP2 binders

6.3 TWO STAGED EXTRACTION AND ASSESSMENTS

6.3.1 Two staged extraction and DSR master curve for HMA mixture

In previous sections, different trends were observed in the changes in the properties of the HMA mixture and RAP mixtures with the SATS conditioning. For example, the RAP mixtures did not show a reduction in retained stiffness, whereas the HMA mixture showed a significant drop in stiffness with SATS conditioning. It was also found that the RAP mixtures showed a longer fatigue life than the HMA mixture after SATS conditioning. In addition, the RAP mixtures showed a higher stripping resistance compared to the HMA mixture. These trends were more pronounced for higher RAP contents.

However, no significant change was observed in the properties of the binders extracted from the HMA and RAP mixtures with SATS conditioning. Therefore, the fatigue test results indicate different trends between the mixture and binder, despite the general expectation that the trend should be the same. To examine this contradiction, the RAP binder without SATS conditioning was investigated in more detail using two-stage extraction with reference to Carpenter *et al*. (1980). The two-staged extraction was conducted on the 60% RAP1 mixture without SATS conditioning. First, the RAP mixtures were soaked in dichloromethane for 3 min, and then the outer layer binder was extracted (see Figure 6.3). The same procedure was conducted for the rest of the RAP mixture to obtain the inner layer binder. Both the outer and inner layer binders were examined through frequency sweep tests using a DSR. Figure 6.4 shows the master curves of the inner and outer layer binders as extracted from the 60% RAP1 mixture without SATS conditioning. The master curve of the binder extracted from the HMA mixture without SATS conditioning in Figure 4.8 is also shown in the figure. The difference in the master curve between the outer and inner layer binders can be clearly seen for the 60% RAP1 mixture. The inner layer binder demonstrates a higher complex modulus G^* than the outer layer binder at all frequencies. Meanwhile, the outer layer binder shows a modulus G^* similar to that of the binder extracted from the HMA mixture. These facts suggest that the inner layer binder is older than the outer layer binder and HMA binder. Thus, it can be presumed that the inner layer binder adheres to aggregate better than HMA binder.

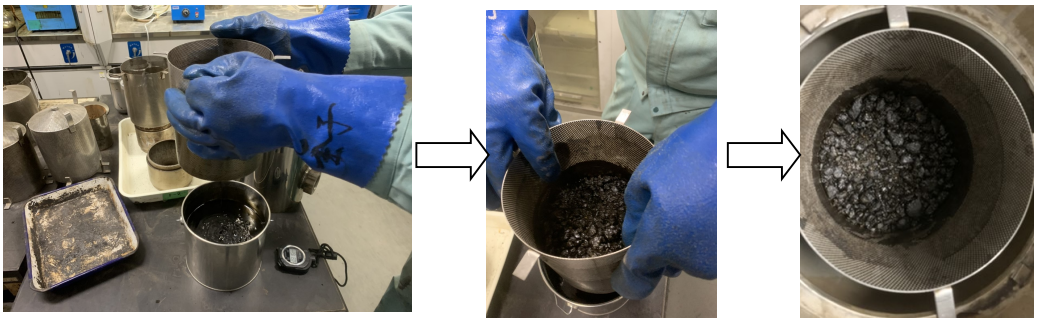

(a)

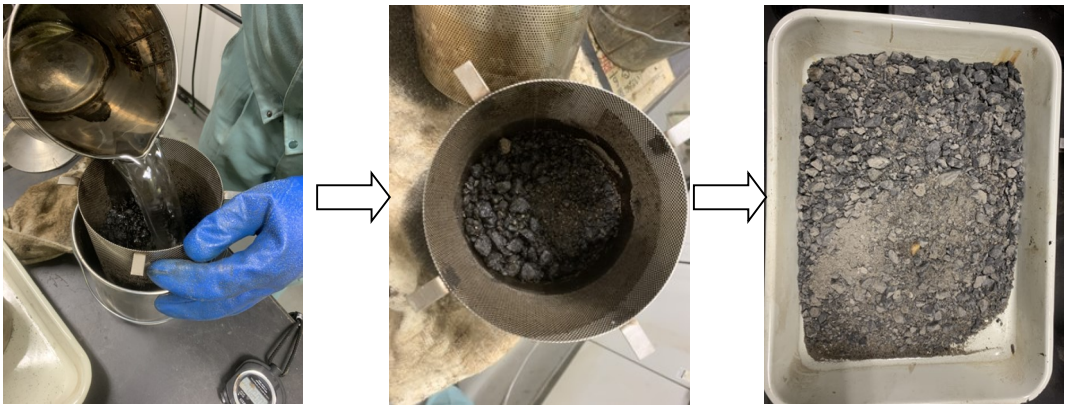

(b)

Figure 6.3 Two-staged extraction process (a) 1st extraction, (b) 2nd extraction

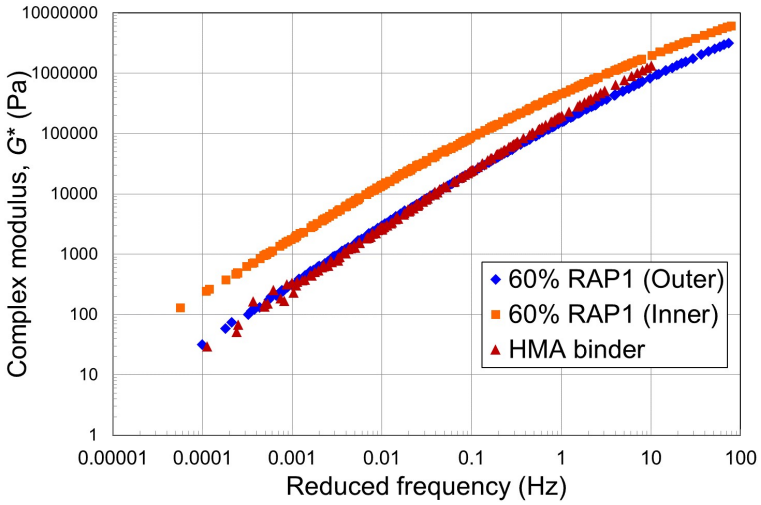

Figure 6.4 Master curves of the two-steps extracted binders at a reference temperature of 34 °C

6.3.2 Two staged extraction and DSR master curve for WMA

In previous chapters, it was observed that the properties of the WMA mixture and the RAP-WMA mixture changed with the SATS conditioning, and those changes were different between the WMA and the RAP-WMA mixtures. For example, WMA mixtures illustrated significant drop in the stiffness with the conditioning whilst RAP-WMA mixtures showed different trend in retained stiffness between RAP1 and RAP2 WMA mixtures. It was also found that RAP-WMA mixtures showed longer fatigue life than that of WMA mixture after the SATS conditioning. In addition, RAP-WMA mixtures showed higher stripping resistance compared to the WMA mixture although differences in average stripping ratio was seen between RAP1 and RAP2 WMA mixtures.

In terms of binder properties, it was also observed that there was significant change in the properties of the binders extracted from the WMA and RAP-WMA mixtures with the SATS conditioning. Therefore, the fatigue test results indicated different trend between the mixture and the binder, despite the general expectation that the trend would be the same. In order to examine this contradiction, RAP binder was investigated in more detail with using the two-stage extraction by following the same protocol as that of HMA extraction. The two-stage extraction was carried out on the 30% and 60% RAP1-WMA and RAP2-WMA mixtures. At first, the RAP mixtures were soaked into dichloromethane for three minutes, and then the outer layer binder was taken through the extraction process. Consequently, the same procedure was conducted for the rest of RAP mixture to obtain the inner layer binder. Both outer and inner layer binders were examined by DSR tests.

Figures 6.5 to 6.8 demonstrates the frequency sweep test results for the extracted binders from WMA and RAP-WMA mixtures with and without SATS conditioning. From the results, it was found that the master curve for the extracted binders were harmonized with the stripping results. Figures 6.5 and 6.6 show the master curve of the five binders (i.e. WMA binder, 30% RAP1-WMA binder, 60% RAP1-WMA binder, 30% RAP2-WMA binder, 60% RAP2-WMA binder) without the

conditioning. For RAP1-WMA binders, both the 30% and 60% binders exhibit differences between outer and inner layers. As can be seen in the results, outer binder shows lower value whilst inner binder demonstrates higher value in complex modulus, G^*. In terms of RAP1-WMA binder, WMA binder is exhibited between outer and inner layers both in 30% and 60% RAP1-WMA binders, although differences in outer and inner layers can be seen between 30% and 60% RAP1-WMA binders. Meanwhile, different trend from the RAP1 binder can be seen in the RAP2 binder. For the 30% RAP binder, both outer and inner layers show similar master curves closely plotted with that of WMA binder. However, clear differences can be seen in the 60% RAP2 binder as these two curves show significant differences between outer and inner binder showing the master curve of WMA binder in the middle. Since the chemical composition of RAP2 binder is similar to that of virgin binder, it appears that 30% RAP2 binder behaves similar to that virgin binder.

For the binders extracted from the specimen after the conditioning, different trends were confirmed both in RAP1 and RAP2 binders. Figures 6.7 and 6.8 shows the master curve of the RAP1 and RAP2 binders after the SATS conditioning. For 30% and 60% RAP1 binders, both outer and inner layer binders were paralleled showing WMA binder master curve closed to outer layer. In other words, the inner layer of RAP1 binder has larger complex modulus than that of WMA and outer RAP1 binders. Meanwhile, RAP2 binder indicates different trend from RAP1 binder. Of interest, 30% RAP2 binder exhibits similar manner among the WMA and the inner binders whilst 60% RAP2 binder demonstrates paralleled curves between outer and inner binders showing that of WMA binder in the middle. Considering the results obtained from 30% RAP2 binder, it is speculated that inner binder of 30% RAP2 binder behaves like WMA binder because of the similarity in chemical composition between WMA and RAP2 binders.

These results might explain the mixture stiffness and fatigue results related to retained stiffness ratio and saturation. Looking at stiffness and fatigue results as mixtures, RAP-WMA mixture tend to indicate lower retained saturation than that

of WMA mixtures. This trend was more pronounced as the RAP contents were increased. The retained stiffness depicted in Figure 5.1, also showed reduction in stiffness in WMA mixture whilst that of RAP mixtures tend to be remained original stiffness even after SATS conditioning, especially in 60% RAP-WMA mixtures. As to fatigue, the test results shown in Figure 5.4 indicated that WMA mixture demonstrated changes in initial strain and fatigue life whereas that of RAP-WMA mixture showed longer life showing similar initial strain to that without SATS conditioning. In addition, RAP-WMA mixtures demonstrated high in stripping resistance compared with that of WMA mixture after the condition.

These results might be related to coated state of RAP aggregate between outer and inner layers. Considering the results obtained from the two stage extraction and the mechanical tests, RAP-WMA mixtures have stronger bonding between aggregate and binder than that of WMA mixture. This trend is more pronounce when RAP contents increase so that reduction in stiffness and fatigue life would not be seen much. This result may support the evidence that WMA mixture has low adhesive strength between binder and aggregate. This leads to reduction in stiffness and fatigue life causing stripping of WMA mixture after SATS condition.

Meanwhile, for RAP-WMA mixture, it is assumed that adhesion between aggregate and RA binder has become strong during long-term service life. In addition, it is speculated that better cohesion between RAP aggregate and added binder (i.e. 70 pen bitumen) has been obtained due to the effect of rejuvenator. Moreover, better adhesive and cohesive strength leads to the prevention of moisture intrusion in RAP-WMA mixture, thus this avoids the loss of stiffness and fatigue life from moisture damage. Furthermore, good cohesion would be expected if similar chemical composition is made between RAP aggregates and rejuvenator. This assumption may be the evidence that RAP1-WMA mixtures showed better stripping resistance than that of RAP2-WMA mixture since both aged binder and RAP1-WMA binder illustrated similarity in resin component, compared with RAP2-WMA binder. In other word, high in stripping can be seen in 30% RAP2-WMA mixture because of similarity in WMA and its inner layer binders, in terms of chemical composition and mechanical properties. In fact, the inner layer of 30% RAP2-WMA binder exhibited similar master curve to WMA binder which demonstrated largest stripping. Inevitably, it can be said that the inner layer of 30%

RAP2-WMA binder has less adhesion than other RAP binders. This implies that 30% RAP2-WMA mixture showed similar retained stiffness and saturation to that of WMA mixture, thus larger stripping can be seen in the 30% RAP2-WMA mixture.

As a result, it can be said that the results obtained from the two staged extraction and the frequency sweep test results harmonized with the stripping results obtained from the SATS conditioning. This might be related to the retained saturation of WMA and RAP mixtures, and fatigue properties after the combined aging. Therefore, this result might imply that RAP mixture have advantage for stripping to avoid intrusion of moisture. In particular, it can be said that high RAP contents and moisture resistance rejuvenator might be beneficial for stripping.

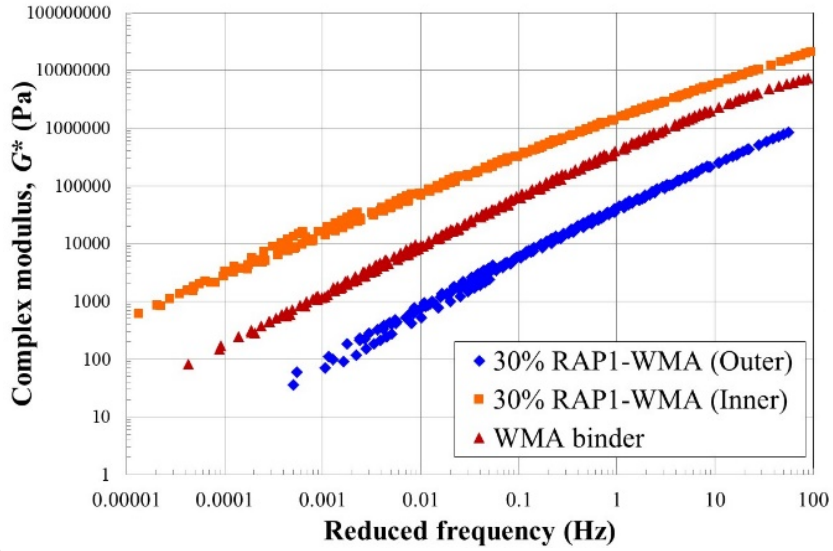

(a)

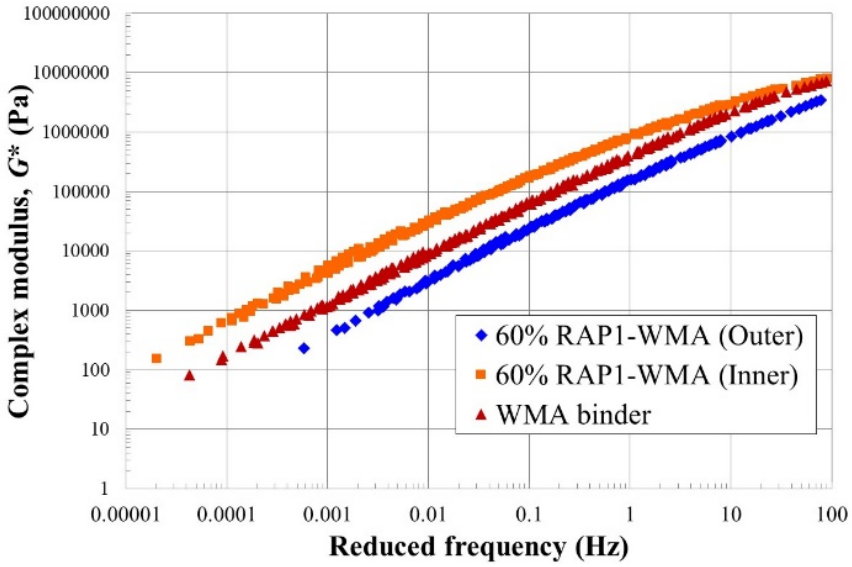

(b)

Figure 6.5 Master curves of the two-steps extracted binders without SATS conditioning at a reference temperature of 34 °C (a) WMA & 30% RAP1-WMA binders, (b) WMA & 60% RAP1-WMA binders

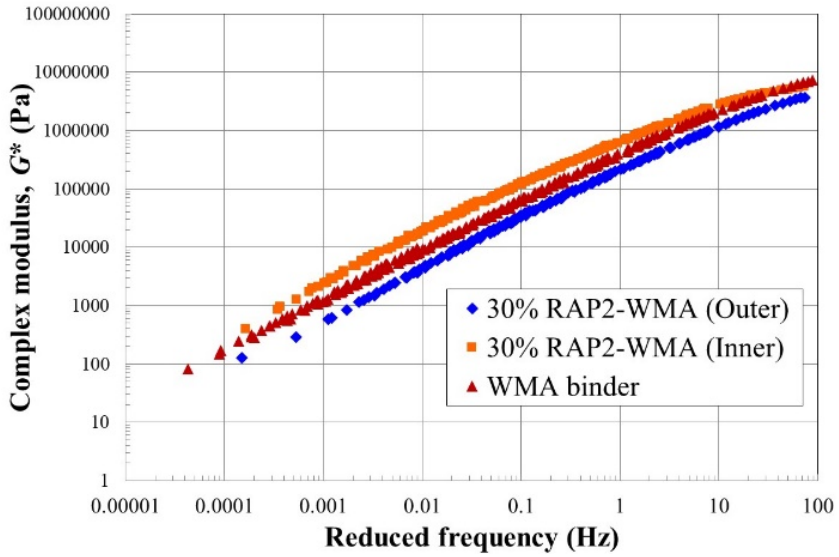

(a)

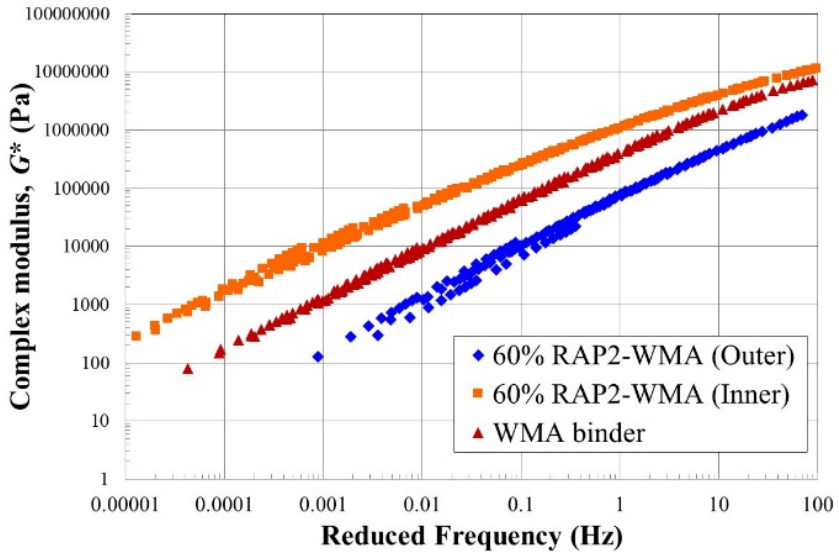

(b)

Figure 6.6 Master curves of the two-steps extracted binders without SATS conditioning at a reference temperature of 34 °C (a) WMA & 30% RAP2-WMA binders, (b) WMA & 60% RAP2-WMA binders

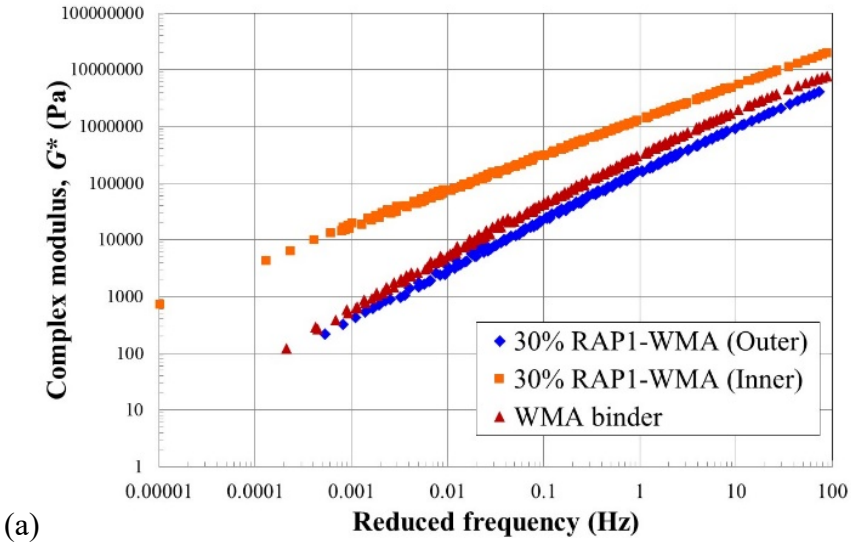

(a)

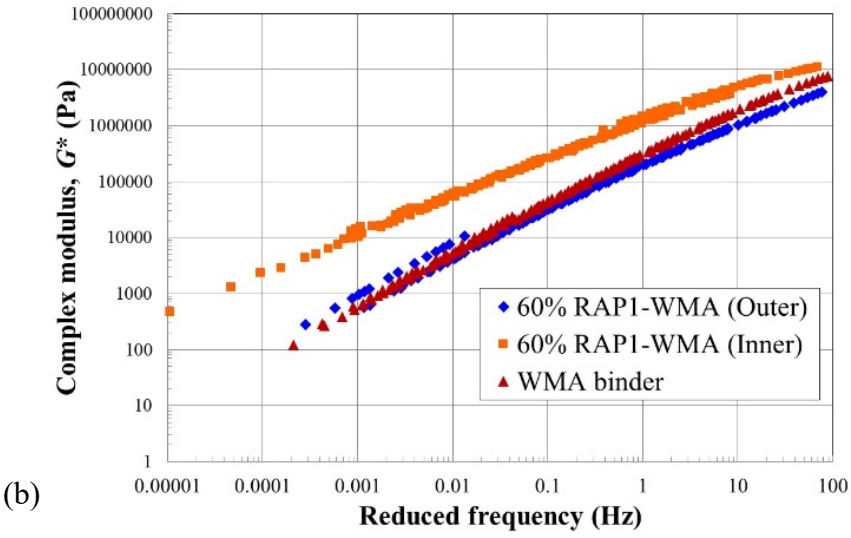

(b)

Figure 6.7 Master curves of the two-steps extracted binders with SATS conditioning at a reference temperature of 34 °C (a) WMA & 30% RAP1-WMA binders, (b) WMA & 60% RAP1-WMA binders

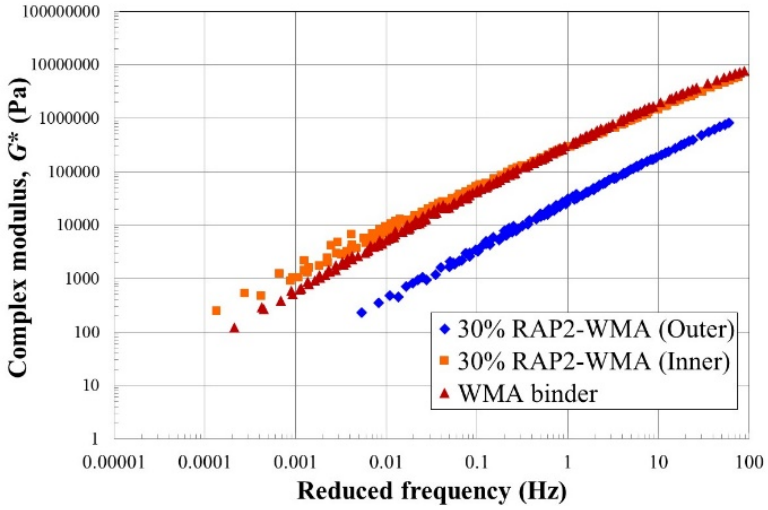

(a)

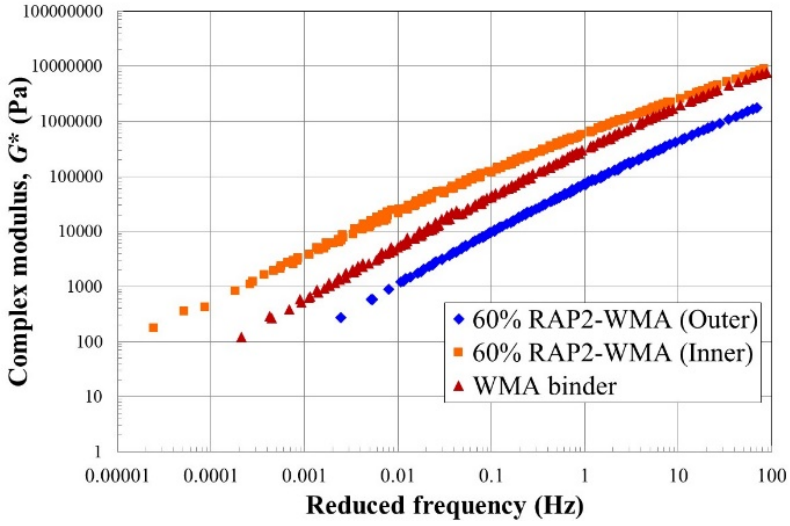

(b)

Figure 6.8 Master curves of the two-steps extracted binders with SATS conditioning at a reference temperature of 34 °C (a) WMA & 30% RAP2-WMA binders, (b) WMA & 60% RAP2-WMA binders

6.4 G-R PARAMETER AFTER TWO STAGED EXTRACTION

6.4.1 Two staged extraction and black diagram for HMA

Binders obtained from the two-stage extraction were also analyzed through G-R parameter. Figure 6.9 captured the G-R parameter for the five binders with and without the SATS conditioning. As can be seen in the figure, the results exhibited that the extracted binders were divided into two regions: Inner and Outer regions. The two regions were separated at around 73 degrees in phase angle. The four (i.e. 30%RAP1, 30%RAP2, 60%RAP1, 60%RAP2) inner binders were plotted in the inner region, whilst the four outer binders were indicated in the outer region. There were remained in the same regions with and without the condition.

However, as can be seen in the figure, G-R value for 30%RAP2 inner binder crossed from outer region to inner region after the SATS condition. It should be noted that both HMA and 30%RAP2 mixtures exhibited larger stripping ratio with the condition as shown in Figure 4.7. Therefore, the stripping results might be related to this G-R parameter results. In addition, it is speculated that both HMA and RAP2 binder have similar chemical composition as shown in Figure 4.1, the two binders have similarity in mechanical and chemical properties, in terms of bonding with aggregate and binders, thus 30%RAP2 mixture showed larger stripping ratio. Therefore, it can be said that this G-R parameter results are harmonized with the stripping result.

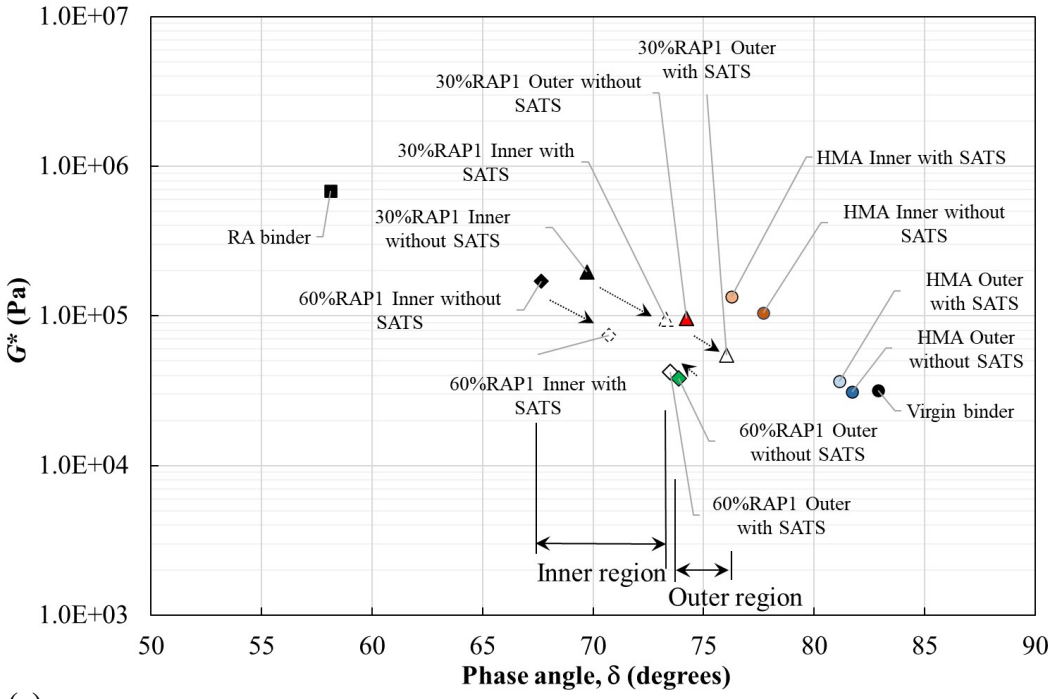

(a)

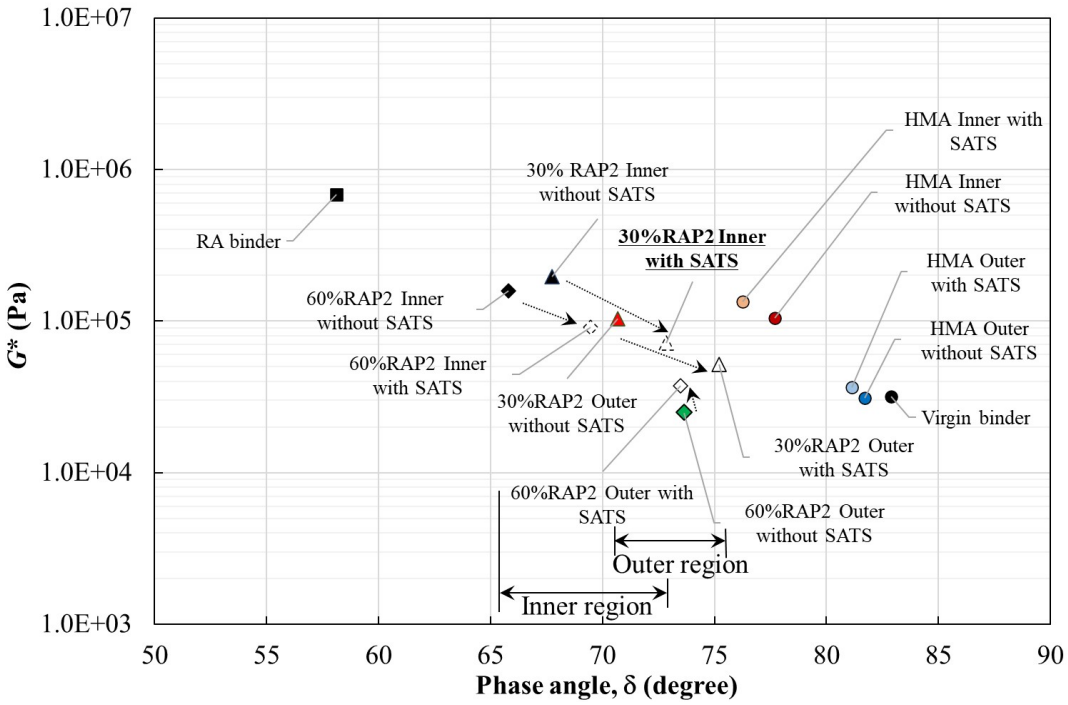

(b)

Figure 6.9 G-R parameter for the five extracted binders with and without SATS conditioning after two-stage extraction from HMA and RAP HMA mixtures (a) 30% and 60% RAP1 binders, (b) 30% and 60% RAP2 binders

6.4.2 Two staged extraction and black diagram for WMA

Binders obtained from the two-stage extraction were also analyzed through G-R parameter. Figure 6.10 captured the G-R parameter for the five binders with and without the SATS conditioning. As can be seen in the figure, the results exhibited that the extracted binders were divided into two regions: Inner and Outer regions. The two regions were separated at around 73 degrees in phase angle. The four (i.e. 30% RAP1, 30% RAP2, 60% RAP1, 60% RAP2) inner binders were plotted in the inner region, whilst the four outer binders were indicated in the outer region. There were remained in the same regions with and without the condition.

However, as can be seen in the figure, G-R value for 30% RAP2 inner binder crossed from outer region to inner region after the SATS condition. It should be noted that both WMA and 30% RAP2 mixtures exhibited larger stripping ratio with the condition as shown in Figure 5.6. Therefore, the stripping results might be related to this G-R parameter results. In addition, it is speculated that both WMA and RAP2 binder have similar chemical composition as shown in Figure 4.1, the two binders have similarity in mechanical and chemical properties, in terms of bonding with aggregate and binders, thus 30% RAP2 mixture showed larger stripping ratio. Therefore, it can be said that this G-R parameter results are harmonized with the stripping result.

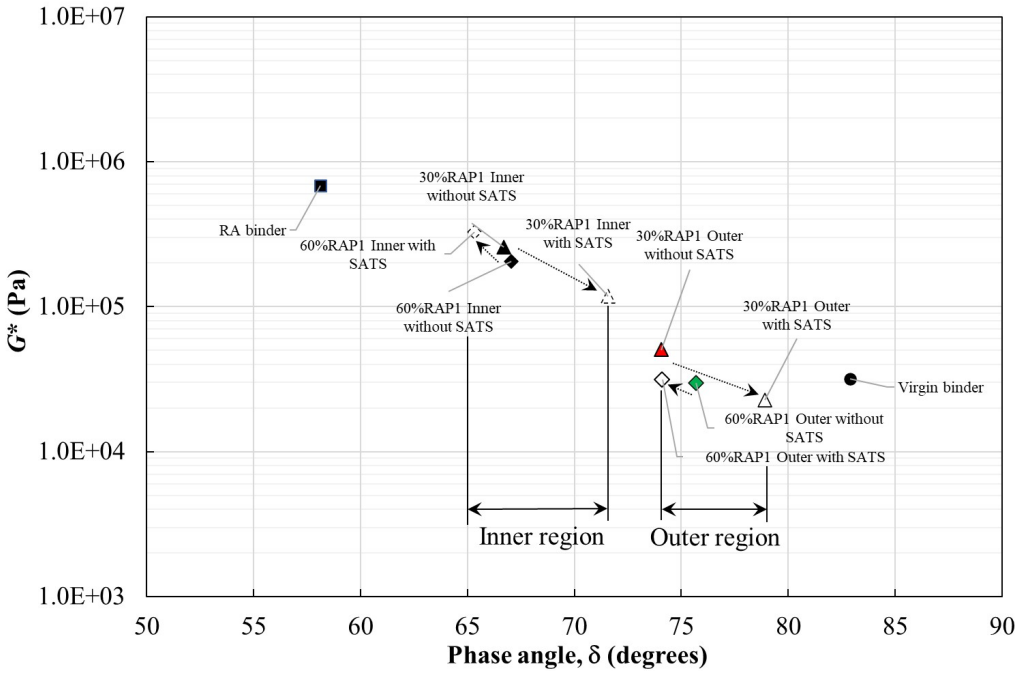

(a)

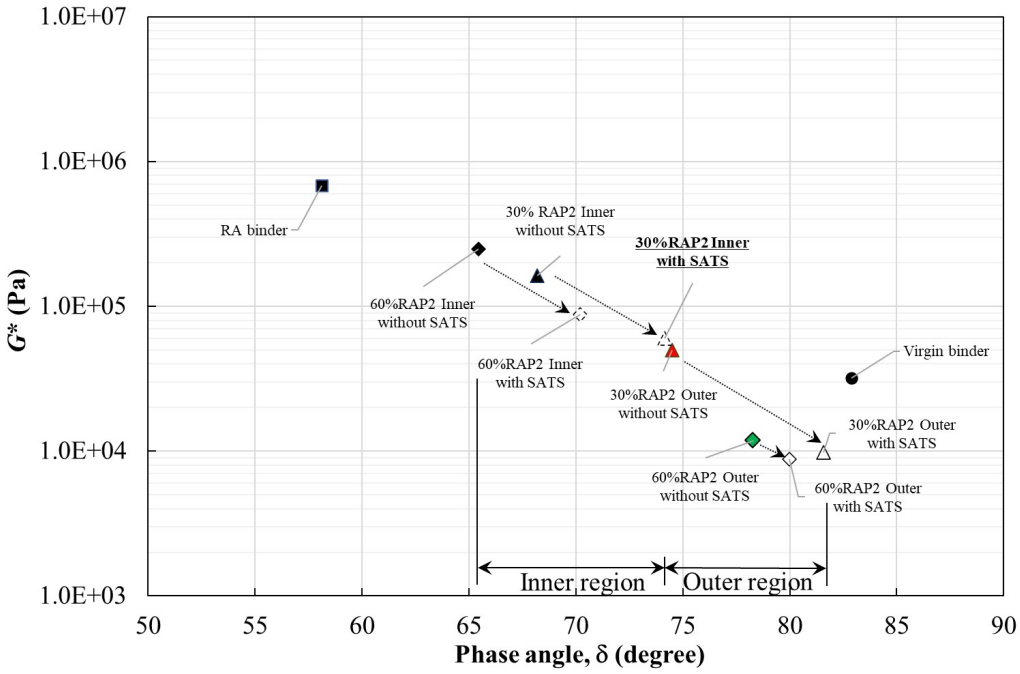

(b)

Figure 6.10 G-R parameter for the five extracted binders with and without SATS conditioning after two-stage extraction from WMA and RAP WMA mixtures (a) 30% and 60% RAP1 binders, (b) 30% and 60% RAP2 binders

6.5 ASSUMED DETERIORATION MECHANISM

As mentioned above, the properties of the binder extracted from the HMA and WMA mixtures did not change significantly with SATS conditioning. However, in the case of both the HMA and WMA mixtures, the retained saturation was high with SATS conditioning. Owing to this situation, as shown in Figure 6.11 (a), the adhesion between the aggregate and binder might be lost after the SATS conditioning. Then, water might infiltrate into the voids that had not been continuous before being subjected to SATS conditioning. The loss of adhesion between the aggregate and binder could allow the aggregate to move more easily during loading. This could be in accordance with the lower stiffness and higher initial strain of the mixtures with the SATS conditioning compared to those without the conditioning, as observed in the ITSM tests and in the ITFTs, respectively.

In contrast, in the case of the RAP mixture, although the properties of the binder did not change much when subjected to SATS conditioning, as in the case of the HMA mixture, the retained saturation remained relatively low. This indicates that, as shown in Figures 6.11 (b) and (c), the RAP mixture was expected to have little water infiltration into the discontinuous voids, even after SATS conditioning. Therefore, it is natural to assume that the adhesion between the binder and aggregate was not lost. In fact, the results shown in Figures 6.9 and 6.10 support the idea that the inner layer binder adheres to the aggregate better than the HMA and WMA binder. This mechanism is consistent with the fact that the stiffness in the ITSM tests and the initial strain in the ITFTs did not change significantly for the RAP mixture with the SATS conditioning.

In addition, these adhesion states depend on the types of rejuvenator, especially in 30% RAP as shown in Figures 6.9 and 6.10. These results are related to stripping results. Notably, because changes in binders properties can be seen in each rejuvenator after the SATS conditioning as indicated in Figures 6.9 and 6.10, it was assumed that the bonds in the binders were not lost in either the HMA, WMA or RAP mixtures, as shown in Figure 6.11.

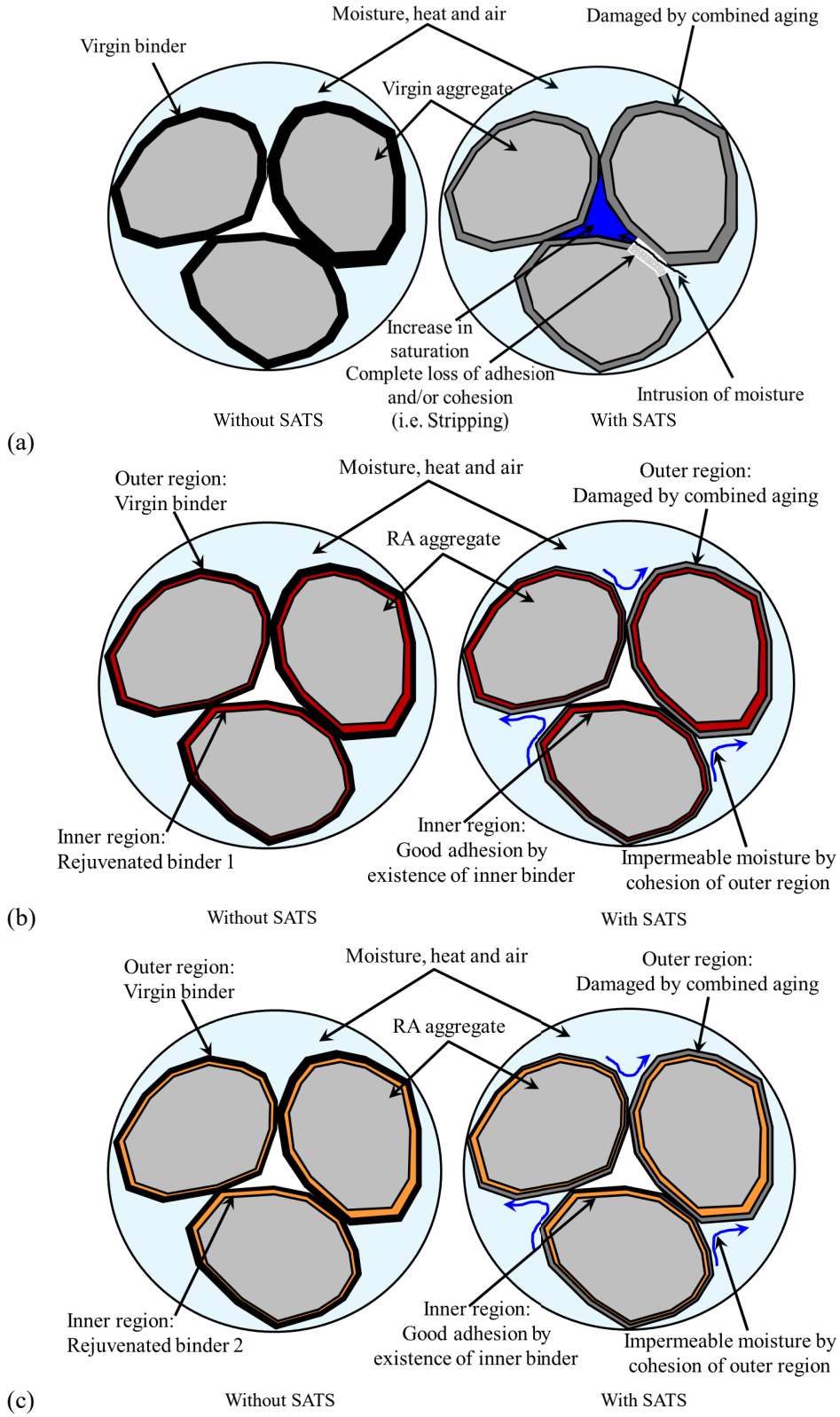

Figure 6.11 Assumed deterioration mechanism induced by the combined aging (a) HMA and WMA mixtures, (b) RAP mixture-Rejuvenator 1, (c) RAP mixture-Rejuvenator 2

6.6 SUMMARY

In order to assess the rheological properties of HMA, RAP, WMA and RAP-WMA mixtures, the extracted binders were analysed using two staged extraction method. Based on the findings obtained from the extracted binder, the following summary are described in this section.

1. As to G-R parameter for binders, similar trend to G^* ratio can be seen in G-R parameter. The result reveals that G-R parameter was shifted toward lower phase angle as RAP ratio increases. In addition, differences in rejuvenator is more pronounced after SATS conditioning. These results show similarity in G^* ratio and binder fatigue tests results. Therefore, G-R parameter might also be harmonized with binder stiffness and fatigue results.

2. For binders obtained from two-staged extraction, the results drawn from master curve exhibited that the inner layer binder shows high in complex modulus than that of the outer layer. In addition, there seems significant changes in master curve, especially in 30% RAP2 after the conditioning. Furthermore, the rheological assessment plotted in black diagram also captured significant changes in inner and outer binders with the conditioning, especially for 30% RAP2 binder. Since 30% RAP2, 30% RAP2-WMA, HMA and WMA mixtures demonstrated significant changes in average stripping ratio, these results might imply corelation to average stripping ratio of mixtures.

3. To assess the deterioration mechanism, DSR tests were conducted on the binders using a two-stage extraction of the RAP mixture. The results indicated that the inner layer binder of the RAP mixture adhered to the aggregate better than the HMA and WMA binders. Based on these observations, it is proposed that the RAP mixture did not lose adhesion between the binder and aggregate, whereas the adhesion could be lost in the case of the HMA and WMA mixtures with the SATS conditioning. The proposed mechanism could reasonably explain the trends in the changes in the properties of binders and mixtures with SATS conditioning, as obtained from the experiments in this study.

CHAPTER 7

Conclusions and Further Research

7.1 INTRODUCTION

Provisional conclusions have been described through this thesis. This chapter provides conclusions obtained from RAP, RAP-WMA mixtures and rheological assessment results through Saturation Aging Tensile Stiffness (SATS) conditioning. These conclusions are followed by further research that could be related to this study.

7.2 CONCLUSIONS FOR RAP-HMA WITH REJUVENATOR

In order to assess the durability of RAP mixtures, the mechanical and physical properties of RAP mixtures with 30 and 60% RAP contents blended with two types of oil-based rejuvenator agents (denoted as 30% RAP1, 60% RAP1, 30% RAP2, and 60% RAP2 mixtures, respectively), both with and without combined aging, were experimentally investigated in Chapter 4. The properties of the HMA mixtures were investigated in the same way as comparison. The following conclusions were obtained from the test results using SATS conditioning.

In terms of mixture properties, remarkable trends were confirmed in the changes in the properties of the HMA and RAP mixtures with SATS conditioning. The results obtained from ITSM tests indicated that the RAP mixtures with rejuvenators did not show a reduction in retained stiffness, while the HMA mixtures demonstrated a significant drop in stiffness with SATS conditioning. Furthermore, in the ITFTs,

the RAP mixtures with rejuvenators showed a longer residual service life than the HMA mixture after the damage from SATS conditioning. These trends were more pronounced as RAP content increased. In addition, detailed analyses showed that there were differences in the fatigue behaviors of RAP mixtures with different rejuvenators. These differences might be attributed to differences in the compaction performances of the RAP mixtures with different rejuvenators, which could (in turn) be due to the different components of the chemical properties of the RAP binders.

As to stripping result, the RAP mixtures with rejuvenators showed a lower stripping ratio with SATS conditioning than that of the HMA mixture. This trend became more pronounced for higher RAP content. As a results, all the experimental results suggested that the adhesion states of the binder and aggregates caused a difference in durability between the HMA mixture and RAP mixtures with SATS conditioning.

With respect to binder, asphalt binders were extracted from the laboratory specimens of five types of the mixtures (HMA, 30% RAP1, 60% RAP1, 30% RAP2 and 60%), in order to investigate the binder properties with and without the SATS conditioning. The properties of the extracted binders were evaluated through frequency sweep tests and fatigue tests using DSR. The results demonstrated that there was no significant change in the properties of each binder with the conditioning. This was probably due to the fact that the low pressure of 0.5 MPa and the curing period of 24 hours set by the SATS conditioning in this study. The detailed analyses of the test results demonstrated that there were differences in the stiffness and the fatigue results among the RAP binders with different rejuvenators with the SATS conditioning. The different trends in the effects of the SATS conditioning on the RAP1 and RAP2 binders might be attributed to the difference in the chemical composition of the binders, which were brought by different rejuvenators.

7.3 CONCLUSIONS FOR RAP-WMA WITH REJUVENATOR

To evaluate the durability of RAP-WMA mixtures, mechanical and physical properties of RAP-WMA mixtures having 30 % and 60 % RAP contents blended with two types of rejuvenator agents (Rejuvenator 1 and 2), with and without combined aging, were examined through experiments in Chapter 5. WMA mixtures prepared from virgin binder and virgin aggregates, with and without combined aging, were also investigated for the purpose of comparison. SATS conditioning were used to simulate the combined aging. Properties of the binders extracted from the RAP and the WMA mixtures were also examined by extracting binder from mixture. The following findings were obtained from the test results.

As mixture properties, the SATS conditioning reveals that retained stiffness and fatigue test results are harmonized after the conditioning. 30% RAP1-WMA, 60% RAP1-WMA and 60% RAP2-WMA mixtures remained similar stiffness with and without the SATS conditioning, while WMA and 30% RAP2-WMA indicated reduction in stiffness with the condition.

With respect to fatigue properties, similar trend can be seen in fatigue results. RAP1-WMA and 60% RAP2-WMA mixtures did not show significant changes in initial strain with and without the condition, 30% RAP2-WMA and WMA mixtures indicates changes in the initial strain with the condition. In addition, the initial strain of 30% RAP2-WMA mixture were closed to that of WMA mixtures after the condition. Furthermore, the results summarized by stress level revealed that RAP-WMA mixture has longer fatigue life than that of WMA mixture.

With regard to stripping characteristics of mixtures, average stripping ratio is also corelated to retained stiffness and fatigue results. RAP1-WMA mixtures remained lower stripping ratio in 30% and 60% RAP ratios, whilst RAP2-WMA mixtures were shifted as RAP contents increase. Since similar trend can be seen in the retained stiffness and fatigue test results, stripping ratio is also harmonizing with these results.

With regard to binder properties, the G^* ratio ($G^*_{conditioned}/G^*_{unconditioned}$) is harmonized with fatigue test results. 60% RAP1-WMA binder showed slight increase in the G^* ratio whilst that of WMA binder indicated significant drop in the ratio. 30% RAP1-WMA, 30% RAP2-WMA and 60% RAP2-WMA binders also showed changes in the G^* ratio with and without the SATS conditioning. The same trend can be seen in fatigue test results. In particular, 60% RAP1-WMA binder showed increase in failure cycles whereas WMA binder demonstrated significant reduction in failure life, with and without the condition. Other binders also exhibited changes in failure cycles after the condition. Therefore, it implies that both the G^* ratio and the fatigues results are harmonizing. In addition, experiment results showed that the effect of wax could be neglected if wax was remained in binder.

7.4 CONCLUSIONS FOR RHEOLOGICAL ASSESSMENT

The rheological properties of HMA, RAP, WMA and RAP-WMA mixtures, the extracted binders were analysed using two staged extraction method. Based on the findings obtained from the extracted binder, the following summary are described from Chapter 6.

In terms of G-R parameter for binders, similar trend to G^* ratio can be seen in G-R parameter. The result reveals that G-R parameter was shifted toward lower phase angle as RAP ratio raises. In addition, differences in rejuvenator is more pronounced after SATS conditioning. These results show similarity in G^* ratio and binder fatigue tests results. Therefore, this suggests that G-R parameter might also be harmonized with binder stiffness and fatigue results.

As to binder obtained from two-staged extraction, the results drawn from master curve exhibited that the inner layer binder shows high in complex modulus than that of the outer layer. In addition, there seems significant changes in master curve, especially in 30% RAP2 after SATS conditioning. Furthermore, the rheological assessment plotted in black diagram also captured significant changes in inner and

outer binders with the conditioning, especially for 30% RAP2 binder. Since 30%RAP2, 30%RAP2-WMA, HMA and WMA mixtures demonstrated significant changes in average stripping ratio, these results might imply corelation to average stripping ratio of mixtures.

With regard to assessment of the deterioration mechanism, DSR tests were conducted on the binders using a two-stage extraction of the RAP mixture. The results demonstrated that the inner layer binder of the RAP mixture adhered to the aggregate better than the HMA and WMA binders. Based on these observations, it is proposed that the RAP mixture did not lose adhesion between the binder and aggregate, whereas the adhesion could be lost in the case of the HMA and WMA mixtures with the SATS conditioning. The proposed mechanism could reasonably explain the trends in the changes in the properties of binders and mixtures with SATS conditioning, as obtained from the experiments in this study.

7.5 CONCLUSIONS FOR RESEARCH PURPOSE

Based on the above findings and conclusions obtained from each chapter, following conclusions can be drawn in this study.

In terms of the effect of RAP ratio, increase in RAP contents would contribute to the improvement of durability in pavement. For the results of retained stiffness and saturation after the SATS conditioning, retained stiffness tends to increase as RAP contents increase. This result is harmonized with fatigue test and stripping ratio results. Thus, RAP contents might be related to the durability of RAP mixture.

With regard to influence of rejuvenator, chemical composition of RAP binder with rejuvenator might be related to the durability of RAP mixture. For RAP mixture with rejuvenator 2, similar mechanical properties to HMA mixture can be seen, especially for 30% RAP mixture. This trend was more pronounce for retained stiffness and saturation and stripping ratio. Looking at its chemical composition of binder, it shows similar composition to virgin binder. Therefore, it seems that binder chemical composition adjusted by rejuvenator influences the durability of RAP mixture.

With respect to WMA additive, a wax examined in this study did not give negative effect on the durability. In terms of mixture properties, there seems no negative results for retained stiffness and saturation, fatigue tests and stripping ratio. In addition, black diagram obtained from DSR test drew similar curve to HMA and RAP binders after SATS conditioning. Therefore, it seems that wax additive did not give negative influence to the durability of RAP mixture.

Based on the findings shown above, the deterioration mechanism for high RAP mixtures are highlighted looking at the three factor.

Firstly, the improvement of the durability for high RAP mixture might be attributed to adhesion between aged aggregate and binder. This trend is confirmed from both mixture tests and rheological properties results.

Secondly, Saturate-rich rejuvenator would lead to stripping of the RAP mixture since less adhesion state between aggregate and binder might be predicted. This means that chemical composition of recovered binder would be related to the durability of high RAP mixture. This trend is more pronounced for 30% RAP2 mixture and binder test results, which might have similar chemical composition to virgin binder.

Finally, Wax used in this study would be dissipated after paving and service, and there seems no negative effect on the durability if it was remained in binders and mixtures. In other words, WMA additive (i.e. wax) used in this study does not provide negative effect on the durability of RAP mixture since rheological property was closed to the binder results extracted from HMA and RAP mixtures after SATS conditioning.

7.6 RECOMMNEDATION AND FUTHER RESEARCH

Some significant features related to aggregate, rejuvenator and warm-mix additive were found through this research. Some of the results might be related to mechanical properties of asphalt mixtures, whilst others are not explained. Based on findings obtained from experiment, following recommendations are described in

this study.

In terms of application, the use of high RAP mixture with rejuvenator should be promoted. The SATS condition results obtained in this study demonstrated that high RAP mixture has high in durability, compared with that of HMA mixture. The results of retained stiffness and saturation showed that high RAP mixture tends to indicated low in saturation and high in retained stiffness, and this result is related to that of stripping results. Fatigue test results support this evidence that high RAP mixture has high in failure life that that of HMA mixture. The same trend as RAP mixture was seen in RAP-WMA mixture. Therefore, the application of high RAP mixture with rejuvenator should be promoted in practice.

With regard to chemical composition of rejuvenator, it was found that the durability of high RAP mixture is different in each rejuvenator. This might be attributed to chemical composition of rejuvenator types. Therefore, the types of rejuvenator should be assessed and selected using rheological assessments before it is laid in service. In particular, the application of saturate-rich rejuvenator should be noted, in terms of durability improvement.

With respect to the durability assessment based on rheological property, rheological assessment is a powerful tool to assess the durability of RAP-WMA mixtures with rejuvenator as well as RAP-HMA mixtures with rejuvenator. This assessment would be useful, especially when resistance for stripping is assessed for different types of rejuvenators and additives. This result might be good indicator for the durability prediction of high RAP mixtures. In particular, two-staged extraction is also good assessment method for high RAP mixture with rejuvenator. Immersion state of binder with rejuvenator can be evaluated through this method. This might be related to the prediction of adhesion and cohesion state of the RAP mixture with rejuvenator. Therefore, this assessment method should be applied for the evaluation of high RAP mixture with rejuvenator.

Finally, the amount of wax should be appropriately decided by looking at both mixture performance and rheological properties. Although remained wax does not give negative effect on the durability of RAP-WMA mixture in this research, the appropriate amount of wax contents should take into account in practice. If

optimum amount of wax is decided through rheological assessment, it might be benefit for engineering works, in terms of cost reduction. Therefore, optimum amount of wax should be considered for practical application.

References

1. Ahmad, M., Mannan, U. A., Islam, M. R., & Tarefder, R. A. Chemical and mechanical changes in asphalt binder due to moisture conditioning. *Road Materials and Pavement Design*, *19*(5), 1216-1229, 2018.
2. Airey, G. D. Rheological characteristics of polymer modified and aged bitumens, PhD Thesis, University of Nottingham, 1997.
3. Airey, G. D, Use of black diagrams to identify inconsistencies in rheological data use of black diagrams to identify inconsistencies in rheological data. Road Materials and Pavement Design, 3 (4), pp. 403-424, 2002.
4. Airey G. D. and Choi, Y-K., State of the art report on moisture sensitivity test methods for bituminous pavement materials. International Journal of road materials and pavement design, 3 (4), pp. 355-372, 2002.
5. Airey, G. Optimizing the returns from long life roads, durability review: volume III – Review of durability test methods. Scott Wilson Pavement Engineering Limited, Nottingham, 2002.
6. Airey, G. D., Choi, Y. K., Collop, A. C., & Elliott, R. C. Development of an accelerated durability assessment procedure for high modulus base (HMB) materials. In *Proceedings of the 6th international RILEM symposium on performance testing and evaluation of bituminous materials, PTEBM* (Vol. 3, pp. 160-166), 2003.
7. Airey, G. D., Choi, Y. K., Collop, A. C., Moore, A. J., & Elliott, R. C. Combined laboratory ageing/moisture sensitivity assessment of high modulus base asphalt mixtures (with discussion). *Journal of the Association of Asphalt Paving Technologists*, *74*, 2005.
8. Airey, G. D., Collop, A. C., Zoorob, S.E., & Elliott, R. C. Moisture damage assessment of asphalt mixtures using the UK saturation aging tensile stiffness test. Transportation Research Board 86th Annual, Meeting. pp. 21-25 January. Washington, DC. 2007.
9. Airey, G.D., Rowe, G. M., Sias, J. E., Di Benedetto, H., Sauzeat, C. & Dave, E. V., Black Space Rheological Assessment of Asphalt Material Behavior. Journal of Testing and Evaluation, 50(2), 2021.
10. Ameli, A., Nasr, D., Babagoli, R., Pakshir, A. H., Norouzi, N. & Davoudinezhad, S. Laboratory evaluation of rheological behavior of binder

and performance of stone matrix asphalt (SMA) mixtures containing zycotherm nanotechnology, sasobit, and rheofalt warm mixture additives. Construction and Building Materials 262, 120757, 2020.

11. Arabani, M., & Mirabdolazimi, S. M. Experimental investigation of the fatigue behaviour of asphalt concrete mixtures containing waste iron powder. Materials Science and Engineering: A, 528(10-11), 3866-3870, 2011.
12. Ascenbrener, T., McGennis, R.B and Terrel, R.L. Comparison of several moisture susceptibility tests to pavements of known field performance. Journal of the association of asphalt paving technologists, 64, pp. 163-208, 1995.
13. ASTM D 1856-95, Standard Test Method for Recovery of Asphalt From Solution by Abson Method. ASTM International, West Conshohocken, PA, 1995.
14. ASTM D5-97, Standard Test Method for Penetration of Bituminous Materials, ASTM International, West Conshohocken, PA, 1997.
15. ASTM D4402-02, Standard Test Method for Viscosity Determination of Asphalt at Elevated Temperatures Using a Rotational Viscometer, ASTM International, West Conshohocken, PA, 2002.
16. ASTM D36 / D36M-14 (2020), Standard Test Method for Softening Point of Bitumen (Ring-and-Ball Apparatus), ASTM International, West Conshohocken, PA, 2020.
17. Bhasin, A., Masad, E., Little, D. and Lytton, R. Limits on adhesive bond energy for improved resistance of hot mix asphalt to moisture damage. Transportation research record: Journal of the transportation research board, 1970, pp. 3-13, 2006.
18. Bhasin, A., Chowdhury, A., Button, J. and Little, D.N. Evaluation of material property tests to predict moisturesusceptibility of HMA. 10th International conference on asphalt pavements (ISAP), Quebec, Canada, pp. 701-710, 2006.
19. Bonnetti, K. S., Nam, K., and Bahia, H. U., Measuring and Defining Fatigue Behavior of Asphalt Binders, *Transportation Research Record 1810*, pp. 33-43, Transportation Research Board, National Research Council, Washington D.C., 2002.
20. BS EN 12697-45, Bituminous mixtures. Test methods. Saturation Ageing Tensile Stiffness (SATS) conditioning test. London: British Standards Institution (BSI) Publication, 2012.

21. BS EN 12697-26, Bituminous mixtures. Test methods. Stiffness, 2012.
22. BS EN 12697-24, Bituminous mixtures. Test methods. Resistance to fatigue, 2012.
23. BS EN 12697-4, Bituminous mixtures. Test methods. Bitumen recovery: Fractionating column, 2015.
24. Copeland, A., Kringos, N. and Scarpas, N. Determination of bond strength as a function of moisture content at the aggregate – mastic interface. 10th International conference on asphalt pavements (ISAP), Quebec, Canada, 711–719 [in CD-ROM], 2006.
25. Carpenter, S. and Wolosick, J. R., Modifier Influence in the Characterization of Hot-Mix Recycled Material. *Transportation Research Record 777*, pp. 15-22, Transportation Research Board, National Research Council, Washington D.C., 1980.
26. Caro S., Masad, E., Bhasin, A. and Little D. N., *Moisture susceptibility of asphalt mixtures, Part 1: mechanisms*, International Journal of Pavement Engineering Vol.9, No. 2, pp. 81- 98, 2008.
27. Cocurullo, A., Airey, G. D., Collop, A. C. and Sangiorgi, C. *Indirect tensile versus two-point bending fatigue testing*, Proceedings of the Institution of Civil Engineers - Transport 2008 161:4, 207-220.
28. Chen, J., Lin, K. and Young, S. Effects of crack width and permeability on moisture-induced damage of pavements. Journal in materials in civil engineering, ASCE 16 (3), pp. 276-282, 2004.
29. Choi, Y.C., Development of the saturation ageing tensile stiffness (SATS) test for high modulus base materials, Thesis (PhD), School of Civil Engineering, University of Nottingham, UK, 2005.
30. Cocurullo, A., Airey, G. D., Collop, A. C. & Sangiorgi, C., Indirect tensile versus two-point bending fatigue testing. In Proceedings of the institution of civil engineers-transport (Vol. 161, No. 4, pp. 207-220) (2008, November). Thomas Telford Ltd.
31. Collop, A. C., et al, Development of the Saturation Ageing Tensile Stiffness (SATS) test. *Proceedings of the Institution of Civil Engineers (ICE)*, 157 (3), pp. 163-171, 2004a.
32. Collop, A.C., Choi, Y.K. and Airey, G.D., Development of a combined ageing/moisture sensitivity laboratory test, Eurasphalt and Eurobitume

Congress, Vienna, Austria, 2004b.

33. DeCarlo et al., Comparative Evaluation of Moisture Susceptibility Test Methods for Routine Usage in Asphalt Mixture Design, *Journal of Testing and Evaluation*, Volume 48, Issue 1, 2019.
34. Farooq, M. A., Mir, M. S. & Sharma, A., Laboratory study on use of RAP in WMA pavements using rejuvenator. *Construction and Building Materials*, *168,* pp. 61-72, 2018.
35. Gabrera, J.G. and Zoorob, S.E. Design of Low Energy Hot Rolled Asphalt. European Symposium on Performance and Durability of Bituminous Materials, pp.289-308, 1994.
36. Gabrera, J.G. and Zoorob, S.E. Field Performance of Low Energy Hot Rolled Asphalt. Second National Conference on Bituminous Mixtures and Flexible Pavements, pp.130-150, 1996.
37. Ghabchi, R., Singh, D., Zaman, M. & Tian, Q. Application of asphalt-aggregates interfacial energies to evaluate moisture-induced damage of warm mix asphalt. *Procedia-Social and Behavioral Sciences*, *104*, 29-38, 2013.
38. Glover, C. J., Davison, R. R., Domke, C. H., Ruan, Y., Juristyarini, P., Knorr, D. B., & Jung, S. H. Development of a new method for assessing asphalt binder durability with field validation. Texas Dept Transport, 1872, 1-334, 2005.
39. Method for Assessing Asphalt Binder Durability with Field Evaluation, FHWA/TX-05/1872-2 (Austin, TX: Texas
40. Department of transportation, Research and Technology Implementation Office, 2005).
41. Goli, H. & Latifi, M. Evaluation of the effect of moisture on behavior of warm mix asphalt (WMA) mixtures containing recycled asphalt pavement (RAP). *Construction and Building Materials,* 247, 118526, 2020.
42. Grenfell, J., Airey, G., Collop, A., Elliott, R, Nicholls, J. Assessment of Asphalt Durability Tests: Part 1, Widening the Applicability of the SATS Test, Published Project Report PPR 535, Transportation Research Laboratory (TRL), Berkshire, 2011.
43. Grenfell, J., Ahmad, N., Airey, G., Collop, A., & Elliott, R. Optimising the moisture durability SATS conditioning parameters for universal asphalt mixture application, *International Journal of Pavement Engineering*, 13, pp. 433-450, 2012.

44. Grenfell, J., Apeagyei, A., and Airey, G., Moisture damage assessment using surface energy, bitumen stripping and the SATS moisture conditioning procedure. *International Journal of Pavement Engineering*, 16 (5), pp. 411-431, 2015.
45. Haggag, M. M., Mogawer, W. S., & Bonaquist, R. Fatigue evaluation of warm-mix asphalt mixtures: Use of uniaxial, cyclic, direct tension compression test. Transportation research record, *2208*(1), 26-32, 2011.
46. Hamzah, M. O., Jamshidi, A., & Shahadan, Z. Evaluation of the potential of Sasobit® to reduce required heat energy and CO2 emission in the asphalt industry. *Journal of Cleaner Production*, *18*(18), 1859-1865, 2010.
47. Hearon, A., & Diefenderfer, S. Laboratory evaluation of warm asphalt properties and performance. In Airfield and Highway Pavements: Efficient Pavements Supporting Transportation's Future (pp. 182-194), 2008.
48. Hefer, A.W., Little, D.N. and Lytton, R.L. A synthesis of theories and mechanisms of bitumen–aggregate adhesion including recent advances in quantifying the effects of water. Journal of the association of asphalt paving technologists, 74, pp. 139-196, 2005.
49. Hirato, T. Effect of Long-term Aging on Rheological Properties of Asphalt, PhD Thesis, Chuo University, 2017.
50. Hurley, G. C., & Prowell, B. D. Evaluation of Sasobit for use in warm mix asphalt. *NCAT report*, *5*(6), 1-27, 2005.
51. Huschek, S. Moglichkeiten zur Verringerung der Misch- und Einbautemperatur von Asphalt, asphalt, pp.46-49 (in German), 1994.
52. IPCC. Climate Change 2021: The Physical Science Basis. Contribution of Working Group I to the Sixth Assessment Report of the Intergovernmental Panel on Climate Change. Cambridge University Press, Cambridge, United Kingdom, 2021.
53. Jamshidi, A., Hamzah, M. O., & Shahadan, Z. Selection of reclaimed asphalt pavement sources and contents for asphalt mix production based on asphalt binder rheological properties, fuel requirements and greenhouse gas emissions. *Journal of Cleaner Production*, *23*(1), 20-27, 2012.
54. Jamshidi, A., Hamzah,M., and You, Z. Performance of warm mix asphalt containing Sasobit®: State-of-the-art. Construction and Building Materials, Vol. 38, pp. 530-55, 2013.

55. Japan Institute of Country-ology and Engineering, retrieved January 29th , 2023 from https://www.jice.or.jp/award/detail/47.
56. Japan Road Association, Handbook for Reclaimed Asphalt Pavement Mixture, 2010.
57. Japan Road Association, Method of Immersed Wheel Tracking Test, Reference for pavement test method, B004, 2007.
58. Kandhal P.S., *Field and laboratory evaluation of stripping in asphalt pavements: state-of-the-art report*. Transportation Research Record 1454, TRB, 1994.
59. Kanitpong, K., Charoentham, N., & Likitlersuang, S. Investigation on the effects of gradation and aggregate type to moisture damage of warm mix asphalt modified with Sasobit. *International Journal of pavement engineering*, *13*(5), 451-458, 2012.
60. Kassem, E.A., Masad, E., Bulut, R. and Lytton, R. Measurements of moisture suction and diffusion coefficient in hot mix asphalt and their relationships to moisture damage. Transportation research record: journal of the transportation research board, pp. 45‑54, 2006.
61. Karlsson, R. and Isacsson, U. Material-related aspects of asphalt recycling—State-of-the-art. Journal of Materials in Civil Engineering (ASCE), 18 (1), pp. 81-92, 2006.
62. Kennedy T.W., *Prevention of water damage in asphalt mixtures.* STP 899, American Society for Testing and Materials, pp. 119-133, 1985.
63. Krishnan, J.M. and Rao, C.L. Permeability and bleeding of asphalt concrete using mixture theory. International journal of engineering science, 39 (6), pp. 611-627, 2001.
64. Levy, S. M. Public-private partnerships in infrastructure. *Leadership and Management in Engineering*, *8*(4), 217-230, 2008.
65. Little, D. N., Allen, D. H., & Bhasin, A. *Modeling and design of flexible pavements and materials*. Berlin: Springer, 2018.
66. Little, D.N. and Jones, D. Chemical and mechanical mechanisms of moisture damage in hot mix asphalts pavements. Moisture sensitivity of asphalt pavements: a national seminar, San Diego, California. Washington DC: National Academies Press, 2003.

67. Lottman, R. P. Predicting moisture-induced damage to asphaltic concrete: field evaluation. National cooperative Highway Research Program 246, 1982, Washington, DC: National Academies Press.
68. Lu, D. X., Saleh, M., Laboratory evaluation of warm mix asphalt incorporating high RAP proportion by using evotherm and sylvaroad additives. *Construction and Building Materials 114,* pp. 580-587, 2016.
69. Lu, D. X., Saleh, M. & Nguyen, N. H., Effect of rejuvenator and mixing methods on behaviour of warm mix asphalt containing high RAP content. *Construction and Building Materials*, *197,* pp. 792-802, 2019.
70. Mainichi Shinbun, retrieved January 29th , 2023 from https://mainichi.jp/articles/20180910/k00/00e/040/143000c.
71. Masad, E., Castelblanco, A. and Birgisson, B., 2006c. Effects of air voidsize distribution, pore pressure, and bond energy on moisture damage. Journal of testing and evaluation, 34 (1), pp. 1-9, 2006.
72. Masad, E., Arambula, E., Abbas, A.R., Ketcham, R.A. and Epps-Martin, A. Non-destructive measurement of moisture transport in asphalt mixtures. Journal of the association of asphalt paving technologists, 2007.
73. Masad, E., Al-Omari, A. and Lytton, R. A simple method for predicting laboratory and field permeability of hot mix asphalt. Transportation research record: journal of the transportation research board, pp. 55-63, 2006.
74. Masad, E., Zollinger, C., Bulut, R., Little, D. and Lytton, R. Characterization of HMA moisture damage using surface energy and fracture properties. Journal of the association of asphalt paving technologists, 75, pp. 713-754, 2006.
75. Mirhosseini, A. F., Tahami, S. A., Hoff, I., Dessouky, S., & Ho, C. H. Performance evaluation of asphalt mixtures containing high-RAP binder content and bio-oil rejuvenator. *Construction and Building Materials*, *227*, 116465, 2019.
76. Mogawer, W., et al. Performance characteristics of plant produced high RAP mixtures. Road Materials and Pavement Design, 13, pp. 183-208, 2012.
77. Mogawer, W. S., Booshehrian, A., Vahidi, S., & Austerman, A. J. Evaluating the effect of rejuvenators on the degree of blending and performance of high RAP, RAS, and RAP/RAS mixtures. *Road Materials and Pavement Design*, *14*(sup2), 193-213, 2013.
78. Mogawer, W. S., Austerman, A., Roque, R., Underwood, S., Mohammad, L.,

& Zou, J. Ageing and rejuvenators: evaluating their impact on high RAP mixtures fatigue cracking characteristics using advanced mechanistic models and testing methods. *Road Materials and Pavement Design*, *16*(sup2), 1-28, 2015.

79. National Asphalt Pavement Association. Asphalt Pavement Industry Survey on Recycled Materials and Warm-Mix Asphalt Usage Information Series 138, 2017.
80. Nicholls, J. C. and Whiteoak, C.D., Test procedures for durability and adhesion in asphalt, Published Project Report PPR 187, Transportation Research Laboratory (TRL), Berkshire, 2006.
81. Nicholls, J., Harper, K., Green, K., Elliott, R. Assessment of Asphalt Durability Tests: Part 3, Review of SATS test to evaluate existing base layers, Published Project Report PPR 537, Transportation Research Laboratory (TRL), Berkshire, 2010.
82. Pradhan, S. K., & Sahoo, U. C. Influence of softer binder and rejuvenator on bituminous mixtures containing reclaimed asphalt pavement (RAP) material. *International Journal of Transportation Science and Technology*, *11*(1), 46-59, 2022.
83. Qin, Q., Farrar, M., Turner, T. F., & Planche, J. P. Characterization of the Effects of Wax (Sasobit®) on Asphalt Binder. *Western Research Institute. Laramie: Federal Highway Administration,* 2015.
84. Read, J. and Whiteoak, D. (ed) *The Shell Bitumen Handbook* (Fifth edition). London: Thomas Telford, 2003.
85. Rowe, G. M., King, G. & Anderson, M. The influence of binder rheology on the cracking of asphalt mixes in airport and highway projects. *Journal of Testing and Evaluation*, *42*(5), 1063-1072, 2014.
86. Sasolwax. Sasol wax. Retrieve http://www.sasobit.com, 2023.
87. Silva, H. M. R. D. D., Oliveira, J., Ferreira, C. I., & Pereira, P. A. Assessment of the performance of warm mix asphalts in road pavements, 2010.
88. Simnofske, D., Mollenhauer, K., Butz, T. & Oelkers, C., Benefits of FT wax based warm asphalt mixes for short-term binder aging and pavement durability. In *6th Eurasphalt & Eurobitume Congress, https://doi. org/10.14311/EE, 2016*.
89. Sobhi, S., Yousefi, A., & Behnood, A. The effects of Gilsonite and Sasobit on the mechanical properties and durability of asphalt mixtures. *Construction and Building Materials*, *238*, 117676, 2020.

90. Solaimanian, M., Harvey, J., Tahmoressi, M. and Tandon, V. Test methods to predict moister sensitivity of hot mix asphalt pavement. Moisture sensitivity of asphalt pavements: a national seminar, San Diego, California. Washington DC: Transportation Research Board, 2003.
91. Song, I., Little, D.N., Masad, E. and Lytton, R.L. Comprehensive evaluation of damage in asphalt mastics using X-ray CT, continuum mechanics, and micromechanics. Journal of the association of asphalt paving technologists, 74, pp. 885-920, 2005.
92. Song, W., Huang, B. & Shu, X., Influence of warm-mix asphalt technology and rejuvenator on performance of asphalt mixtures containing 50% reclaimed asphalt pavement. *Journal of Cleaner Production*, *192*, pp.191-198, 2018.
93. Shu, X., Huang, B., Shrum, E. D., & Jia, X. Laboratory evaluation of moisture susceptibility of foamed warm mix asphalt containing high percentages of RAP. Construction and Building Materials, 35, pp. 125-130, 2012.
94. Terrel R.L., Al-Swailmi S., *Water sensitivity of asphalt-aggregate mixes: test selection,* SHRP-A-403, Strategic Highway Research Program, National Research Council, Washington, D.C., 1994.
95. Terrel, R.L. and Al-Swailmi, S., The role of pessimum voids concept in understanding moisture damage to asphalt concrete mixtures. Transportation research record: journal of the transportation research board, 1386, pp. 31-37, 1993.
96. Terrel, R. L., Shute, J.W. Water sensitivity of asphalt-aggregate mixes: test selection, SHRP-A-403, Strategic Highway Research Program, National Research Council, Washington, D.C., 1989.
97. Tarbox, S. and Daniel, J. S. Effects of long-term oven aging on reclaimed asphalt pavement mixtures. Transportation Research Record: Journal of the Transportation Research Board, 2294 (1), pp. 1-15, 2012.
98. Tran, N.H., Taylor, A., and Willis, R. Effect of rejuvenator on performance properties of HMA mixtures with high RAP and RAS contents. NCAT Report 12-05, National Center for Asphalt Technology, Aurburn University, Auburn, Alabam-a, 2012.
99. Venkatachalam, A., & Devadas, M. P. Design of high performance bituminous mix using tannery waste. In *Proceedings of 27th IRF International Conference* (p. 81), 2015.
100. Wang, D., Li, D., Yan, J., Leng, Z., Wu, Y., Yu, J., & Yu, H. Rheological and

chemical characteristic of warm asphalt rubber binders and their liquid phases. *Construction and Building Materials*, *193*, 547-556, 2018.

101. Wasiuddin, N. M., Zaman, M. M., & O'Rear, E. A. Effect of sasobit and aspha-min on wettability and adhesion between asphalt binders and aggregates. *Transportation Research Record*, *2051*(1), 80-89, 2008.
102. Yang, Y., Zhang, H., & Wu, Y. Laboratory evaluation of the Warm Mix Asphalt performance in liaoning. In *ICCTP 2009: Critical Issues In Transportation Systems Planning, Development, and Management* (pp. 1-7), 2009.
103. Yin, F., et al. Long-term ageing of asphalt mixtures. Road Materials and Pavement Design, 18, pp. 2-27, 2017.
104. Yousefi, A., Behnood, A., Nowruzi, A. & Haghshenas, H., Performance evaluation of asphalt mixtures containing warm mix asphalt (WMA) additives and reclaimed asphalt pavement (RAP). *Construction and Building Materials 268,* 121200, 2021.
105. Zhang, J., Guo, C., Chen, T., Zhang, W., Yao, K., Fan, C.,& Yao, Z. Evaluation on the mechanical performance of recycled asphalt mixtures incorporated with high percentage of RAP and self-developed rejuvenators. *Construction and Building Materials*, *269*, 121337, 2021.
106. Zhao, S., et al. Laboratory performance evaluation of warm-mix asphalt containing high percentages of reclaimed asphalt pavement. Transportation Research Record: Journal of the Transportation Research Board, 2294 (1), pp. 98-105, 2012.
107. Ziari, H., Moniri, A., Bahri, P., & Saghafi, Y. The effect of rejuvenators on the aging resistance of recycled asphalt mixtures. *Construction and Building Materials*, *224*, 89-98, 2019.